USE OF AIR SIDE ECONOMIZER FOR DATA CENTER THERMAL MANAGEMENT

A Thesis
Presented to
The Academic Faculty

By

Anubhav Kumar

In Partial Fulfillment
of the Requirements for the
Masters Degree in the
School of Mechanical Engineering

Georgia Institute of Technology
August 2008

USE OF AIR SIDE ECONOMIZER FOR DATA CENTER THERMAL MANAGEMENT

Approved by:

Dr. Yogendra Joshi, Advisor
School of Mechanical Engineering
Georgia Institute of Technology

Dr. Srinivas Garimella
School of Mechanical Engineering
Georgia Institute of Technology

Dr. Ruchi Choudhary
College of Architechture
Georgia Institute of Technology

Date Approved: July 7, 2008

ACKNOWLEDGEMENT

I would like to thank Dr. Yogendra Joshi for his technical mentoring, direction, and support during this research. I would also like to thank Dr. Srinivas Garimella and Dr. Ruchi Choudhary for their technical review and support as my thesis reading committee.

I wish to thank all my family and friends for their moral support during my graduate study. I would like to express my deepest gratitude to my company General Electric and my manager for supporting my graduate studies. I am thankful for all my current and former colleagues for the valuable suggestions and advice during the course of my study.

TABLE OF CONTENTS

Page

LIST OF TABLES

Page

LIST OF FIGURES

Page

NOMENCLATURE

ρ	Density
μ	Viscosity
u_i, u_j	Fluid Velocity
μ_t	Turbulent Viscosity
G_k	Turbulent kinetic energy generation due to mean velocity gradient
G_b	Turbulent kinetic energy generation due to mean buoyancy
β	Coefficient of thermal expansion
T	Temperature
S	Modulus of mean rate-of-strain tensor
T_{ref}	Reference Temperature
k	Turbulent kinetic energy
ε	Turbulent dissipation
λ	Thermal conductivity of the fluid
J_j	Diffusion flux of species
S_h	Volumetric energy source
h	sensible enthalpy
Y_j	Mass fraction of species
D_{H_2o}	Diffusion coefficient of water vapor into air
Sc_t	Schmidt number

SUMMARY

Sharply increasing power dissipations in microprocessors and telecommunications systems have resulted in significant cooling challenges at the data center facility level. Trends indicate that the room level heat densities will increase from 1000 W/m^2 to 3000 W/m^2 in the near future, along with a net power demand of upto hundreds of MW. Energy efficient cooling of data centers has emerged as an area of increasing importance in electronics thermal management.

One of the lowest cost options for significantly cutting the cooling cost for the data center is an airside economizer. If outside conditions are suitable, the airside economizer introduces the outside air into the data center, making it the primary source for cooling the space and hence a source of low cost cooling.

Full-scale model of a representative data center was developed, with the arrangement of bringing outside air. Commercially available fluid flow and heat transfer software, FLUENT, was used for all numerical simulation. Four different cities over the world were considered to evaluate the savings over the entire year.Results show a significant saving in chiller energy (upto 50%). The limits of relative humidity can be met at the inlet of the server for the proposed design, even if the outside air humidity is higher or lower than the allowable limits. The saving in the energy is significant and justifies the infrastructure improvements, such as improved filters and control mechanism for the outside air influx.

CHAPTER 1

INTRODUCTION TO DATA CENTER THERMAL MANAGEMENT

A **data center** is a facility used to house computers and associated infrastructure, such as telecommunications and storage systems. It generally includes redundant or backup power supplies, redundant data communications connections, environmental controls (e.g., air conditioning, fire suppression), and special security devices. These computing facilities are used by industries with large data processing needs, such as telecommunications switching, and supercomputing nodes. Figure 1.1 shows such a data center facility, which typically houses thousands or tens of thousands of heat producing processors. The trends show a rapid increase in heat fluxes and volumetric heat generation rates from these microprocessors [1]. The excess heat generated by equipment can concentrate within the cabinet and cause equipment to critically overheat and shutdown, costing companies time and money. The much higher heat generation rates and their concentrated nature make the design guidelines for comfort cooling in office space or auditoria inapplicable to such environments.

Thermal management of data center is critical as it is one of the most power-consuming overheads for the center [4]. Due to high heat loads, data center layout and design cannot rely on intuitive design of air distribution. Detailed experimental measurements and numerical computations of heat transfer and fluid flow are needed for the proper equipment placement and design of the data center for reliable operation.

The thermal management community, in the past, has extensively looked at heat removal from the data center [2, 3]. The focus has been on recirculation of the air while

rejecting heat to the ambient. The predominant architecture for cooling data centers since the inception of the mainframe has been raised-floor air delivery from perimeter computer room air handlers (CRAH). In this approach, CRAH units are placed around the perimeter of the room and distribute cold air through a raised floor, with perforated floor tiles or vents to direct the air into the room [44]. A similar air delivery system that has been used to cool data centers is central air handler units (CAHU). These systems utilize larger, more centralized cooling units, with air delivery similar to perimeter CRAH cooling of either raised-floor or custom overhead ductwork [44]. The challenges to such systems have been mixing of the hot and cold fluid within the space of the data center and recirculation of hot air through the equipments [3].

Figure 1.1. Data center layout with racks arranged in hot and cold aisle [7]

1.1. Data Center Power Density Trends

Microprocessor driven escalation of heat dissipation needs has resulted in significant cooling challenges at the data center facility level. Data centers are currently

designed for handling heat densities of 1000 W/m ^{2} at the room level [3]. Trends indicate that these heat densities will exceed 3000 W/m ^{2} in the near future [3]. Lawrence Berkeley National Laboratory has studied the trends of power consumption for a number of data centers [1]. Figure 1.2 summarizes their findings. The trends show that the heat production rate has doubled in two years (2003-2005) at the sever level. Therefore, cooling of data center has emerged as an area of increasing importance for electronics thermal management. Let us consider a 1000 m^2 data center, a facility with total power supply of 1MW over the entire 8,760 hours of the year [31]. The cost of driving that 1MW computer load could be up to $700,000 per year (assuming a cost of electricity of $0.08 / kWh) {1000 x 8760 x 0.08}. The cooling load associated with the 1MW load would be around 285 tons (1,002 kW). At an average chiller efficiency of 0.5 kW/ton, the cost of running that chiller at full load year-round is approximately $100,000 per year.

Studies have revealed that the current thermal management practices such as increased air flow rate, extra fans and baffles will soon become incapable for handling the high thermal load and would also become formidably expensive [44]. So, alternative methods such as row-based cooling systems [44], liquid cooling [35] and economizers [31] for cooling the data centers have to be implemented.

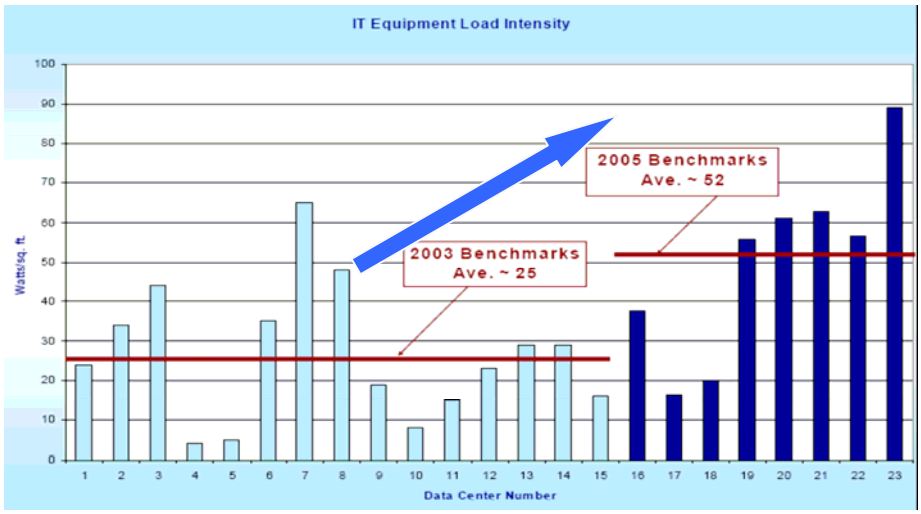

Figure 1.2. IT equipment load intensity over the years for date centers [3].

1.2. Data Center Layout

The trend of putting more functionality into data processing and telecommunication equipment while maintaining the same total volume occupied has lead to continual increase in volumetric power density. In a data center, this equipment is arranged in an Electronics Industry Standard (EIA) Rack. The data processing equipment is then organized in these racks in discrete vertical units, called 'U', where a rack is approximately 40U tall. The racks are arranged in rows of hot aisle and cold aisle as discussed in next section. Racks are provided with fans and baffles designed to move cooling air in a specified direction and often, at a specified rate. Most racks provide connections for electrical power. Some provide electromagnetic interference (EMI) and radio frequency interference (RFI) shielding to meet standards established by various regulatory agencies.

1.3. Airflow Configuration

Airflow distribution within a data center has a major impact on the thermal environment of the data processing equipment located in these rooms. To provide an

environment of controlled temperature and humidity, two types of air distribution configurations are commonly utilized for such equipment: raised-floor and non-raised-floor layouts [45].

In a non-raised floor cooling system, the chilled air enters the room from diffusers in the ceiling and exits the room via vents that may be placed at different locations as shown in figure 1.3. Cooling air can be supplied from the ceiling in the center of the room, where computers are located, with exhausts located near the walls. Short partitions are installed around the supply openings to minimize short-circuiting of supply air to returns (short-circuiting occurs when air takes the path of least resistance) [45].

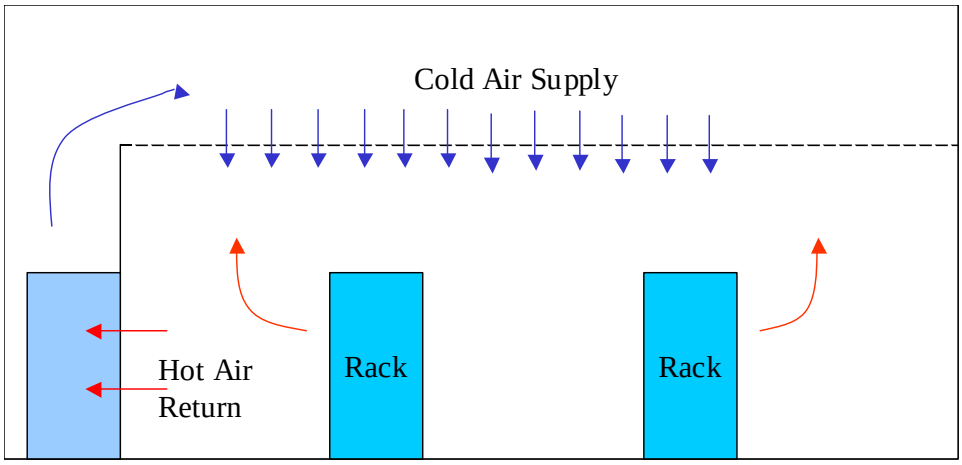

Figure 1.3. Non-raised floor air distribution system [45]

A majority of today's data centers use computer room air conditioning (CRAC) units to supply the facility with cooling air through a raised floor, designed to provide an adequately low cabinet air temperature for reliable server operation. Because of the typical front-to-back airflow of the systems, the ideal placement of the cabinets and racks have the systems installed front-to-front and back-to-back. This configuration is referred to as a *hot-aisle/cold-aisle layout.*

A hot-aisle/cold-aisle layout enables cool air to flow through the aisles to the systems' front air intake and enables heated air to flow away from the systems' back exhaust to the air conditioner return ducts. This layout eliminates direct transfer of hot exhaust air from one system into the intake air of another system. Figure 1.4 illustrates a hot-aisle/cold-aisle layout. Rows of racks or cabinets perpendicular to air conditioners are formed. This formation facilitates an unobstructed flow of heated air down the aisles to the air conditioner return ducts. A cold aisle has perforated floor tiles or grates that enable cold air to rise from the raised floor. A hot aisle has no tiles or grates so that hot air and cold air do not mix. Seal cable cutouts in both hot aisles and cold aisles increase underfloor pressure and eliminate cold or hot air redirection.

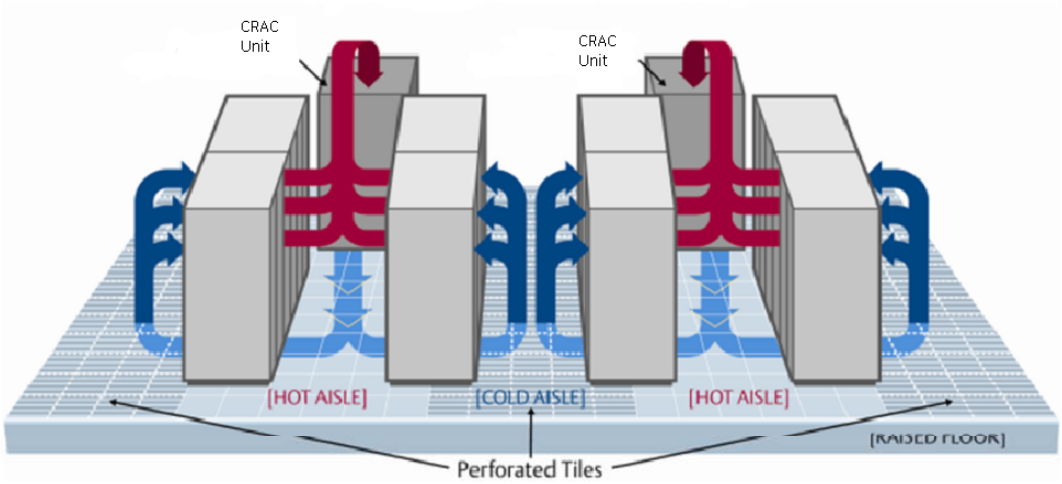

Figure 1.4. Hot-Aisle/Cold-Aisle layout in a raised floor data center [8]

The temperature at inlet of the racks is the key performance metric in evaluating the cooling performance of the data center facility. The chiller is typically the largest energy consumer of all the facility's HVAC equipment. The cooling requirements of data centers represent up to 50% of the total energy consumption [2], corresponding to a significant cost and environmental impact. An example of an energy benchmarking

survey, measuring the percentage of total power consumed by the Heating Ventilation and Air Conditioning (HVAC) equipment, compiled by Lawrence Berkeley National Labs is presented below in Figure 1.5. Significant HVAC energy saving can be realized by reducing the chiller energy. This can be achieved by using energy efficient chillers. However, reducing the number of hours of chiller operation could have a have the larger impact on lowering energy usage in a facility than by selecting a more energy-efficient chiller.

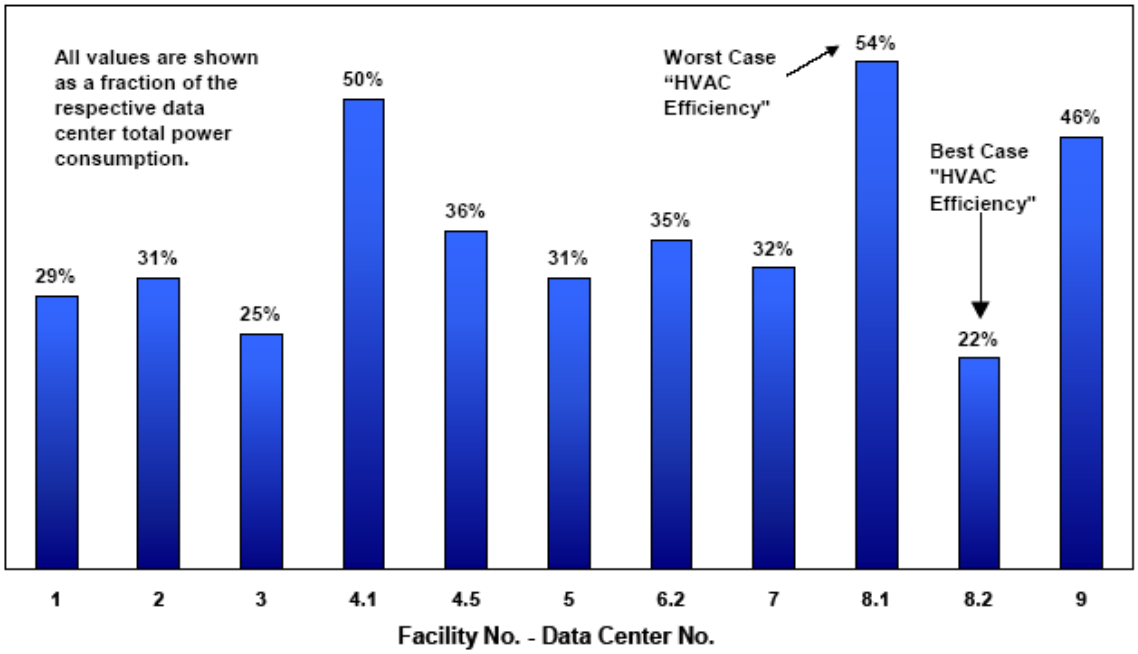

Figure 1.5. HAVC power consumption of 11 surveyed data center [3]

1.4 State-of-the-Art and Future Trends in Data Center Thermal Management

Over the past several years, supplemental thermal solutions in the form of ceiling mounted air-cooling units and additional rack level fans have been used to deal with high power density at the rack level. This has proportionally increased the power consumed by the chiller and the fans.

Liquid cooling has the potential to reduce power consumption and noise levels. Systems with air-to liquid heat exchangers mounted within the rack to cool the hot air to form a self-contained cooling loop are commercially available [35]. Figure 1.6 illustrates a system with coupled air to liquid cooling. This approach reduces the distance the hot exhaust air must travel before reaching the CRAC units, which minimizes the adverse effects of hot air recirculation. Moving heat exchanger to the rack still relies on air as the heat transfer medium for heat removal from the servers and performance of such systems are limited by airside heat transfer coefficient. There is ongoing research and development on extending the liquid cooling path to the chip level.

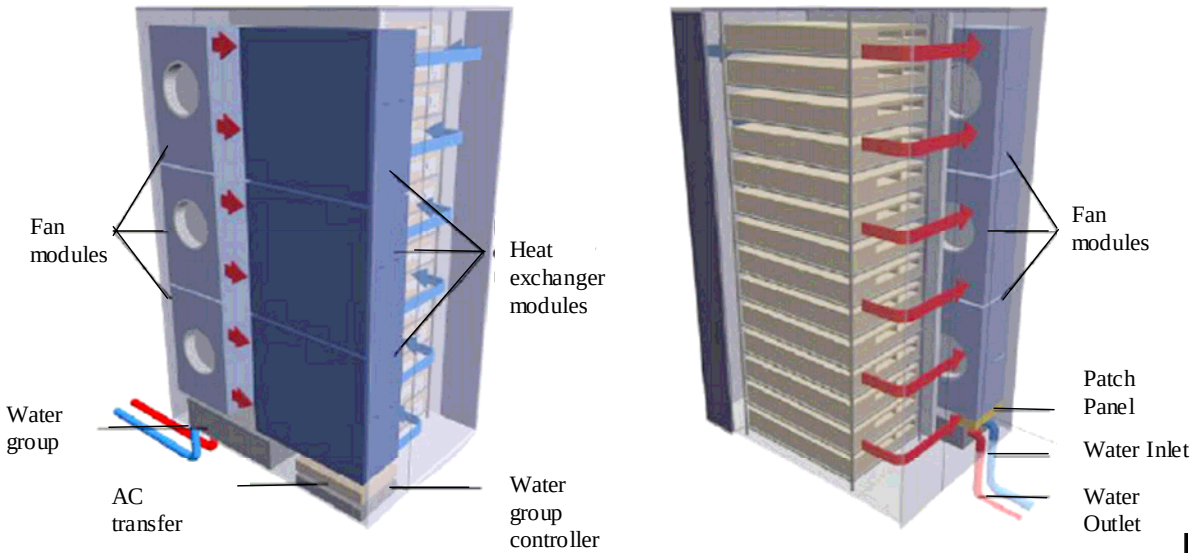

Figure 1.6. Racks with air to liquid heat exchangers [35]

One of the lowest cost options for significantly cutting the cooling costs for a data center is an airside economizer. Depending on the climate, the steady, 24-hour cooling load of a typical data center is well suited to take advantage of seasonal and night-time temperature variations to provide a source of low cost cooling. With an economizer, when the outside air is cooler than the return air, the hot return air is exhausted and

replaced with cooler, filtered outside air - essentially "opening the windows" for free cooling. The term free cooling has been used by the data center community though the fan power and humidification power has to be considered. In many cases, economization can reduce annual cooling energy consumption by more than 50% [34].

This thesis presents computational fluid dynamics/heat transfer (CFD/HT) analysis of a representative data center with an airside economizer. Numerical simulation of the flow, heat and moisture transport was carried out at four locations around the world for different months of the year. The savings in energy used by the CRAC are reported for these different locations, while maintaining humidity and cabinet air inlet temperature levels within ASHRAE allowable limits.

CHAPTER 2

INTRODUCTION TO ECONOMIZERS

The use of economizer systems is one method that has been adopted to lower energy usage, lessen wear and tear on precision air conditioning equipment and decrease operational costs. The two primary types of economizer systems are airside economizers and fluid-based economizers. The stringent temperature and humidity requirements of data centers, coupled with the need for 24-hour cooling 365 days per year, motivate a detailed study of economizers.

Computational equipment has much more stringent requirements on operating ambient conditions as compared to comfort cooling in buildings. It is required to maintain an average inlet dry bulb temperature of 20-25 ^{0}C with 40-55 % relative humidity [7]. A detailed discussion of these is given in section 2.2.2.

2.1 Economizer Systems and their Usefulness

Economizer systems use outside air, when conditions are favorable, to help meet cooling requirements and provide so-called “free cooling” cycles for computer rooms and data centers. When an economizer system is operating, the use of an air conditioning system’s compressor(s) and related electro-mechanical components is reduced or eliminated. In certain geographical locations, economizers can satisfy a large portion of data center cooling requirements [34].

2.2 Airside Economizer

A standard data center cooling system can remove heat from the data center it serves only by running compressor(s), a major electrical cost. With an airside economizer, when the outside air is cooler than the return air, hot return air is exhausted and replaced with cooler, filtered outside air – essentially 'opening the windows' for free cooling. An **airside economizer** system serves as a control mechanism to regulate the use of outside air for cooling in a data center. It utilizes a system of sensors, ducts and dampers to allow entry of the appropriate volume of outside air to satisfy cooling demands. The sensors measure the outside and inside air conditions. If outside conditions are suitable for the use of outside air for cooling, the economizer adjusts the dampers to introduce the outside air, making it the primary source of air for cooling the space with the help of a motorized actuator system. This reduces or eliminates the need for the air conditioning system's compressor(s), which results in a significant energy savings for cooling the space. The economizer also has the facility to mix the hot return air with the outside cold air in cases when the outside air temperature is below the minimum operating temperature ($20\ ^{0}C$). Airside economizers also include exhaust air dampers to prevent the facility from becoming over-pressurized when large amounts of outside air are introduced.

Economization must be engineered into the air handling system. Low cost, mass produced package units may economically serve small data centers. Larger data centers typically justify a more efficient chilled water system with central air handlers and economizer system integrated during the data center design. The schematic of such a data center is shown in figure 2.1 [7]. An outdoor economizing system is best implemented

starting at the schematic design stage, where any required architectural accommodations can be made at little or no additional cost. The key objective is for all data center air handlers to have access to 100 percent outside air as well as return air. This is typically easiest with a central air handling system.

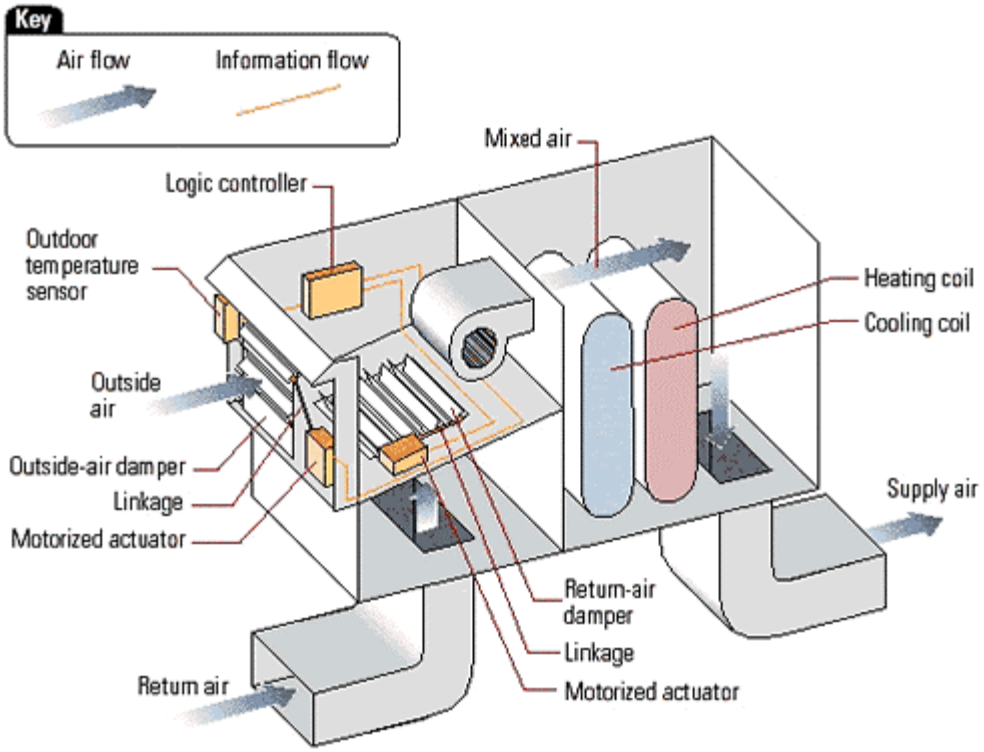

Figure 2.1 Schematic of airside economizer with airflow path [7]

The figure 2.2 shows the control logic of the controller for deciding the opening and closing of the airside economizer dampers. There are sensible heat and enthalpy sensors on the outside as well as inside the data center. The control logic looks at the differential of the sensible heat of the return air and the outside air as shown in the figure.

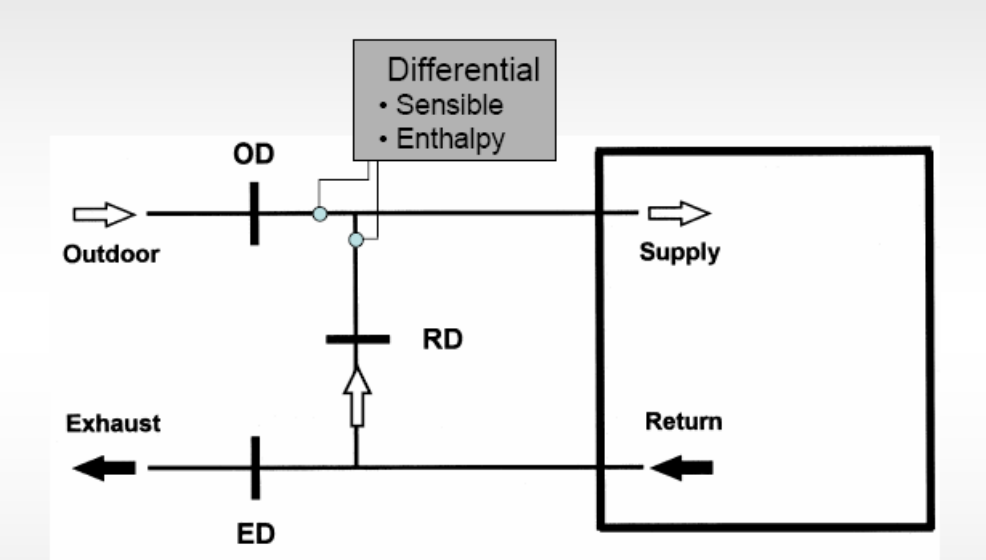

Figure2.2 Control logic of the airside economizer for damper actuation

Figure 2.3, 2.4 and 2.5 show when the outside air can be used. For example, when the outside air temperature (OAT) is higher than the return air temperature (RAT), no outside air is brought into the data center space as shown in figure 2.3. In this case, the outside air damper (OD) is completely closed resulting in no economization.

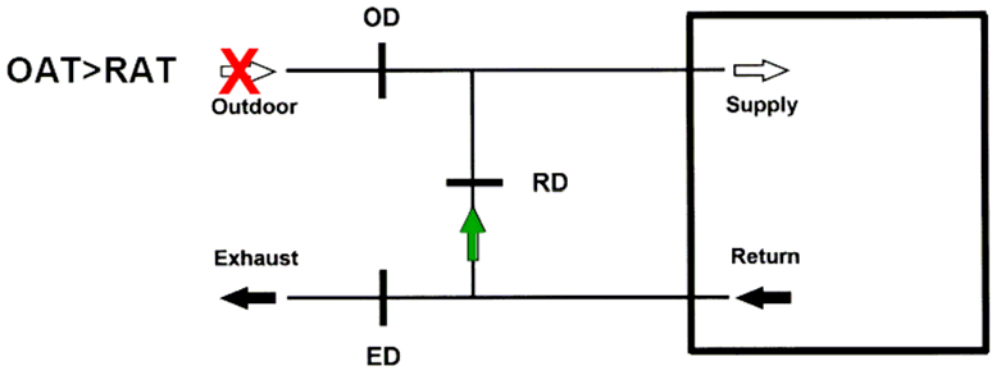

Figure2.3 Case for which no cooling is available from the economizer

Figure 2.4 shows the case when the outside air temperature (OAT) is lower than the return air temperature (RAT), outside air is brought into the data center space. In this

case, the return air damper (RD) is completely closed not allowing the return air to mix with the outside air. This case results in partial economization and additional cooling should be provided with the chillers.

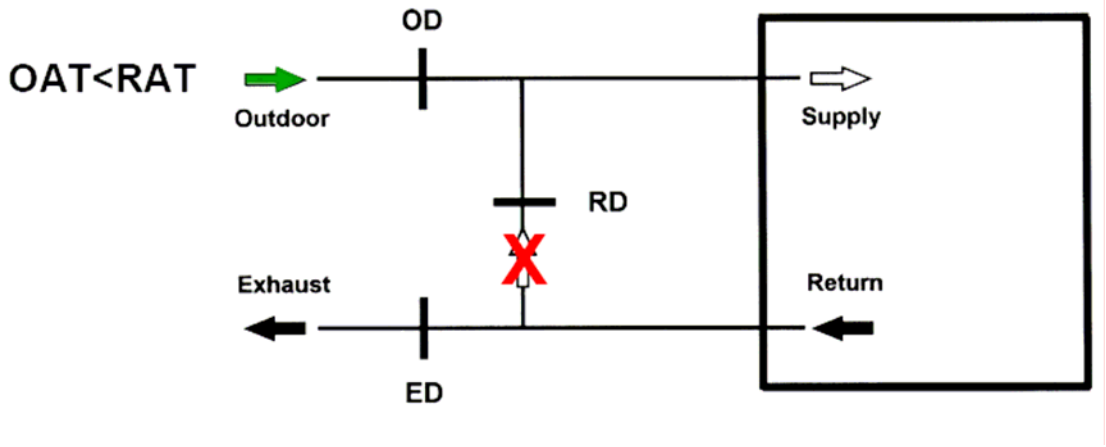

Figure2.4 Case for which partial cooling is available from the economizer

Figure 2.5 shows the case when the outside air temperature (OAT) is lower than the supply air temperature (SAT), outside air is brought into the data center space. In this case the return air is mixed with the outside air so that the temperature falls in the ASHRAE recommended region. This leads to 100% cooling and chillers can be switched off but additional humidification or dehumidification may be required.

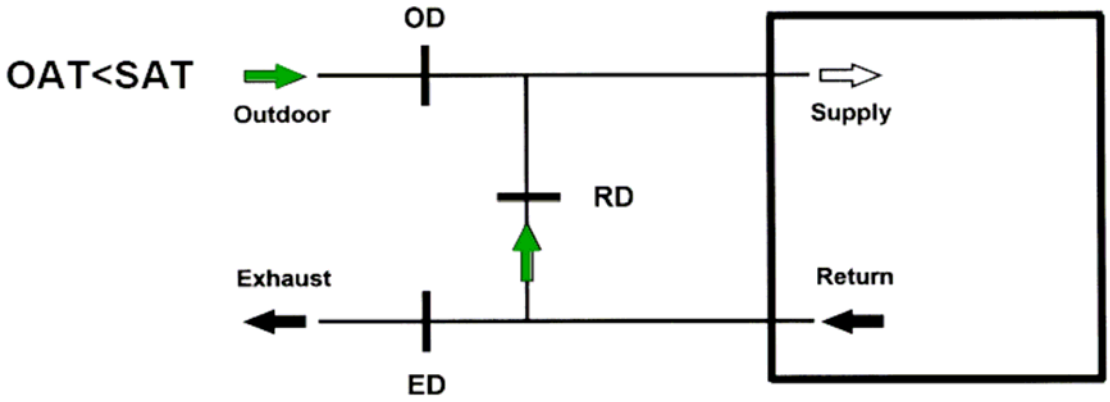

Figure2.5 Case for which 100% cooling is available from the economizer

The use of economizers is also now required by some building codes. The energy code adopted by the City of Seattle in 2001 requires the application of economizer systems in computer rooms and data centers. The State of Massachusetts Energy Code for Commercial and High-Rise Residential New Construction, effective in 2001 [35], requires, with some exceptions, air or water economizers for all cooling systems with a total cooling capacity of at least 19 kW (65,000 Btu per hour).

2.2.1 Use of Airside Economizers for Data Centers – Issues and Solution

Historically, the industry generally has avoided using outside air economizers when dealing with data centers. ASHRAE's Technical Committee 9.9, the technical committee which deals with the issues of data center design and operation, has avoided making any recommendations about the application of outside air economizer until more research can be provided to either support or reject its use for data center [7].

The main points to be considered when using such large quantities of outside air are introduced into a data center are as follows:

- Introduction of outside air into the data center can be a source of dirt, dust, and other airborne particulate or gaseous contaminants that can place the investment of computer equipment at risk; and
- Introduction of outside air into the data center can make relative humidity control difficult.
- The increased cost of additional infrastructure can offset the savings from the economizer system.

All the issues should be addressed during the design phase for any data center facility. Though these issues have been addressed successfully in the past in other type of facilities that have a critical need and requirement for large quantities of outside air, such as hospital and laboratory facilities, data centers need a more careful control, as the recommendations are even more stringent.

2.2.2 Temperature and Humidity Control

With the publication of ASHRAE's 2004 book, *Thermal Guidelines for Data Processing Environments* (prepared by TC 9.9) [7], the industry has come to a consensus about the optimal thermal environment for the data processing equipment. The recommended environment is temperature of 68 ^{0}F to 77 ^{0}F (20 ^{0}C to 25 ^{0}C) dry bulb and relative humidity of 40 % to 55 % at the INLET of the equipment. Figure 2.6 shows a psychrometric chart with ASHRAE's recommended levels of temperature and humidity for reliable operation of the data center. The temperature at any other location within the data center space is not addressed by these specifications. This is a critical point to emphasize as it highlights the basic difference between cooling for comfort and cooling for critical computer equipment.

Figure 2.6 graphically shows psychrometric quantities such as dry bulb temperature, wet bulb temperature, relative humidity (RH), sensible heat ratio and enthalpy. ASHRAE's Design Considerations for Data and Communication Equipment Centers [7] recommends relative humidity between 40% and 55% and temperature between 20 ^{0}C and 24 ^{0}C. However, it allows relative humidity between 20% and 80% with temperature between 15 ^{0}C and 35 ^{0}C. The manufacturers of the data center

equipment have listed a much higher operating range (8% to 95% RH and temperature between 10 ^{0}C and 45 ^{0}C) [27].

In a comfort-cooling environment, the supply air is usually provided by an overhead system within a temperature range of 13 ^{0}C to 16 ^{0}C (55 ^{0}F to 60 ^{0}F dry bulb). The air is then mixed within the occupied space. The temperature perceived by the occupants is represented by this mixed condition. The thermostat that controls the occupied space must be located in the occupied space to ensure optimal comfort. In a data processing space with cooling provided from an underfloor plenum, the cold supply air is separated from the hot discharge air by arranging equipment cabinets in alternating hot and cold isles. The thermostat should be placed in the supply air stream as close to the controlled environment as possible.

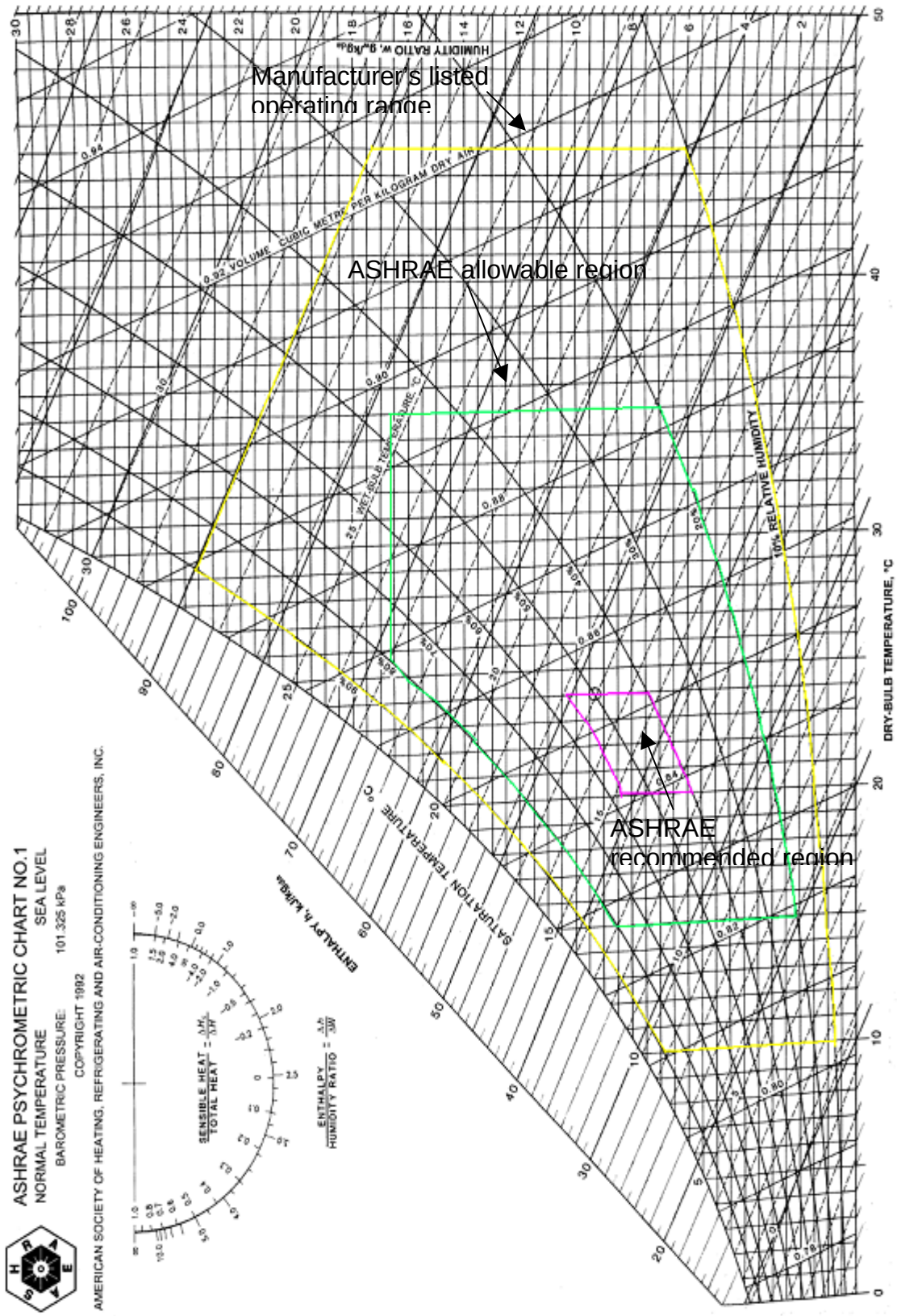

Figure 2.6. Psychrometric chart showing recommended and allowable limits of temperature and RH [47]

Unlike the seasonal and intermittent heating and cooling requirements of office buildings and similar facilities, the controlled environment of a data center requires continuous, year-round cooling. This makes it an ideal candidate for economizer systems during the fall, winter and spring months. Maintaining consistent, acceptable temperature levels can be done with either system (airside economizer or waterside economizer), but humidity control becomes a significant challenge with the airside system. Introducing air via an airside economizer system in the cold winter months is appealing from temperature control standpoint, but care must be taken for RH control.

If a data center room is too humid, condensate can build on computer components causing corrosion and electrical shorts. In addition, high humidity can cause condensate to form on the coils of a cooling unit, in turn leading to wasted cooling (latent cooling), and increased energy cost. Meanwhile, if the humidity is too low, electronic components can experience electrostatic discharge (ESD). Such an event can shut down electronic equipment and possibly damage it, causing loss in productivity and added cost.

Hence, a clean, filtered environment with acceptable control of humidity is mandatory in a data center. Ignoring the impact of humidity can result in serious short and long-term problems, including damage to equipment and to the facility's infrastructure. In most cases, the optimal relative humidity (RH) range for a data center environment is 40-55 %, as recommended by ASHRAE.

2.2.2 Particulate Contamination and Solution

The pollutant of primary concern, when introducing external air to the data center environment, is fine particulate matter that could cause electrical conductor bridging [36]. Outdoor concentrations of fine particulate matter in many locations can be relatively high

compared to other areas within and can be greater than the indoor limits established by ASHRAE. Experimental results show that particulate matter composed of deliquescent salts can cause electronic equipment failure [4]. Other experiments used sulfate salts to demonstrate current leakage from particle deposition under conditions of high humidity [4]. Equipment failure occurs as particles accumulate on electronic equipment and eventually bridge the space between isolated conductors.

While the presence of dry particles between conductors is benign, current leakage or shorts can occur if the particle bridge becomes moist. This happens when the relative humidity of the surrounding air rises to a point where the particles will begin to rapidly absorb moisture. This process is called deliquescence and occurs at a relative humidity point specific to the composition of the particle. Under these moist conditions, the water-soluble ionic salts in particles can dissociate into cations and anions, and become electrically conductive (Weschler and Shields [5]). While particle accumulation by deposition between conductors occurs on a timescale of years, the deliquescence of deposited particles can be a rapid event, on the timescale of minutes or seconds. Sudden spikes in relative humidity have the potential to induce equipment failure.

When introducing large amount of outside air, it is necessary to increase the filtration at the air handlers. With 100% recirculating systems, filters with MERV rating of 8 or 9 (ANSI/ASHRAE52.2-1999; equivalent to 40%efficient based on the older “dust spot” efficiency rating of ANSI/ASHRAE Standard 52.1-1992), as shown in figure 2.7 are typically used [37]. These filters are intended to remove only the particulates that are generated by activity within the space. When outside air is introduced, it is necessary to increase the MERV rating to 10 or 11 (equivalent to 85% efficient based on dust spot

method) so that the filters can extract the increased loading of particulates (i.e., the smaller particles) associated with construction, road highway traffic, industrial processes, and other outdoor pollutants.

In recent case studies published by Lawrence Berkeley National Laboratory (LBNL) [6], it was determined that the challenges surrounding air contaminants and humidity control can be resolved. The approach of using improved air filtration is consistent with their findings. Those studies found slightly higher particulate concentrations (gaseous contaminants were not measured) in data centers with outdoor air economizer when compared to data centers with 100% recirculation systems. For such a system, the particulate concentrations within the spaces were significantly lower than the most conservative particle standards. Result of the finding is shown in figure 2.8. The cleanliness of the indoor air, in terms of particulate content, was to be as good as or better than the cleanliness of a recirculating system with lower MERV rating. The higher MERV rating filter created a higher operating pressure at the fan, and this was associated with an increase in the use of energy. However, this extra energy use was small (1 %) in comparison to the savings associated with reduced operating of chiller plant (30 – 40 %). In conclusion, the study states that the increase in the particle concentration in system with economizers can be negated with improvements in air filtration.

Figure 2.7. MERV 8 filter used for data center air filtration

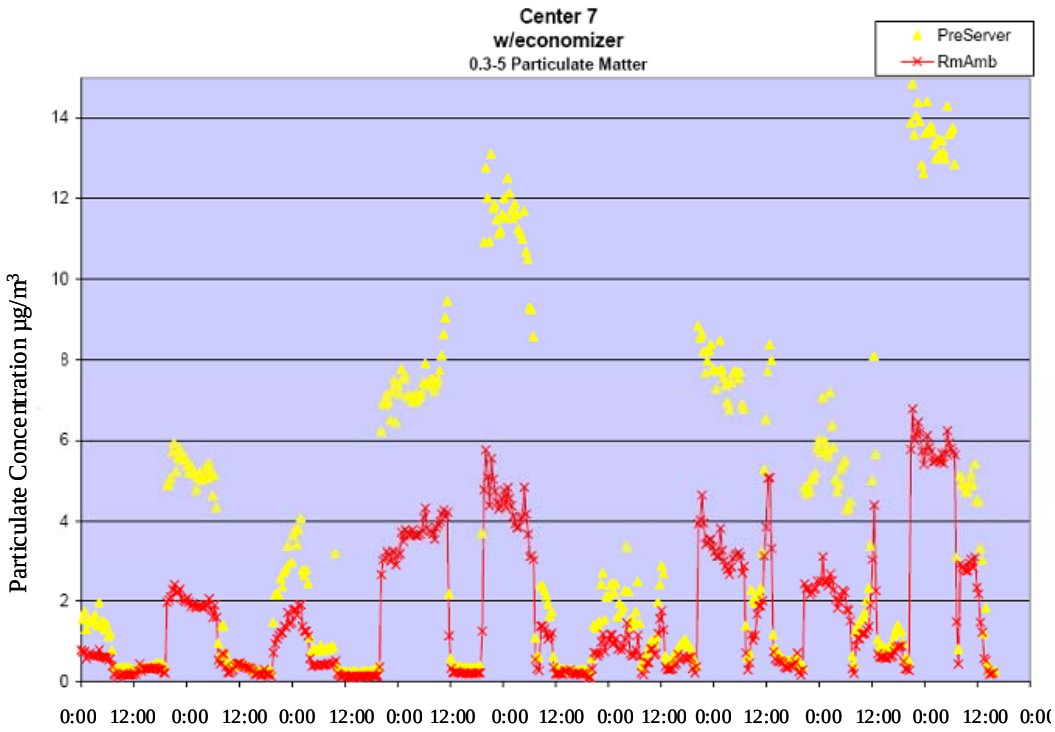

Figure 2.8. Indoor particle concentration with economizer [6]

2.2.3 Added Cost

Added cost for an airside economizer results from dampers used for closing and opening the economizer windows, improved filters, fans and humidification-dehumidification unit. Though the cost of the logic controller and sensors are independent of the economizer size, all other components' cost would depend on the size of the data centre and amount of outside air being brought into the data center space. Table 1 gives the cost of equipments that would be required for the airside economizer for the model data center being considered in the present analysis. The table gives just the equipment cost and extra cost of installation should be added which is depended on the location.

Table 1: List of equipments and their cost for airside economizer

Components	Cost Price	Source
Dampers	$2,000	www.captiveair.com
Honeywell Actuator ML8185	$500	www.americanhvacparts.com
Honeywell W7215 Logic Module	$500	www.partsbuy.com
Honeywell C7400A1004 Enthalpy sensors	$272	www.partsbuy.com
Honeywell C7835A Discharge Sensors	$300	www.air-n-water.com
Air Inlet fan	$400	www.ziehl-abegg.com
Total	$3,972	

Though the infrastructure cost is incurred during the installation of the airside economizer, the cost of humidification would be recurring and can offset the savings from the economizer depending on the location. Liebert Corporation evaluated the cost of humidification for a hypothetical data center with airside economizer [30]. Table 2 summarizes their results. The table shows the cost to humidify flow rate of 6 kg/s of outside air in New York City based on power cost of $0.10 / kWh using a canister-type

humidifier. The humidification cost is not trivial and decreases the energy savings from the economizer.

Table 2: Humidification cost for outside air in New York City

DB Temp Range (F)	<24	25-29	30-34	35-39	40-44	45-49	50-54	55-59	60-64	<64
Moisture to be Added (grains/lb)	49	46.9	42.7	38.5	34.3	28.7	21	12.6	2.8	
Hours/Year in Temp Range	387	344	512	739	791	733	770	722	776	5774
Cost to Humidify*	$457	$386	$518	$667	$629	$483	$367	$205	$48	$3,761

An adiabatic humidifier can significantly cut down the cost of humidification [46]. Adiabatic humidifiers (e.g., evaporative, wetted media) exchange sensible heat of air with the latent heat of water to accomplish evaporation at constant enthalpy. Though supplying air at the data center operating temperature would require refrigeration and would be add to the cost of energy.

2.3 Waterside Economizer

A **waterside economizer** system (often called fluid-side or simply free cooling) works in conjunction with a heat rejection loop consisting of either a cooling tower - evaporative cooler or a dry-cooler to satisfy cooling requirements. A fluid-side economizer system is typically incorporated into a chilled water or glycol-based cooling system. For economizer operation, the fluid used in the cooling system passes through an additional coil to cool the room air, eliminating the need for compressor operation.

The data center community calls the waterside economizer as a source of “free cooling”. But the cost of driving the cooling towers and other components is not free and hence it is more suitable to call it a low-cost cooling. Low-cost cooling operates on the

principle that during cold weather conditions, particularly at night, data center cooling loads can be served with chilled water produced by the cooling tower alone, entirely bypassing an energy intensive chiller. In this scenario, the cooling tower produces low temperature water. A heat exchanger is used to cool the building loop while keeping it clean and isolated from the relatively dirty cooling tower water. Low-cost cooling reduces or eliminates chiller power consumption while efficiently maintaining strict temperature and humidity requirements.

Low-cost cooling can also offer an additional level of redundancy by providing a non-compressor cooling solution for portions of the year. In particular, free cooling can often provide a backup to compressor chillers during cooler nighttime hours when plant staffing may be lower. When the weather allows, free cooling replaces the complex mechanism of a chiller with a simple heat exchanger. The schematic of a typical waterside economizer is shown in figure 2.9.

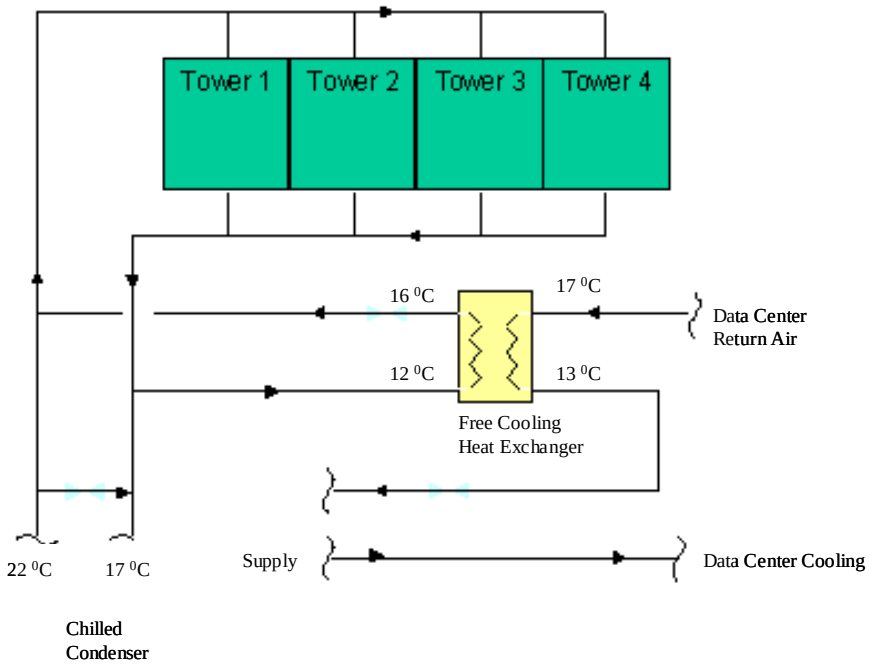

Figure 2.9. Schematic of the airflow in a data center using waterside economizer [31]

However, the return on investment for waterside economizers in data center applications has been a hard sell in most geographic areas [38]. Added costs for a waterside economizer result from increased fan power, controls, heat exchangers, and piping. Some installations also incur additional costs for additional plant floor space or an additional pump. Another challenge in implementing a waterside economizer system is accomplishing the goal of a seamless transition into and out of the economizer operational mode. In most applications today, especially where data centers and other sensitive loads are involved, this changeover needs to occur with little or no interruption of chilled water supply to the building.

Waterside economizers typically involve the use of a cooling tower and heat exchanger to generate chilled water instead of operating a chiller. In order to generate 12 ^{0}C (54 ^{0}F) chilled water, the condenser water temperature leaving the tower would have to be maintained below 6 ^{0}C (43 ^{0}F). The maximum wet bulb temperature required to achieve 6 ^{0}C (43 ^{0}F) condenser water would be in the neighborhood of 4 ^{0}C (40 ^{0}F). As the wet bulb temperature rises above 4 ^{0}C (40 ^{0}F), the economizer system loses its capability to generate 12 ^{0}C (54 ^{0}F) chilled water and its time to initiate mechanical cooling. Making the transition from economizer mode back to mechanical cooling can be precarious because most chillers require a minimum entering condenser water temperature (typically 60 ^{0}F to 65 ^{0}F) to operate properly.

2.4 Data Center Designs with Economizers – A Review

Recently, data center design with airside economizers has become an important topic of research in industry and academia [37,40]. Brandemuehl et al. [40], studied savings that could be achieved using an airside economizer in buildings. They could realize an energy saving of 6% (Denver) to 25% (Miami).

A recent report published by Rumsey Engineers in collaboration with Pacific Gas & Electric Company [34] discussed a new design of a data center with economizer. The schematic of the data center is shown in figure 2.10. A small-scale (130 m^2) data center located in a large office building was considered. Portable air conditioners were also being used to maintain control in the data center space before an airside economizer was implemented. The existing system used chilled water fed CRAC units located in the data center. During normal operating hours, a large house chilled water plant system served the space, while the dedicated chiller was used for off hour (night and weekend) cooling and backup.

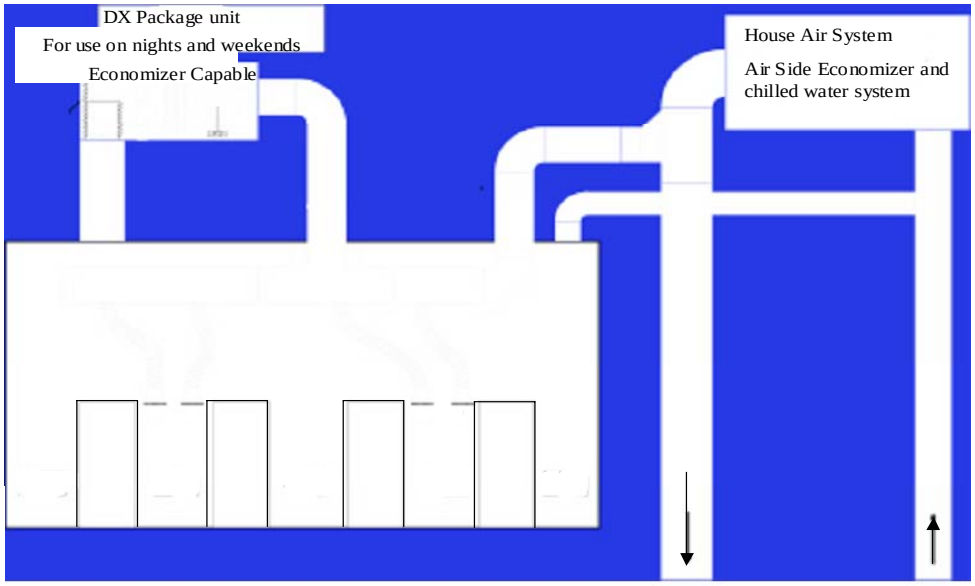

Figure 2.10. Data center converted to be use with an airside economizer [34]

An air-cooled package unit was chosen to replace both the air-cooled chiller and the associated chilled-water CRAC units. The package unit, called the DX package, included full airside economization capability. With this unit, exhaust air was ejected from one end of the air handler, while outside air was drawn in from the opposite end of the unit through louvers in the screenwall. This system had multiple benefits for the data center: it replaced the failing chiller, allowed for airside economization, and eliminated all chilled water piping from within the data center envelope. The main house air handler system, based on a large water cooled chiller plant used for just the data center space alone, was used during the day since the chilled water plant is more efficient than the air-cooled DX package unit system. This system also freed up floor space in the data center by removing the CRAC units. The removal of the CRAC units effectively enlarged the space available for computing equipment, reducing the need for costly future expansions of the space.

Sloan proposed a new design for the airside economizer system [41]. A novel approach for separating the hot aisle and the cold aisle with a physical barrier was proposed as seen in figure 2.11. The surrounding air was brought into the server room after filtration. A variable frequency drive (VFD) operated to remove the hot air from the hot aisle depending on the pressure difference between the hot and the cold aisle. The hot aisle air was either exhausted to the ambient in hot days, or was used to heat the office space in cold winter days.

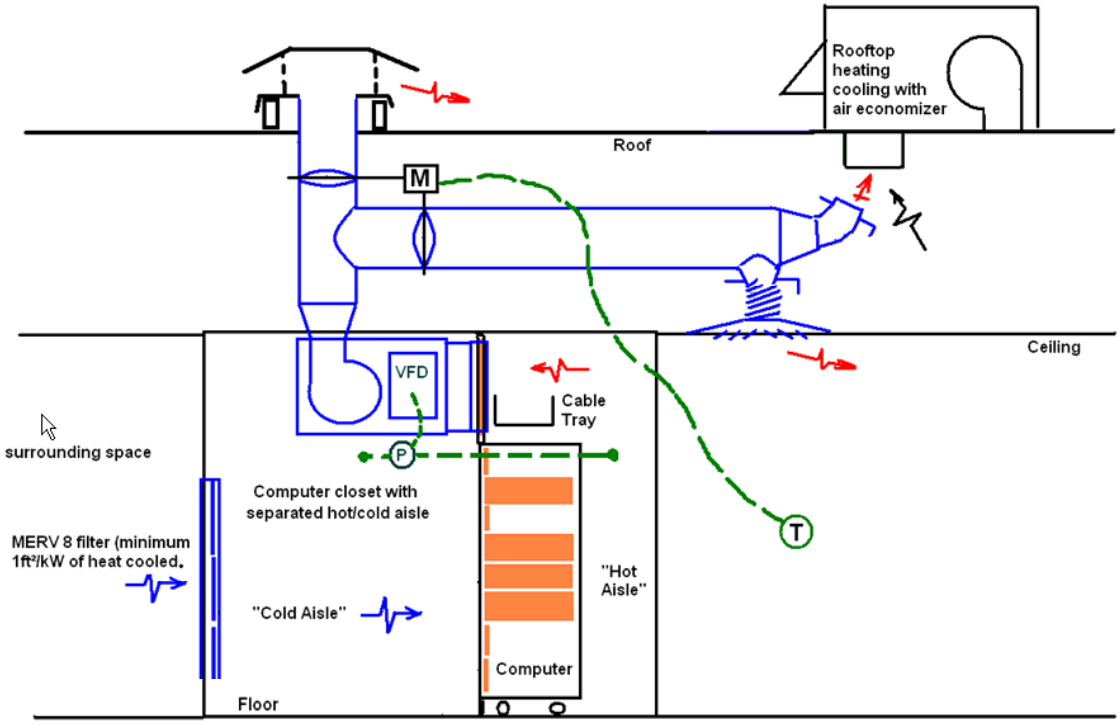

Figure 2.11. Schematic of data center with separated hot and cold aisles [41]

Intel Corp. recently reported large energy savings (40%) by implementing wet side economizers system in data centers [39]. Two cases of wet side economizers were investigated, while designing a high performance data center with a high-density engineering computer server.

Figure 2.12 shows the schematic of the data center with a wet side economizer. The system diverted condenser water cooled by cooling towers around the chillers to a heat exchanger, where it cools down the warm return water in the chilled water system to the required supply temperature. During periods when the economizer was in operation, the chillers were turned off, saving energy. The economizer still used power to operate the tower fans and circulation pumps. However, the savings were considerable (35%)

because chillers accounted for more than half the total energy consumption of the chilled water-cooling system.

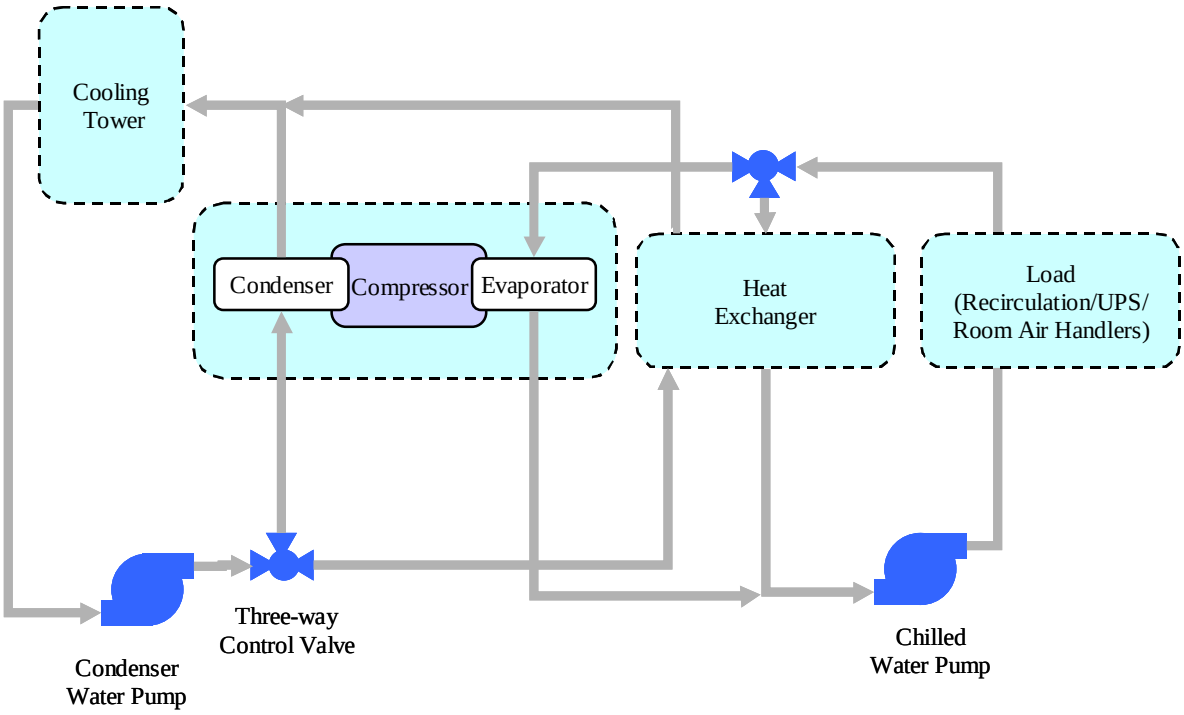

Figure 2.12. Wet side economizer used in a high-density data center [39]

In another system, the wet side economizer was decoupled from the condenser water used to reject chiller heat to cooling towers. Figure 2.13 shows the schematic of such a decoupled wet side economizer. Two isolated condenser water systems were used. The wet side economizer condenser water was used to pre-cool the data center return air. The pre-cooled air is then passed through the chilled water supply to cool the air to desired temperature. This decoupled economizer approach provided a more stable partly loaded chiller operation during spring and fall.

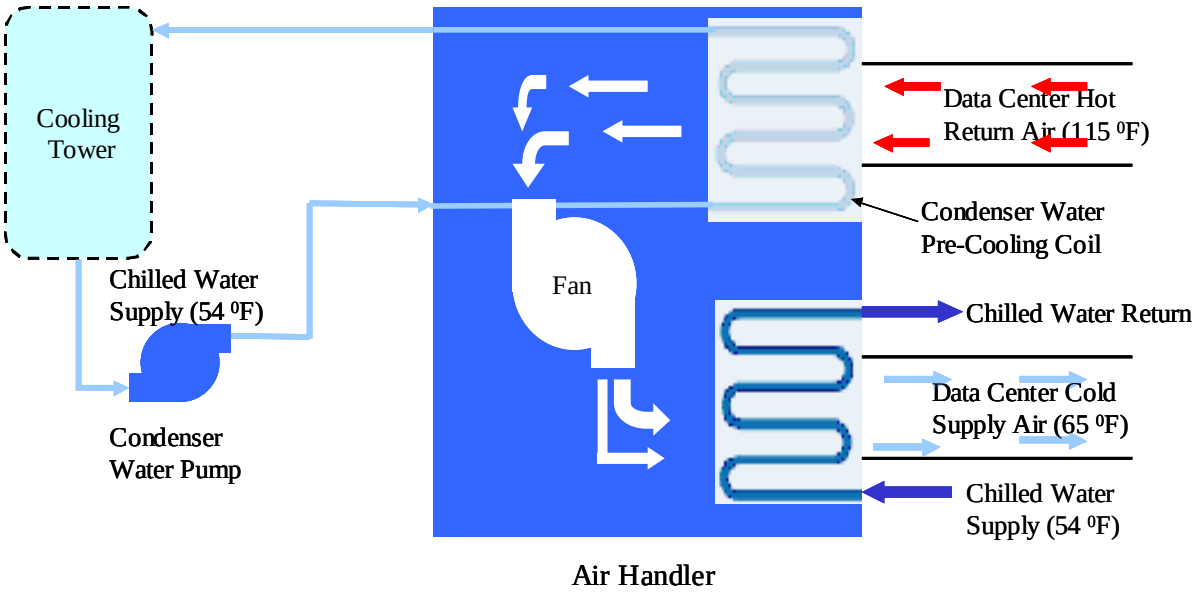

Figure 2.13. Decoupled wet side economizer system used with bladed server [39]

Figure 2.14 gives the saving achieved by implementing the economizers in a data center in terms of HVAC performance index. Energy savings up to 40% could be realized by the new design.

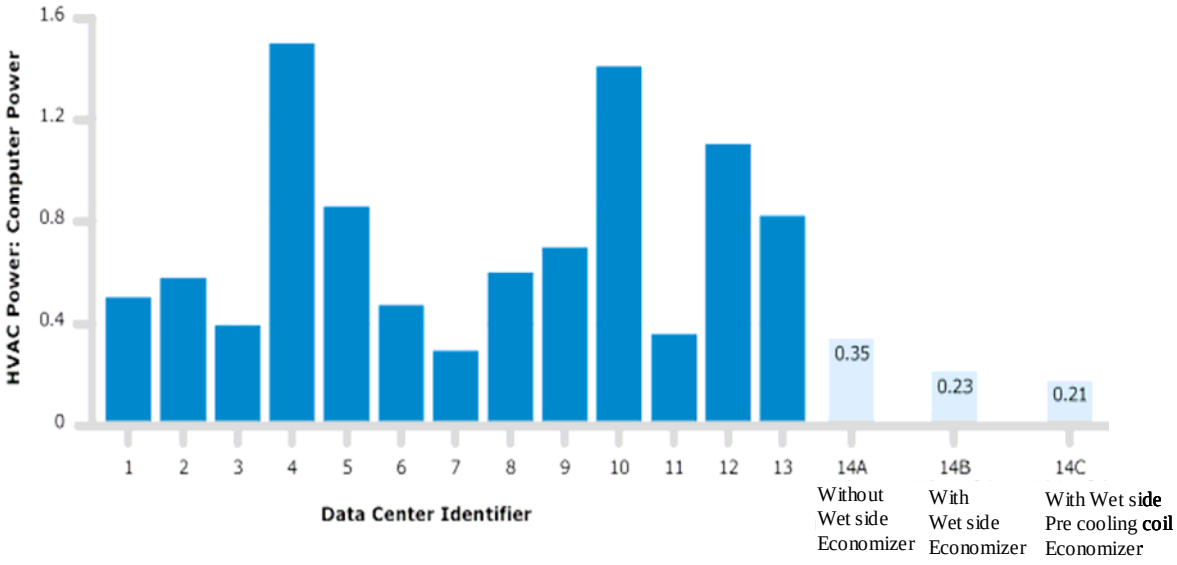

Figure 2.14. Energy saving in terms of HVAC performance index (kW_{HVAC}/kW_{UPS}) [39]

CHAPTER 3

NUMERICAL MODELING OF DATA CENTERS

Due to the complex nature of the flow inside a data center, computational fluid dynamics and heat transfer (CFD/HT) are usually required to investigate the thermal performance of data centers. The heat dissipation at the chip level, causes the temperature rise across each electronic device within each server and consequently inside the whole data center. A rack contains a number of servers, each with their power dissipation and airflow requirements. The heat rejected by the racks should subsequently be taken to the computer room air conditioning unit and cooled air is fed back into the server room.

3.1 Review of Data Center Numerical Modeling

Data center facilities are critical to the data processing needs they serve. They are designed for continuous operation in order to provide a highly reliable environment for the data processing equipment performing essential tasks and often containing highly sensitive material. Access to these environments is limited and performing detailed experimental measurements in operational data centers is difficult. Thus, most previous investigations in data center thermal management are computational in nature and rely on CFD/HT to predict airflow and heat transfer characteristics.

Patel *et al.* [8] performed computations on a model facility and Schmidt *et al.* [9] compared experimental measurements of airflow rate through raised floor data center perforated tiles with 2-dimensional computational models. The various numerical investigations can be classified into the following 4 main categories: 1) raised floor plenum airflow modeling to predict perforated tile flow rates, 2) thermal effects of rack

layout and power distribution and 3) investigation of alternative supply and return schemes and 4) development of thermal performance metrics. A review of data center literature is presented by Schmidt and Shaukatullah [10], which serve to provide a historical perspective considering the rapid growth in data center power density.

Schmidt *et al.* present a depth-averaged (2-dimensional) numerical model for a 0.284 m deep plenum [9] and for a 0.292 m deep plenum [11]. Their experimental validation shows fair overall agreement with selected tile flow rates, with large individual prediction errors. In both papers, it is noted that a 0.1 m diameter pipe and a 0.025 m tall cable tray are located in the bottom of the plenum, although there is no discussion of how these obstructions are accounted for in the depth-averaged equations. Schmidt *et al.* [11] state that for plenum depths less than 0.3 m deep, depth-averaged modeling is adequate as a tradeoff between computational cost and accuracy.

Radmehr *et al.* [12] experimentally investigated the leakage flow, or portion of total CRAC airflow that seeps through the seams of the raised floor tiles, in a 0.42 m deep facility. Distributing the leakage flow uniformly throughout the perforated tile seams and modeling chilled water supply lines, Radmehr *et al.* [12] were able to produce predictions with an overall accuracy of 90%. Van Gilder and Schmidt [13] present a parametric study of plenum airflow for various data center footprints, tile arrangements, tile porosity and plenum depth. A vacant plenum was assumed, which makes the perforated tile resistance much greater than any other flow resistance in the plenum and allows the resulting perforated tile flow rate to scale with the net CRAC flow rate.

Regarding data center rack layouts, Patel et al. [8, 14] have focused on the aisle spacing and the corresponding cooling loads on the CRAC units in conventional raised

floor plenum data centers. These efforts identify the problem of recirculation, or hot exhaust air being drawn into a cold aisle and through electronic equipment before returning to the CRAC units. Schmidt *et al.* [11, 15-17] have also documented the effect of recirculation. Geometrical optimization of plenum depth, facility ceiling height and cold aisle spacing for a single set of CRAC flow rates and uniform rack flow and power dissipation was performed by Bhopte *et al.* [18]. The results showed that increasing the plenum depth or the facility ceiling height, and decreasing the cold aisle width produce an overall reduction in the average inlet temperature to all the racks in the facility. Schmidt and Iyengar [17] have also documented thermal performance variability in several operational data centers and attempted to provide some qualitative explanations for similarly performing racks in different data centers. A cluster of high-power dissipation racks and their effect on the remaining equipment of the facility were considered by Schmidt and Cruz [16].

Each data center has a unique geometrical footprint and rack layout and a common basis is needed to compare the thermal performance of various cooling schemes. Rambo and Joshi [19] formulated unit cell architecture of a raised floor plenum data center by considering the asymptotic flow distribution in the cold aisles with increasing number of racks in a row. The results indicated that for high flow rate racks, 4 rows of 7 racks adequately models the hot-aisle cold-aisle configuration and is representative of a 'long' row of racks.

One of the earliest works in data center CFD/HT modeling analyzed a global flow configuration other than that of the standard raised floor plenum with return to the CRAC unit through the room. The model of Patel *et al.* [8] examined a cooling strategy where

the CRAC unit supply and return are located over top of the cold aisles. A novel concept of introducing cold supply air into the hot aisles to mitigate recirculation effects was proposed by Schmidt and Cruz [15] although computational results showed this modification could diminish the basic cooling scheme's efficiency. Supplying the cold air from above the racks was investigated in [20] where the overhead supply and facility height were investigated parametrically. Shrivastava *et al.* [21] parametrically vary all possible locations of the cold air supply and hot exhaust return for fixed room geometry, uniform rack power and fixed CRAC conditions.

In the previous analysis of data center airflows, researchers have either modeled the rack in a black-box fashion with prescribed flow rate and temperature rise, or as a box with fixed flow rate and uniform heat generation [8, 14, 16, 18]. This less computationally expensive approach is useful for facility quantities such as CRAC unit performance and rack layout are of interest. To characterize the performance variations through a data center, a procedure to model individual servers within each rack was developed in [22]. As far as computational limitations allow, the server sub-models can be increased in complexity to include discrete heating elements to mimic multiple components on a printed wiring board.

Rambo and Joshi [22] presented a formal modeling approach to data centers considering modeling of the CRAC units, perforated tiles and rack sub-models. This investigation considers the distribution of CRAC units through the unit cell architecture and the effect of rack orientation relative to the CRAC units. To develop a mechanistic understanding of convective processes in data centers, the global scheme was divided into the processes of 1) the CRAC exhaust to the cold aisle, 2) cold aisle distribution of

supply air through the racks and 3) the hot exhaust air return to the CRAC units [24]. Numerical modeling of various supply and return schemes, coupled with various orientations between the racks and the CRAC units, identified the causes of recirculation and non-uniformity in thermal performance throughout the data center. The models presented in [8, 14, 16, 17, 19, 25] have used a variety of orientations between the CRAC units and racks.

The performance of the assorted data center models is assessed in various ways by different authors. Sharma *et al.* [24] introduce dimensionless numbers to quantify the effects of recirculation. These dimensionless numbers are arrived at by considering the ratios (cold supply air enthalpy rise before it reaches the racks) / (enthalpy rise at the rack exhaust), and (heat extraction by the CRAC units) / (enthalpy rise at the rack exhaust). These definitions require the air temperature evaluation at arbitrary points near the rack inlet and exhaust. Sharma *et al.* [25] later computed these dimensionless performance metrics in an operational data center by taking a single air temperature measurement just below the top of each rack inlet and outlet. Norota *et al.* [26] used the statistical definition of the Mahalanobis generalized distance to describe the non-uniformity in rack thermal performance. Shah *et al.* [27-29] have proposed an exergy-based analysis method that divides the data center into a series of subcomponents and then CRAC unit operation is optimized given information regarding the rack power dissipation.

Thermal performance metrics for systems level electronics cooling based on the concept of thermal resistance (power dissipation / temperature rise) were formulated and applied to data centers in [22]. The metrics consider the spatial uniformity of thermal performance to characterize poor designs causing local hot spots. Entropy generation

minimization was also proposed as a data center thermal performance metric because poor thermal performance is often attributed to recirculation effects. Since the mixing of hot exhaust air with the supply air in the cold aisles generates entropy, cold aisle entropy generation minimization was employed as a metric.

The use of economizer in the data center has caught the attention of the data center designers and researchers in recent years. Lawrence Berkeley National Laboratory performed extensive experiments on data centers to monitor the effect of outside air particulate contamination on inside space of data centers using airside economizers [1]. They found the contamination level well within the acceptable limits with modest improvement in the filtration system. Liebert Corporation published a white paper on effective utilization of economizers in data center [30]. They found that using glycol-based fluid economizer systems are a good choice to help reduce data center cooling costs, decrease energy usage and provide efficient, economical heat dissipation in a wide range of outdoor temperature and humidity conditions.

Pacific Gas and Electric Company published a design guideline scorebook for high performance data center [31]. They extensively looked at the all the options to improve the data center efficiency including airside and waterside economizers. They demonstrated a total energy saving of 45% (254,000 kWh/yr) on a model data center using airside economizer. A recent publication in ASHRAE journal by Sorell [32] gives a good summary of the issues and solution that designers have faced in the past. The hours available for the use of economizer for different locations based on 68 ^{0}F supply air were also provided.

This thesis examines at a model data center with airside economizer. Whenever the conditions are favorable, i.e. when the outside air temperature is lower than the return air temperature, the outside air is brought into the data center space. A full-scale three-dimensional model of the data center is developed and numerical simulations are carried out to quantify the energy saving of the CRAC units.

3.2 Data Center Model

The model of the data center used for the analysis is shown in figure 3.1. The model data center cell is approximately 110 m^2 (11.68 m x 9.43 m x 3.0 m) facility with 28 racks arranged in 4 rows of 7, as it adequately models the hot-aisle cold-aisle configuration and is representative of a 'long' row of racks [17]. The 7 racks of each row are combined to form a single computing unit. The rows are spaced 1.22 m apart to represent a pair of 2 ft x 2 ft perforated tiles. The walls of the data center are assumed to be adiabatic. Also the plenum wall (connecting the plenum and the server room) is considered adiabatic. The plenum is considered not to have any blockages.

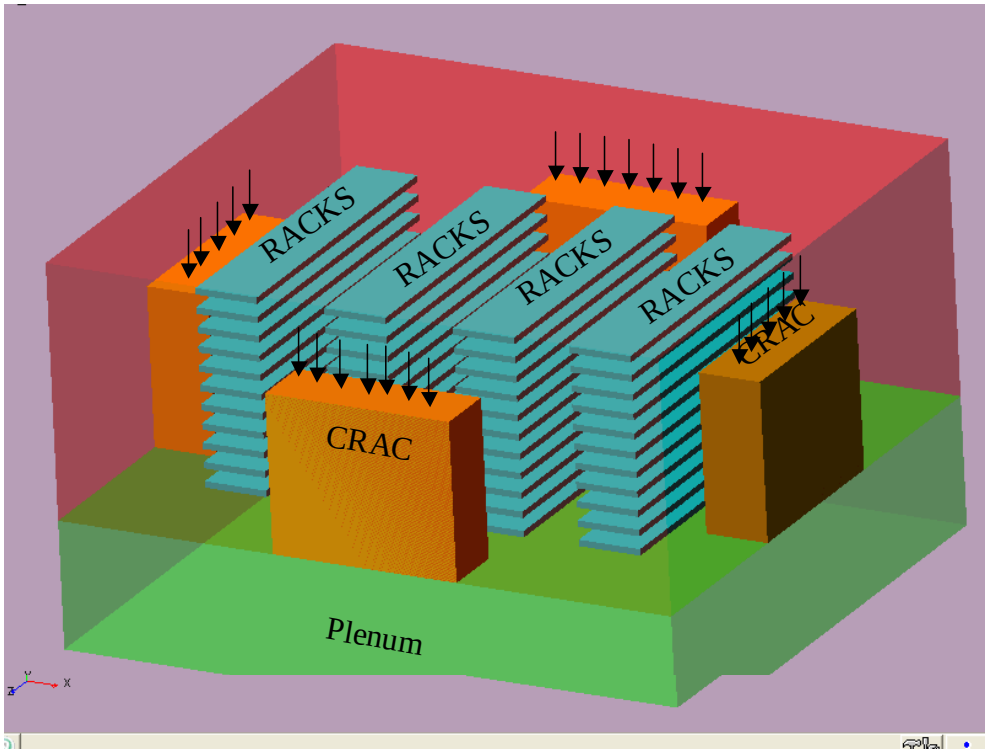

Figure 3.1. Data Center Model

4 CRAC units (approximately 3.0m x 0.9m 1.8m), modeled after the Liebert Deluxe System/3 [7] are placed symmetrically about the facility. These CRAC units output 15 ^{0}C air at the flow rate of approximately 5.7 m^{3}/sec based on the pressure velocity relation given by equation 1, which goes into the plenum before being brought to the facility through the cold aisles. The nominal capacity of each CRAC unit is 95 kW. The CRAC units, placed 1.22 m from the racks to preserve symmetry, feed a 0.83 m deep plenum of the same size of the facility. Each of the 28 racks dissipates 4.23 kW, giving the data center power density of 1076 W/m^{2}. The heat load is uniformly distributed between various racks (4.23 kW per rack). The pressure-velocity relationship for the

induced draft fan was based on cubic polynomial fit to the fan curve of a Papst series 6440 axial fans, given by

$$p(u) = 112.4 - 27.428u + 2.561u^2 - 0.102u^3 \quad (1)$$

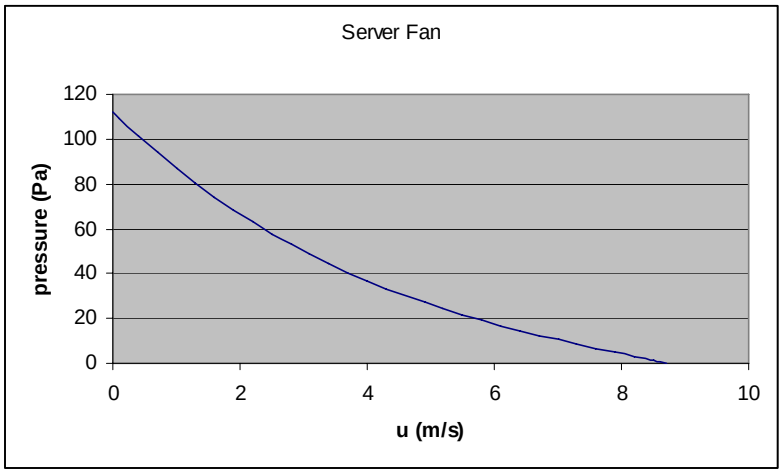

Figure 3.2. Server fan pressure velocity relation

The data center heat transfer computations are modeled as three-dimensional forced convection, taking the buoyancy effect into account. The computation model assumes a steady state of operation with constant heat production from the racks and air circulation through the cooling system (CRAC). Data center layout with the airside economizer system is shown in figure 3.3. There are three main objectives of the proposed design: (1) to utilize the outside air whenever the outside environment temperatures are favorable, (2) to exhaust the hot air from the hot aisle directly to the ambient to minimize the load on the chillers and (3) to make sure the outside air which is brought into the server room does not interfere with the inlet air to the server.

To achieve these targets, the opening for the cold air to be brought into the data center space is directly above the cold aisles, built on the ceiling of the data center.

Similarly, to exhaust the hot air from the server room the hot air outlet is directly above the hot aisle, built on the ceiling.

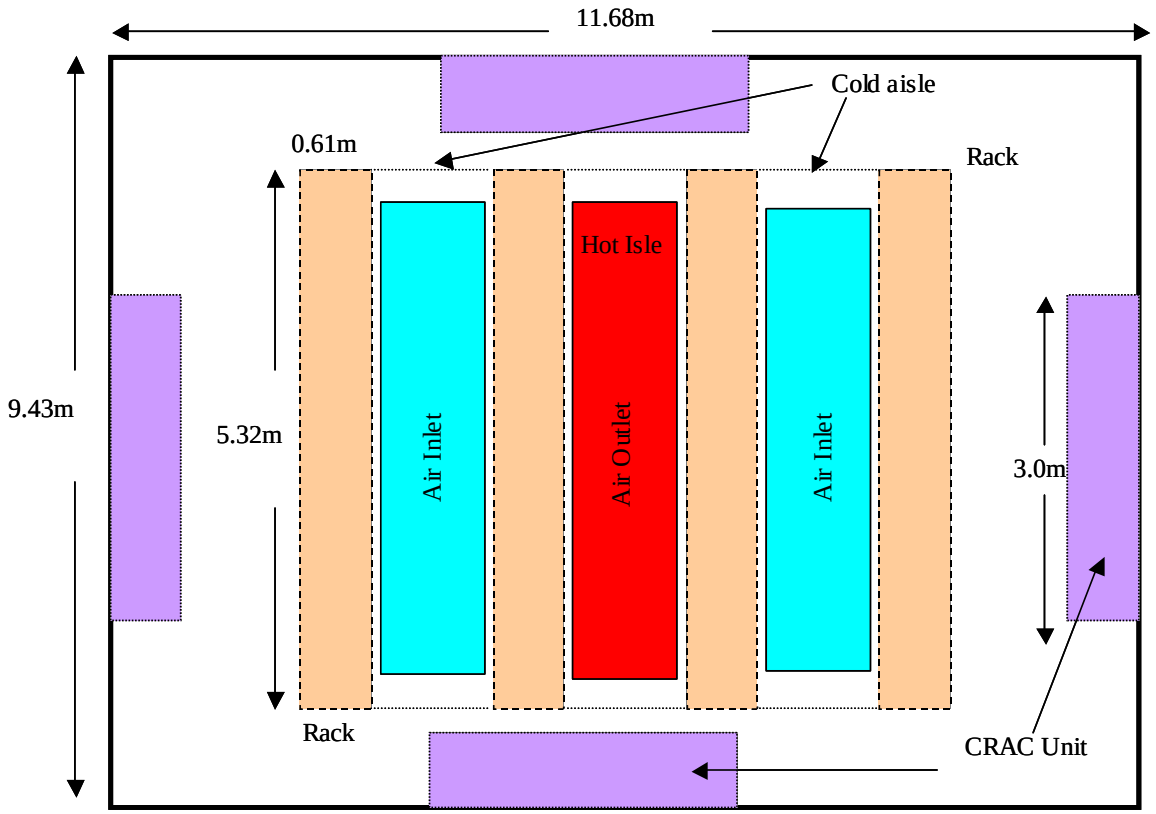

Figure 3.3. Top view of the data center with airside economizer system

The cold air, which is brought into the data center, has temperatures lower than the bulk temperature of the air in the data center space. This air mixes with the space air, and is fed to the CRAC unit. The hot air from the hot aisle, instead of being recirculated through the CRAC unit is made to leave the data center space into the ambient.

Figure 3.4 shows the server room with the airside economizer system with intended flow pattern. The design helps to minimize flow recirculation as well as any hotspot formation. The actual flow pattern is of the air inside the data center is dicussed in section 4.1

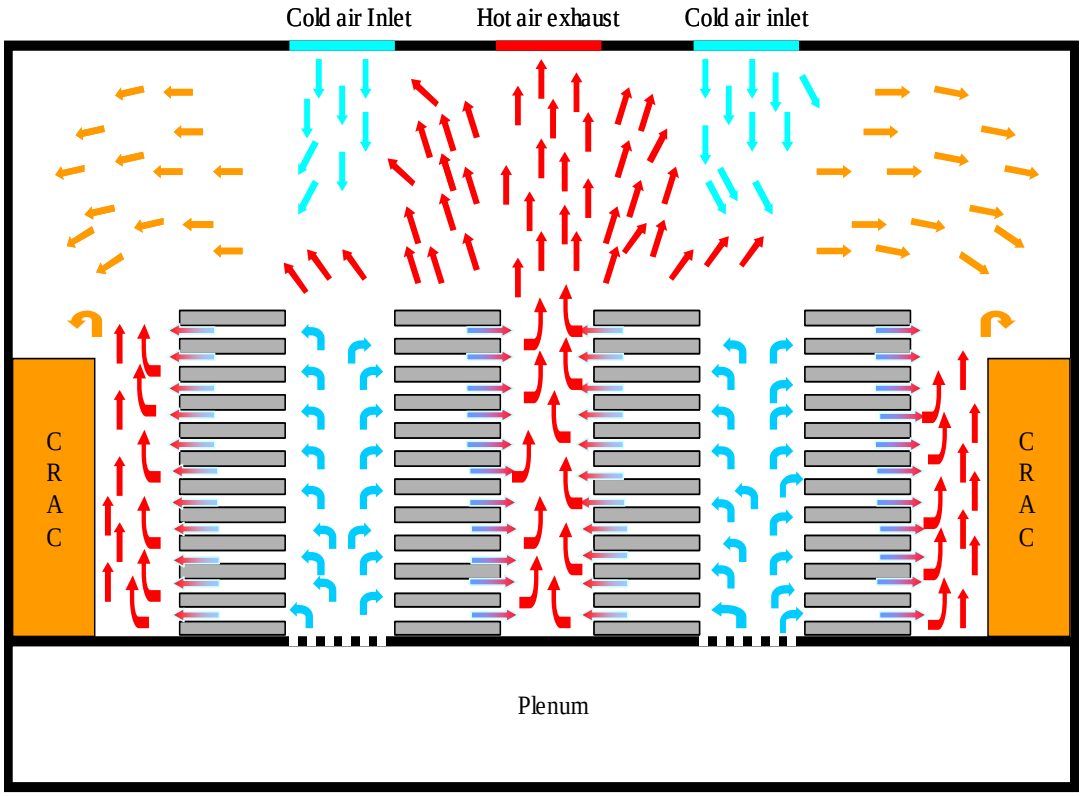

Figure 3.4. Flow pattern inside the data center with economizer

3.3 Governing Equations

The basic assumptions for the CFD / HT simulation include a three-dimensional, fully turbulent, non-isothermal, incompressible flow. The industry standard for turbulence simulation, k-ε model is used because of its robustness at a relatively low computational cost. The transport equations for incompressible turbulent flow in tensor notation take the following form [48].

3.3.1 Continuity Equation

$$\frac{\partial(\rho u_i)}{\partial x_i} = S_m \tag{2}$$

The mass source term S_m is added to or removed from the continuous phase due to evaporation or condensation of the liquid droplets, which is not considered in the present case and hence is set to zero.

3.3.2. Momentum equation

The Reynolds-averaged Navier-Stokes equations governing the flow take the form:

$$\frac{\partial\left(\rho u_i u_j\right)}{\partial x_j} = \frac{\partial p}{\partial x_i} + \frac{\partial}{\partial x_j}\left[\mu\left(\frac{\partial u_j}{\partial x_i} + \frac{\partial u_i}{\partial x_j}\right)\right] + \frac{\partial\left(-\rho\overline{u_i' u_j'}\right)}{\partial x_j} + f_j \tag{3}$$

The Reynolds stresses $\rho\overline{u_i' u_j'}$ are related to the mean velocity gradients by employing the Boussinesq hypothesis:

$$\rho\overline{u_i' u_j'} = \mu_t\left(\frac{\partial u_j}{\partial x_i} + \frac{\partial u_i}{\partial x_j}\right) \tag{3}$$

where μ_t is the turbulent viscosity defined as

$$\mu_t = \rho C_\mu \frac{k^2}{\varepsilon} \tag{4}$$

with

$$k = \frac{1}{2}\overline{u_j' u_i'} \tag{5}$$

and

$$\varepsilon = \nu\overline{\frac{\partial u_i'}{\partial x_j}}.\overline{\frac{\partial u_i'}{\partial x_j}} \tag{6}$$

The Boussinesq model was employed for the calculation of the buoyancy force, f_j. The local density variation is defined as

$$\rho' = \rho[1-\beta(T-T_{ref})] \tag{7}$$

Calculation of the turbulent kinetic energy, k, and dissipation rate, ε, requires two additional partial differential equations that contain four unknown coefficients in addition to C_μ of eq. (4). The two additional partial differential equations take the form:

$$\frac{\partial}{\partial x_j}(\rho k u_i) = \frac{\partial}{\partial x_j}\left[\left(\mu + \frac{\mu_t}{\sigma_k}\right)\frac{\partial k}{\partial x_j}\right] + G_k + G_b - \rho\varepsilon \tag{8}$$

$$\frac{\partial}{\partial x_j}(\rho \varepsilon u_i) = \frac{\partial}{\partial x_j}\left[\left(\mu + \frac{\mu_t}{\sigma_k}\right)\frac{\partial \varepsilon}{\partial x_j}\right] + C_{1\varepsilon}\frac{\varepsilon}{k}(G_k C_{3\varepsilon} G_g) - C_{2\varepsilon}\rho\frac{\varepsilon^2}{k} \tag{9}$$

In Eqs. (8) and (9), the terms G_k and G_b are the generation of turbulent kinetic energy due to mean velocity gradient and buoyancy and could be described as follows:

$$G_k = -\rho\overline{u_i' u_j'}\frac{\partial u_j}{\partial x_i} \tag{10}$$

and G_k is evaluated in a manner consistent with the Boussinesq hypothesis:

$$G_k = \mu_t S^2 \tag{11}$$

where S is the modulus of the mean rate-of-strain tensor, defined as

$$S = \sqrt{2S_{ij}S_{ij}} \tag{12}$$

The buoyancy effect takes the form

$$G_b = \beta g_i \frac{\mu_t}{\mathrm{Pr}_t}\frac{\partial T}{\partial x_i} \tag{13}$$

where the coefficient of thermal expansion, β, is defined as

$$\beta = -\frac{1}{\rho}\left(\frac{\partial \rho}{\partial T}\right)_p \tag{14}$$

The constants in the above equations take the following values:

$C_{1\varepsilon} = 1.44$

$C_{2\varepsilon} = 1.92$

$C_{\mu} = 0.09$

$\sigma_k = 1.30$

$\mathrm{Pr}_t = 0.85$

The degree to which ε is affected by the buoyancy is determined by the constant $C_{3\varepsilon}$. This constant is calculated according to the following relation:

$$C_{3\varepsilon} = \tanh\left|\frac{v}{u}\right| \tag{15}$$

where *v* is the component of the flow velocity parallel to the gravitational vector and *u* is the component of the velocity perpendicular to the gravitational vector. In this way, $C_{3\varepsilon}$ becomes 1 for buoyant shear layers for which the main flow direction is aligned with the direction of gravity. For buoyant shear layers that are perpendicular to the gravitational vector, $C_{3\varepsilon}$ becomes zero.

3.3.3. Energy Equation

For the temperature distribution calculations, the energy equation can be written as:

$$\frac{\partial}{\partial x_j}[u_i(\rho E + p)] = \frac{\partial}{\partial x_j}\left[\left(\lambda + \frac{c_p \mu_t}{\mathrm{Pr}_t}\right)\frac{\partial T}{\partial x_j} - \sum_j h_j J_j\right] + S_h \tag{16}$$

where λ is the thermal conductivity of the fluid, J_j is the diffusion flux of species *j*, and S_h is any volumetric energy source, which is set to zero in the present case. The term *E* in the previous equation is defined as follows:

$$E = \sum_j h_j Y_j + \frac{u^2}{2} \tag{17}$$

where sensible enthalpy *h* is defined for ideal gases as:

$$h_j = \int_{Tref}^{T} c_{pj} dT \tag{18}$$

and *Yj* is the mass fraction of species *j*.

3.3.4. Species Transport Equation

The species transport equation of water vapor into air is written in the form:

$$\frac{\partial}{\partial x_j}[\rho Y_{H_2o} u_i)] = \frac{\partial}{\partial x_j}\left[\left(\rho D_{H_2o} + \frac{\mu_t}{Sc_t}\right)\frac{\partial Y_{H_2o}}{\partial x_j}\right] + S_{H_2o} \tag{19}$$

where S_{H_2o} represents the water vapor added to or removed from the air due to evaporation or condensation. Since there is no vapor added or removed in the domain of calculation (as CRAC is not modeled for numerical simulation), this term is set to zero. The constant D_{H_2o} is the diffusion coefficient of water vapor into air, which is equal to 2.88x 10^{-5} m^2/s; Sc_t is the turbulent Schmidt number, which is equal to 0.7.

3.3.5 Relative Humidity Calculation

The Relative Humidity (RH) is the ratio of the actual water vapor pressure to the saturation water vapor pressure at the prevailing temperature. RH is usually expressed as a percentage rather than as a fraction as is given by

$$RH = p/p_s*100 \tag{20}$$

Where saturation vapour pressure, p_s, in Pa is calculated as

$$p_s = 610.78 *\exp(t / (t + 238.3) *17.2694) \tag{21}$$

where t is the temperature in Celsius

Relative humidity can be converted to water vapor concentration as kg_w/kg_{da} and is used in calculations in above equation as species mass fraction. If the total atmospheric pressure is P and the water vapor pressure is p, the partial pressure of the dry air component is P - p**.** The weight ratio of the two components, water vapor and dry air is:

$$\text{kg water vapor / kg dry air} = 0.018 * p / (0.029 *(P - p)) \quad (22)$$

$$= 0.62 * p / (P - p)$$

At room temperature P - p is nearly equal to P. Hence,

$$Y_{H2O} = \text{kg water vapour / kg dry air} = 0.62 * 10^{-5} * p \quad (23)$$

3.3.6 Fan Power Calculation

As the economizer operates, large quantity of air is required to be brought into the data center space from outside. This would require a fan to operate at the inlet of the economizer to achieve the required mass flow rate. In the model data center, the mass flow rate of the air being brought into the data center was fixed at 3.95 kg/s at each inlet of the economizer giving a total mass flow rate of 7.9 kg/s. The selected flow rate ensures that the low at the inlet of the server is not affected by bringing the outside air into the data center space for the model data center being considered. Density of the air coming through the cold air inlet of the economizer is assumed to be constant at 1.225 kg/m^3. Hence the volume flow rate

$$V = \text{Mass flow rate / Density } (m^3/s) \quad (24)$$

This gives a volume flow rate of 3.22 m^3/s or 6832 ft^3/min (CFM) for each inlet. A fan has to be selected, which can deliver the required flow rate. One of such fans that suit the requirement is RM56D series fan manufactured by Ziehl-AbeggAG Company. The pressure flow characteristic of the fan and operating point are given in figure 3.5.

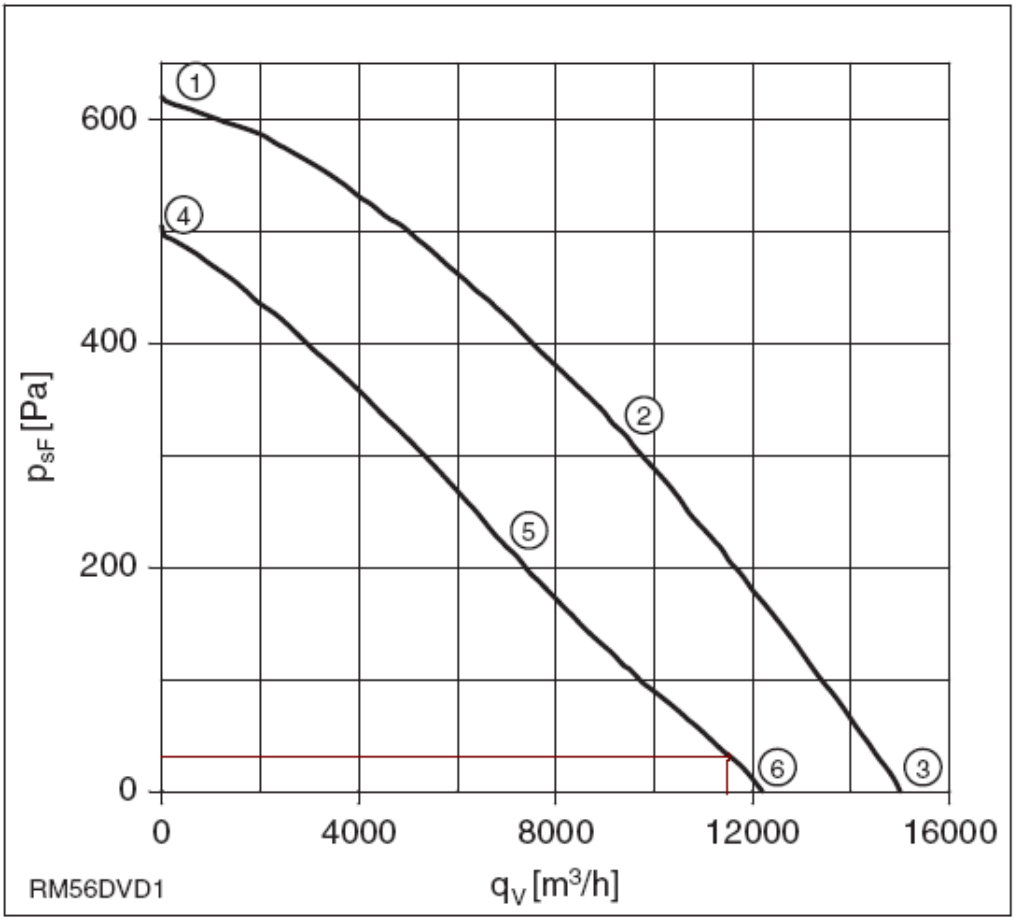

Figure 3.5: Fan characteristics (pressure –flow curve) of the air inlet fan and operating point

The selected fan has a blade diameter of d = 0.407 m. Hence the flow velocity can be calculated as

$$v = V/(\text{fan area}) \quad (m/s) \tag{25}$$

Using the equations 24 and 25, the velocity of air at the exit of the fan is 24.78m/s. The static pressure drop Δp at this velocity is 30 Pa. The efficiency η of the fan is given to be 86%. Hence the power P required for each fan is given by

$$P = (CFM*PSI*746)/(229/\eta) \quad (W) \tag{26}$$

Equation 22 gives a fan power of 750.5 W. For the two fans being used for cold air inlet, the fan power would be 1501 W. Since, in all cases a constant mass flow rate of

the inlet air from the economizer is maintained, the energy savings from the economizer should be reduced by the fan power, which would be constant (1501 W).

3.3.7 Humidification and Dehumidification Power

Humidification and dehumidification requirement of the CRAC units is determined by (1) the RH level to be maintained in the data center space, and (2) the amount of energy and moisture intake at the inlet. Since it is necessary to maintain the server inlet at the ASHRAE's recommended level, moisture must be removed or added to the air as and when required as the outside air being brought into the data center is not necessarily within the range. If dehumidification is required, moist air should be cooled to a temperature below its initial dew point. For humidification, moisture is added to the supply air at the inlet of the CRAC and then cooled to operating temperature of the data center.

Assumptions

1. Area averaged temperature was considered at the inlet and outlet of the CRAC units for property calculations
2. Area averaged mass flow rate of water vapor was considered to calculate the mass fraction at the inlet and outlet of the CRAC units
3. For humidification, moisture was assumed to be added as saturated water vapor at the inlet temperature of the CRAC units
4. During dehumidification, air was cooled to final air temperature before the outlet of the CRAC unit
5. All properties are calculated using psychrometric table provided in ASHRAE Handbook, 2005

6. The refrigeration cycle was assumed to be 100% efficient

The steady-flow energy and material balance equations for dehumidification process [47] are

$$\dot{m}_{da} h_1 = \dot{m}_{da} h_2 + q_1^2 + \dot{m}_w h_{w2} \tag{27}$$

$$\dot{m}_{da} W_1 = \dot{m}_{da} W_2 + \dot{m}_w \tag{28}$$

Thus,

$$\dot{m}_w = \dot{m}_{da} (W_1 - W_2) \tag{29}$$

$$q_1^2 = \dot{m}_{da} [(h_1 - h_2) - (W_1 - W_2) h_{w2}] \tag{30}$$

Similarly for humidification, assuming steady state operation, the governing equations are

$$\dot{m}_{da} h_1 + \sum \dot{m}_w h_w - q_1^2 = \dot{m}_{da} h_2 \tag{31}$$

$$\dot{m}_{da} W_1 + \sum \dot{m}_w = \dot{m}_{da} W_2 \tag{32}$$

Where

$\dot{m}_{da}$ - mass flow rate of dry air (kg/s)

$\dot{m}_w$ - mass flow rate of vapor (kg/s)

h - specific enthalpy of moist air (kJ/kg)

W - humidity ratio of moist air (kg_w/kg_{da})

q_1^2 - rate of addition/withdrawal of heat (kW)

3.3.8. Power Consumption Calculations

With the economizer running, the power consumption of the CRAC units would be lower. The power consumption by the entire data center comprises of three significant components, namely, the humidification/dehumidification power, the cooling power and

the fan power. The fan power calculation is discussed in last section. To calculate the cooling power, power consumption of the case with no humidification or dehumidification was considered. To calculate the humidification power, cooling power was subtracted from the total power (excluding the fan power).

Figure 3.6 shows the states on a schematic psychrometric chart through which the air undergoes during humidification at different stages in the CRAC unit. At the inlet to the CRAC unit, the air is at state 1 as shown in figure. Due to humidification, the enthalpy and the moisture ratio of the air rises and it reaches state 2. Now the air is cooled to operating temperature of the data center with constant humidity ratio to reach state 3, which is supplied to the data center space.

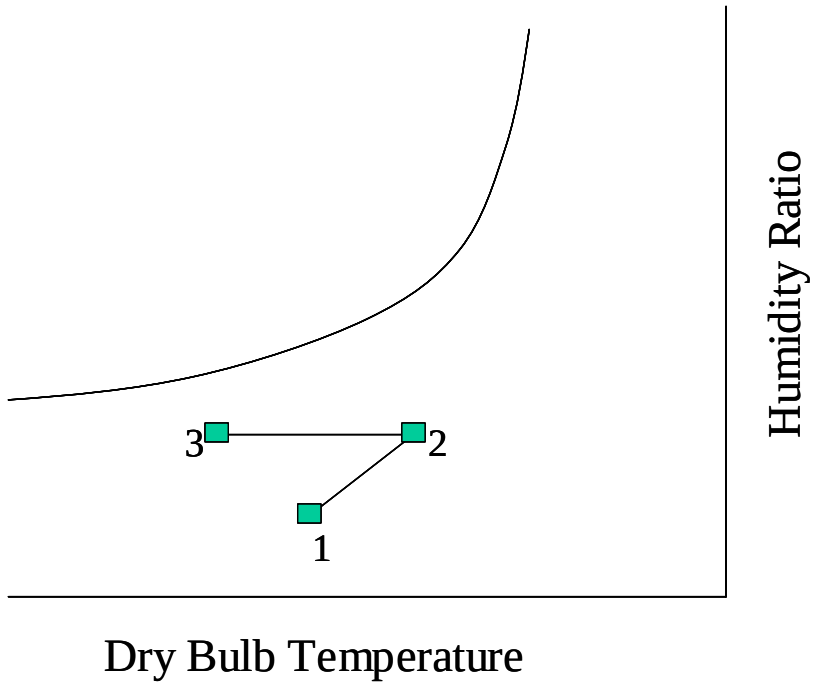

Figure 3.6: Schematic psychrometric chart for humidification

Similarly, figure 3.7 shows the states on a schematic psychrometric chart through which the air undergoes during dehumidification at different stages in the CRAC unit. At the inlet of the CRAC unit, the air is at state 1 as shown in figure. The air then goes through a dehumidifier, during which the moisture ratio and enthalpy of the air go down and it reaches stage 2. Now the air is cooled to operating temperature of the data center with constant humidity ratio to reach state 3, which is supplied to the data center space.

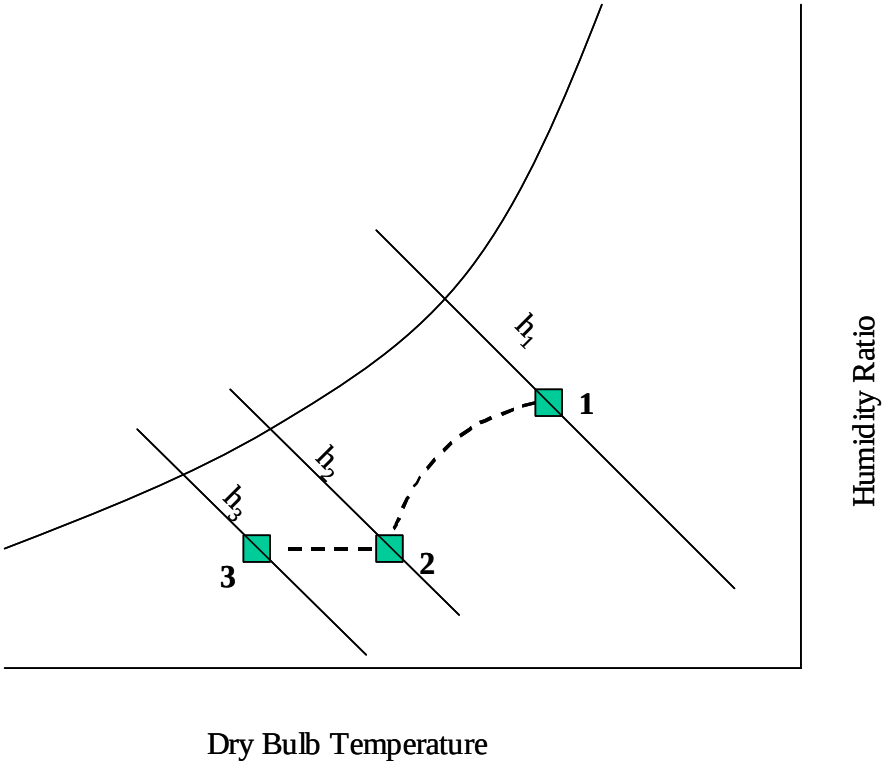

Figure 3.7: Schematic psychrometric chart for dehumidification

3.3.9 Boundary Conditions

Table 3 gives the list of boundary conditions used for simulation in all cases. The CRAC unit is not included in the flow calculation and is used for exit of air from the data center (from the top surface) and supply of cold air to the plenum (at the bottom surface). Initially (before the economizers start operating), the data center space was assumed to be at 15 ^{0}C and RH of 55%.

Table 3: List of boundary conditions used for simulation

Components	Flow	Thermal
Data Center Walls	Wall	Adiabatic
Plenum Walls	Wall	Adiabatic
CRAC		
Top	Outflow	-
Bottom	Velcity inlet (3.5 m/s)	Air at 15 ^{0}C, 55% RH
Sidewall	Wall	Adiabatic
Racks		
Sidewalls	Wall	Adiabatic
Bottom	Wall	Adiabatic
Top	Wall	228 W/m^2
Exit	Fan	-
Economizer Opening		
Cold Air Inlet	Velocity inlet (1 m/s)	Ait at outside temperature and RH
Hot Ait Outlet	Outflow	-

3.4. Model Validation

To build confidence in the modeling method, it is important to validate the model under realistic but well-defined boundary conditions. Experimental results for humidity variation inside a data center are not available in the literature. So, a one-to-one model validation is not possible. But a similar situation of humidity variation occurs in buildings as the HAVC adds or removes moisture from the room to maintain a desired comfort level.

Künzel, Zirkelbach and Sedlbauer [33] studied the indoor temperature and humidity condition including hygrothermal interactions with the building envelope. They developed a combined model, which takes into account moisture sources and sinks inside a room, diffusion and vapor ab- and desorption as a response to the exterior and interior climate conditions, as well as the well-known thermal parameters. Finally, they validated the model with experiments done in controlled environment. Their experimental results are used to validate the simulation methodology by building model of a room similar to the test room and using same boundary conditions. The experiments were carried out in a building erected on the IBP test site in the 80s designed for energy investigations. The ground plan of one of the test rooms and the adjacent spaces is plotted in figure 3.8. The room had a ground area of 20 m^2 and a volume of 50 m^3. They were well insulated (200 mm of polystyrene) towards the ground. In order to avoid moisture flow to or from the ground, the floor had a vinyl covering. The exterior surfaces of the ceiling and partition walls faced the external conditioned space. The external walls consisted of 240 mm thick brick masonry with 100 mm exterior insulation. Special care was taken to make the

separate rooms as airtight as possible. In the room where the experiment was done, the walls and ceiling of the room were rendered moisture inert by sealing them with aluminum foil. Since the envelope of the test room had no sorption capacity due to the aluminum foil it was be used to determine the moisture buffering effect.

The HVAC system of the room continuously moves the air and avoids any stratification. The indoor air temperature and humidity were measured at several levels above the floor. Temperature sensors and heat flux meters were also fixed to the interior surface of external walls.

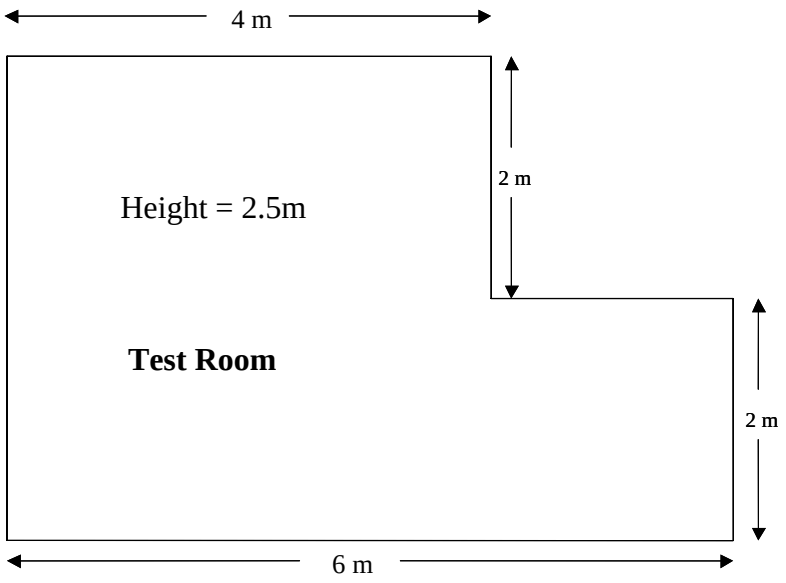

Figure 3.8. Test room plan layout [33]

The test was done with a constant air change rate (ACH) of 0.5 h^{-1}, which is the hygienic minimum rate according to German regulations. The indoor air temperature in the middle of the room was kept above 20 °C. The moisture production was derived from an average moisture load of 0.004 kg/m^3. In reality the production rate will not be

constant over the whole day. Therefore a basic production rate of 0.0005 kg/m³h was assumed with peaks in the morning and in the evening, i.e. 0.008 kg/m³h from 6 AM to 8 AM and 0.004 kg/m³h from 4 PM to 10 PM every day as demonstrated in Figure 3.9. For validation of the model, only 6 hours (from 6 AM to 12 PM) of data was considered.

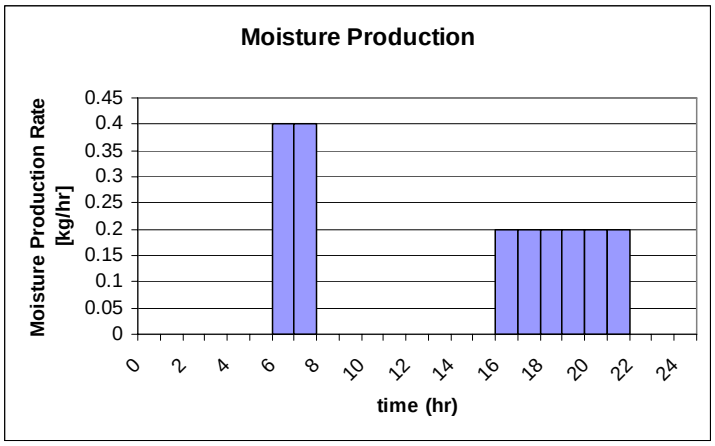

Figure 3.9. Diurnal moisture production pattern in the test room

The average humidity measurement was taken at the horizontal mid plane of the room. The test data and the simulation results show a close match for the for the humidity measurements. Figure 3.10 shows the plot of comparison between the test data and the simulated results. The humidity fluctuations are greatest during the peak load in the morning where the indoor humidity rises from 35% to over 80% which represents an increase of nearly 50% RH.

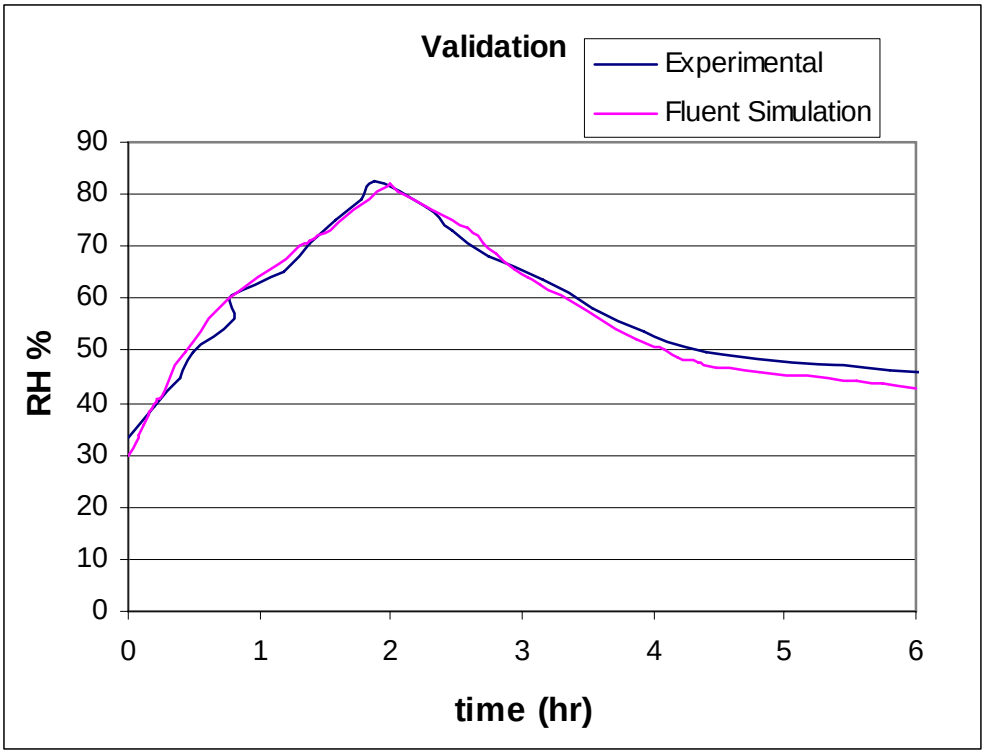

Figure 3.10. Simulated and measured evolution of the indoor air humidity in the test room

CHAPTER 4

RESULTS

4.1. Comparison With Baseline Case (Without Economizer)

A baseline case was considered where no economizer was assumed. This case helps us understand the temperature variation when economizer is implanted. One key aspect to investigate is the temperature variation throughout the rack. The case uses uniformly dissipating racks, each containing the same number of boards, which dissipate heat uniformly in the vertical direction. Figure 4.1 shows the variation of maximum air temperature on the outer racks with and without economizer.

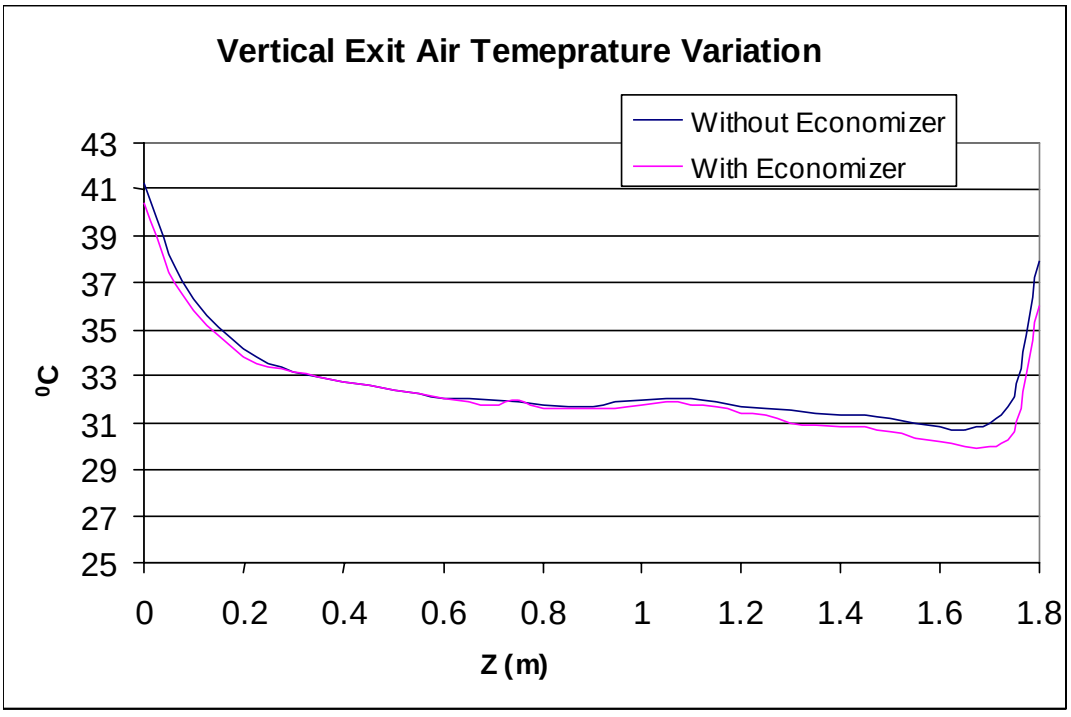

Figure 4.1. Vertical maximum exit air temperature variation throughout the rack

The plot shows a significant variation in temperature throughout the racks. Since all racks have same dissipation, these trends must be attributed to flow rate effects. High temperature near the base was observed due to lower flow rate across the racks and high temperature near the top was observed due to hot air recirculation. The results for the base case agrees with the trends presented in [42] and [43], which examine the effect of flow rate and recirculation on the exit air temperature of the racks.

The rack exit air temperature with the economizer was found to be lower than that without the economizer. This is attributed to the fact that the hot air is recirculated inside the data center space without the economizer as shown in figure 4.2. Instead, in the data center with airside economizer, the hot air is removed from the hot aisle and fresh air is added to the data center space which minimizes the effect of hot air recirculation as shown in figure 4.3. Since the flow rate through the hot aisle is higher than the outflow through the hot air outlet of the economizer, some recirculation would still be present.

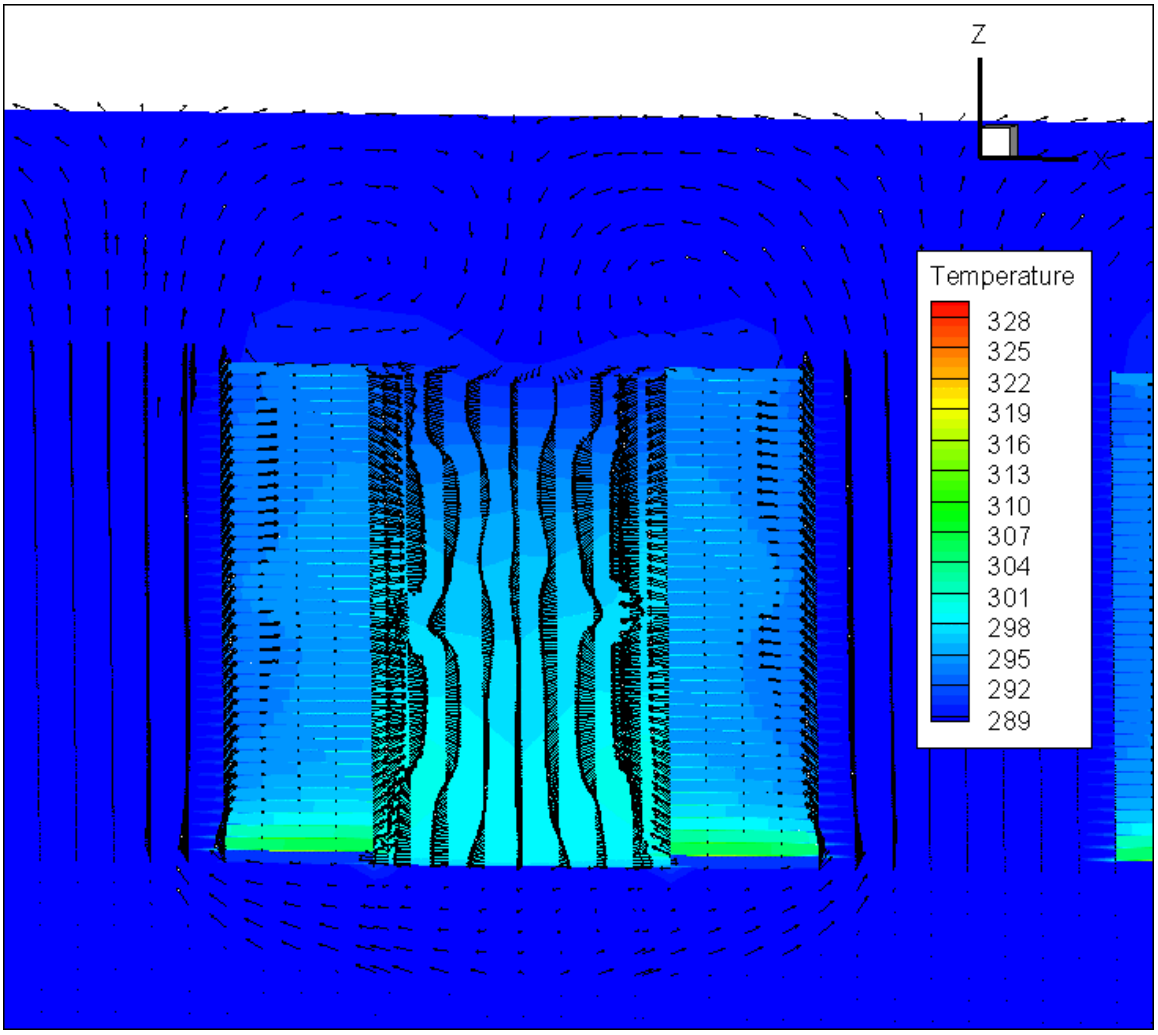

Figure 4.2. Velocity vector plots at the vertical (x-z) mid-plane superimposed on temperature (K) plot; airflow recirculation near the top in the data center without economizer

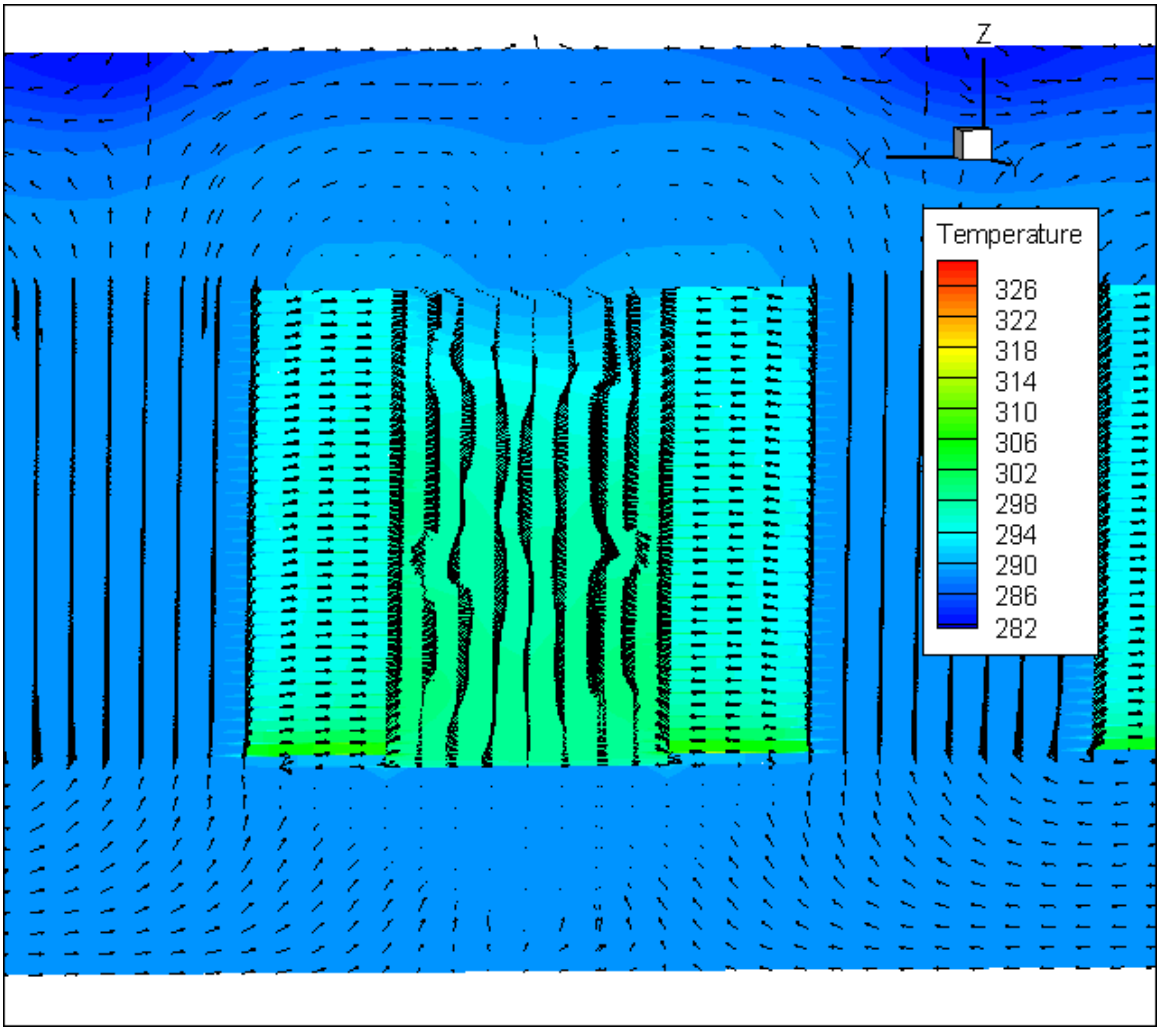

Figure 4.3. Velocity vector plots at the vertical (x-z) mid-plane superimposed on temperature (K) plot; reduced airflow recirculation in the data center with economizer

4.2 Results for Economizer Energy Savings

To evaluate the savings from the implementation of the economizer system to the data center, four locations worldwide were considered. The locations chosen represent hubs of growing energy demand. The locations considered are:

- Atlanta
- New York
- Seattle
- Shanghai

The data for the environmental factors, temperature and humidity, is available from the Russian Meteorology Department website http://meteo.infospace.ru. The website stores data for over 5,000 locations over the world. The temperature and humidity data used for simulations have been monthly averaged for three years, 2004-2007. The plot in figure 4.4 shows the variation of the temperature and humidity of Atlanta over the month of January along with the mean for illustrative purpose.

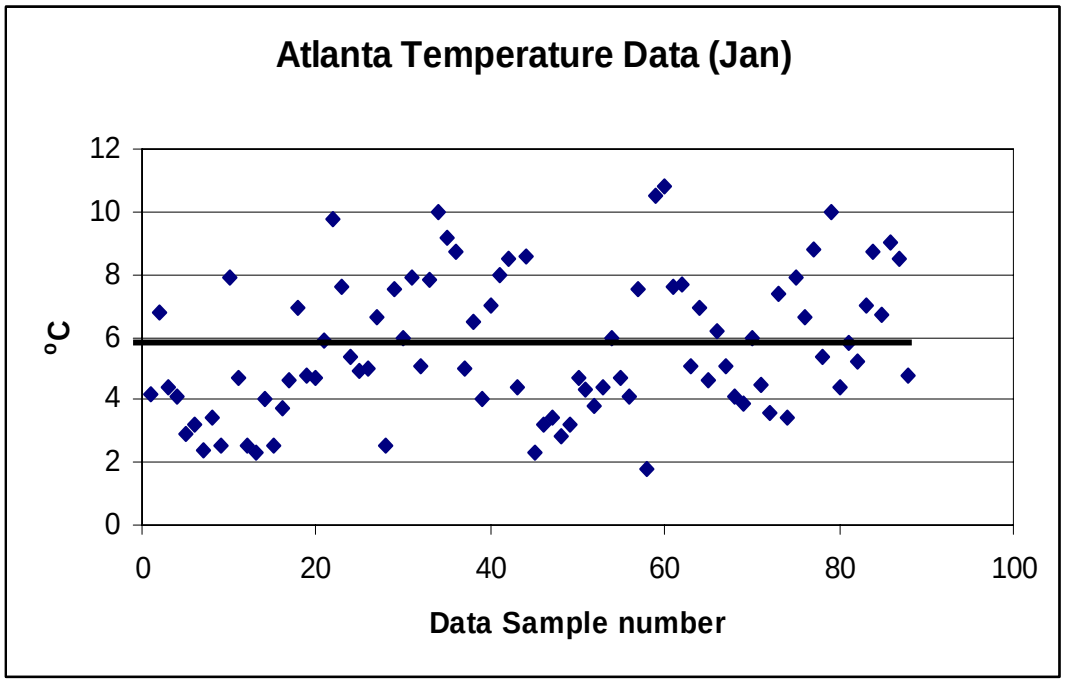

(a)

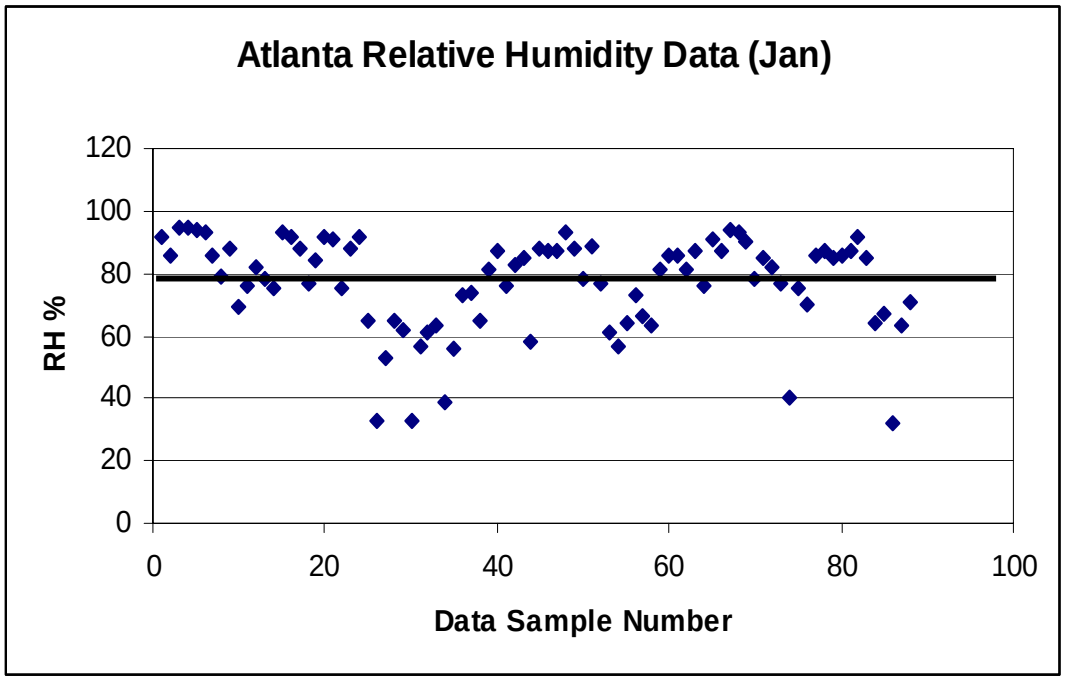

(b)

Figure 4.4. Atlanta a) temperature and b) relative humidity plot for the month of January

4.2.1. Results for Atlanta

Table 4: Weather data (temperature and humidity) for Atlanta

Month	Average Outside Temerature (^{0}C)	Average Outside Humidity (RH %)
January	5.9	79
February	8.2	77
March	12.4	77
April	16.4	79
May	21.0	82
June	24.9	84
July	26.7	88
August	26.1	89
September	22.9	88
October	17.1	84
November	11.9	82
December	7.4	80

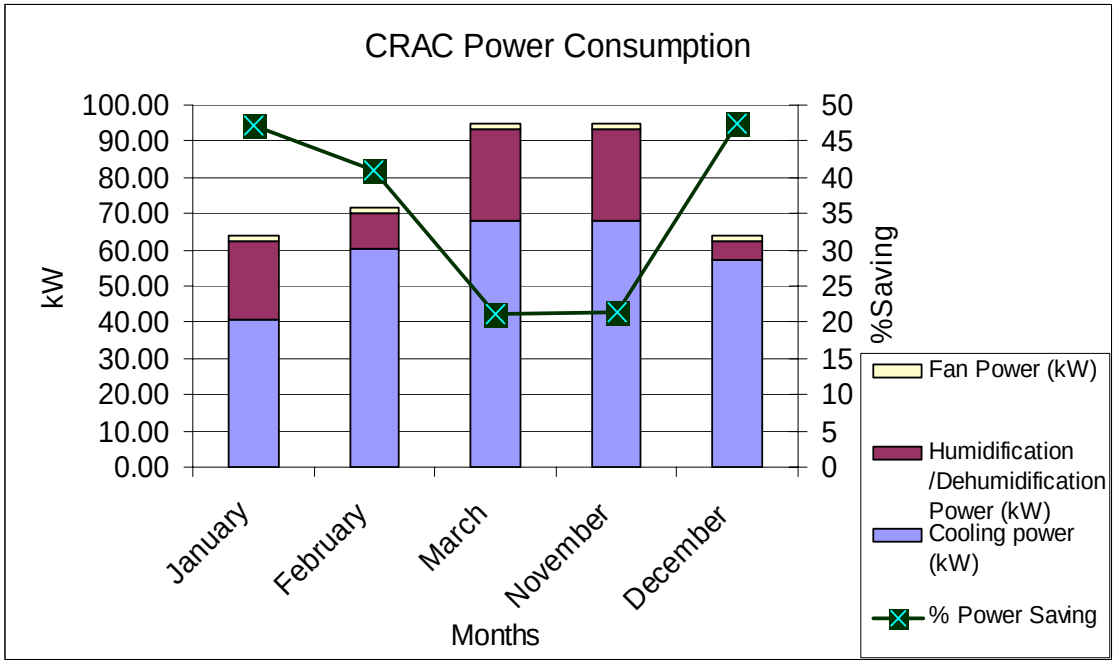

Figure 4.5: CRAC power consumption for various months in Atlanta and percentage energy savings

Energy saving for Atlanta that can be achieved during different months of the year using the economizer in terms of the CRAC power is plotted in figure 4.5. The figure shows different components that need power, namely cooling, humidification /dehumidification and fan when economizer is operating. The percentage energy savings from the baseline power consumption of 118.4 kW is shown on the secondary axis.

Not all months were found to be suitable for the use of economizers. Five months during which the outside temperature falls below the data center operating point, could be used for economizer. The figure shows that though the power of fan is small (1% of the heat load), the power required for humidification or dehumidification could be significant (21% of the heat load). Hence, this power must not be ignored when calculating the energy savings from the economizer. Maximum energy saving of 47% could be realized in Atlanta in the month of January. Rather than waiting until the outside air temperature falls below the supply air temperature set point, the integrated economizer should open when the outside air temperature falls below the economization set point, which for data centers is ideally the current return temperature.

Similar plots of the power consumptions and energy savings can be seen in figure 4.6,4.7 and 4.8 for Seattle, New York and Shanghai respectively. Different levels of saving can be achieved for different months and different locations depending on climate and humidity levels. Energy savings as high as 80% could be realized in month of January in New York where only power consumption is due to humidification requirement and fan power. Actual tables used for the plotting the savings are given in Appendix B.

4.2.2. Results for Seattle

Table 5: Weather data (temperature and humidity) for Seattle

Month	Average Outside Temerature (^{0}C)	Average Outside Humidity (RH %)
January	5.3	82.0
February	6.6	81.0
March	8.3	83.0
April	10.5	84.0
May	15.7	84.0
June	16.2	83.0
July	18.6	82.0
August	18.9	84.0
September	16.3	87.0
October	11.9	88.0
November	7.8	85.0
December	5.2	83.0

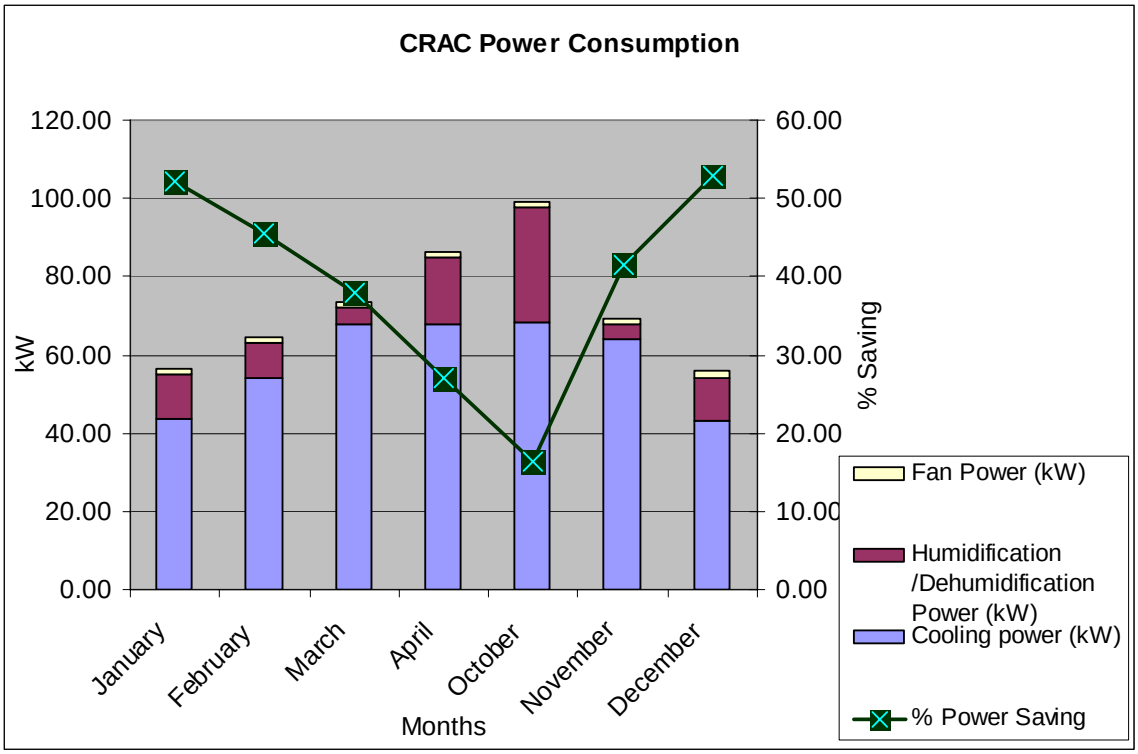

Figure 4.6: CRAC power consumption for various months in Seattle and percentage energy savings

4.2.3. Results for New York

Table 6: Weather data (temperature and humidity) for New York

Month	Average Outside Temerature (^{0}C)	Average Outside Humidity (RH %)
January	-0.1	71
February	0.8	71
March	4.9	71
April	10.1	70
May	15.4	73
June	20.4	75
July	23.8	75
August	23.4	78
September	19.6	80
October	13.6	78
November	8.2	76
December	2.9	72

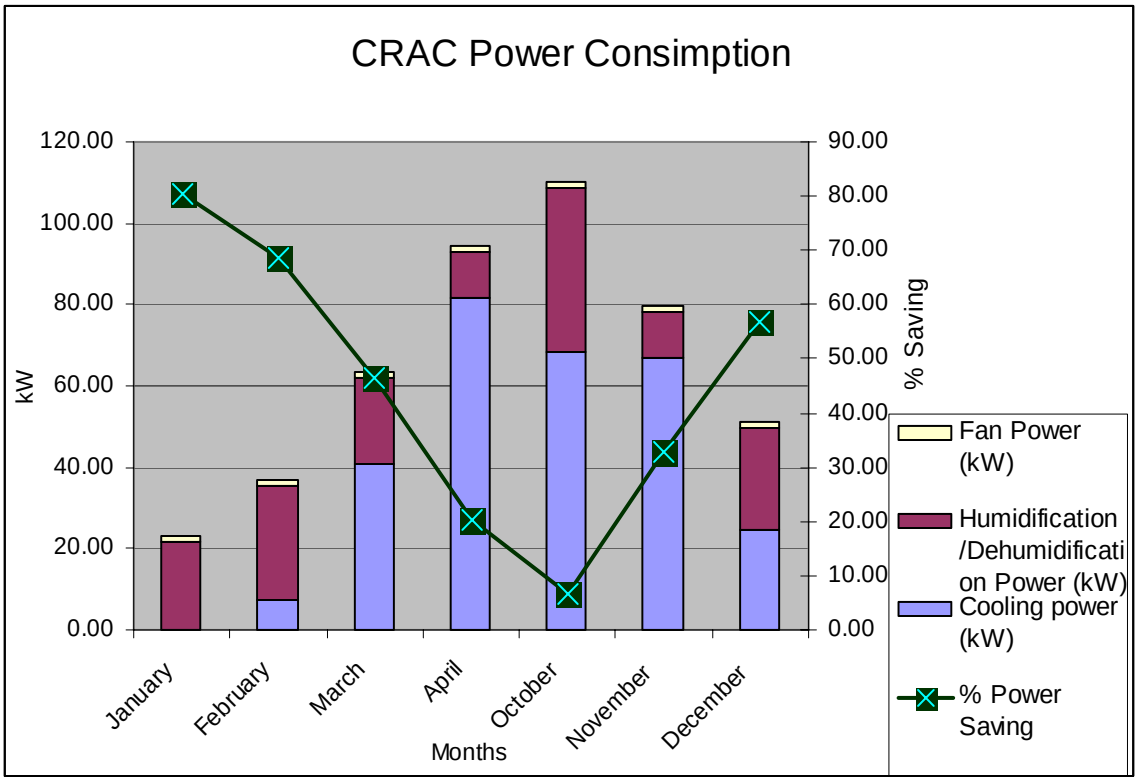

Figure 4.7: CRAC power consumption for various months in New York and percentage energy savings

4.2.4. Results for Shanghai

Table 7: Weather data (temperature and humidity) for Shanghai

Month	Average Outside Temerature (^{0}C)	Average Outside Humidity (RH %)
January	3.9	74.1
February	7.1	81.9
March	10.1	76.7
April	15.9	80.9
May	20.1	77.5
June	24.8	76.3
July	29.7	76.1
August	29.4	73.5
September	26.3	73.2
October	18.8	70.2
November	14.1	75.3
December	6.6	68.6

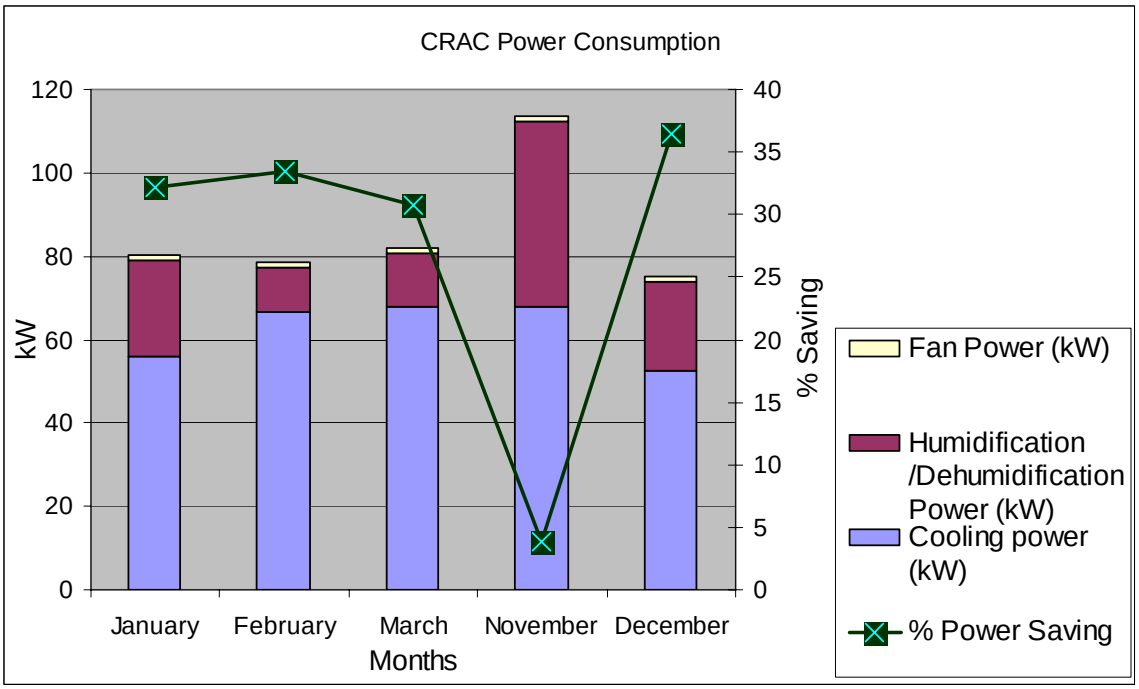

Figure 4.8: CRAC power consumption for various months in Shanghai and percentage energy savings

4.2.5. Temperature contour

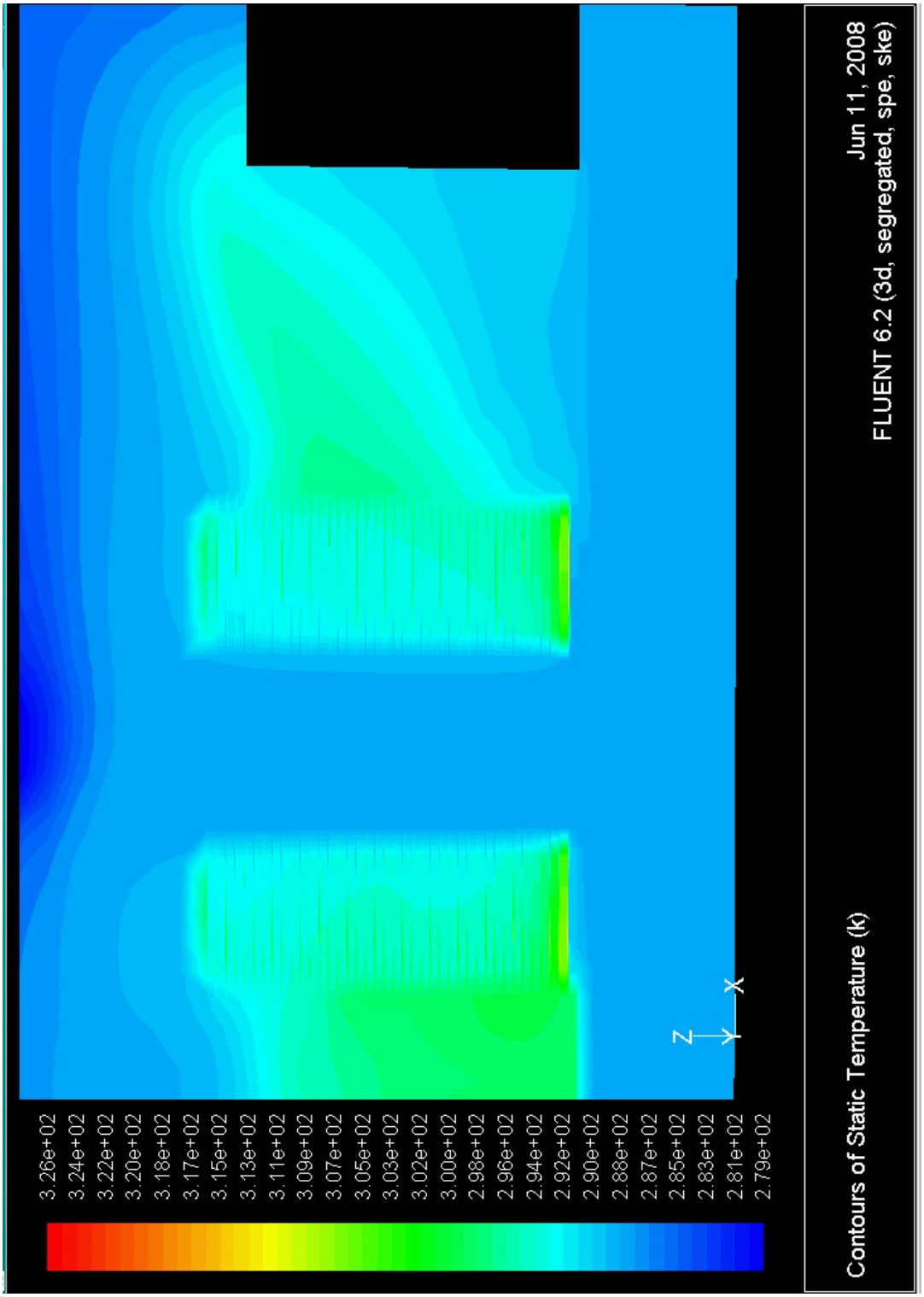

Figure 4.9. Temperature plot through the vertical (x-z) mid plane for the month of January inside the data center in Atlanta

Figure 4.9 shows the temperature variation of the air inside the data center space in vertical mid-plane. Only half the plane is plotted because of symmetric boundary conditions. CRAC units supply cold air at 15 ^{o}C to the plenum, which is fed to the data center space in the cold aisles. The draft fans on the server direct the airflow over the racks, which pick up heat from the servers. Higher temperatures are observed near the base of the racks, as the airflow rate is lower resulting in lower convective heat transfer coefficient. The two openings at the roof are used to bring hot air from the outside into the data center space. This air is much colder (depending on the outside air temperature) and mixes with the data center air, which is at a higher tempertaute, and hence the bulk temperature of the air inside the data center comes down. This mixed air is the directed towards the CRAC units, which cool it down further to the data center operating temperature. The hot air rising from the hot aisle is exhausted from the hot air outlet on the roof.

4.2.6. Relative Humidity contour

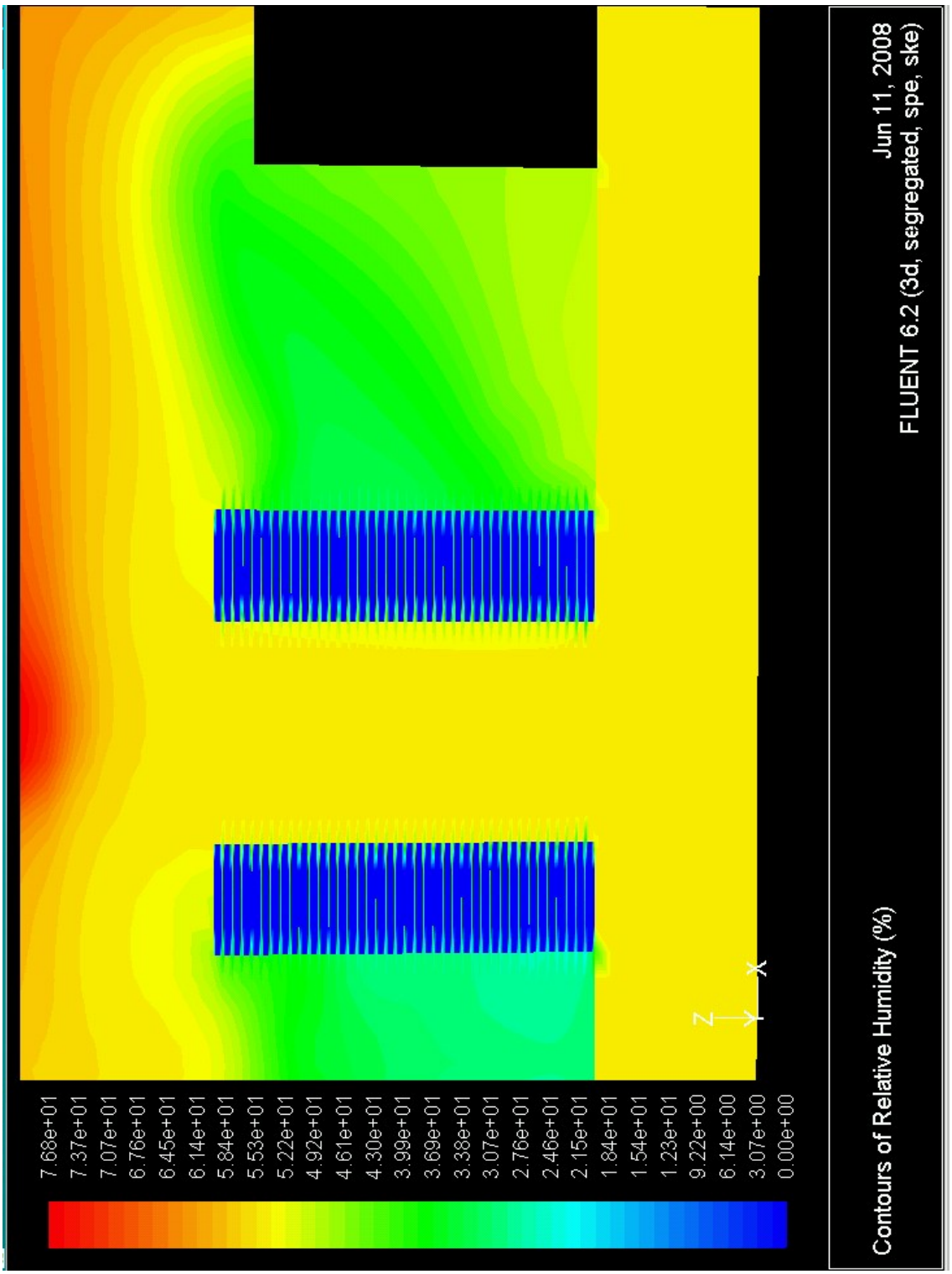

Figure 4.10. RH plot through the vertical mid plane for the month of January inside the data center in Atlanta

CRAC units supply air with 55% RH to the plenum which is fed to the data center space. When this passes over the racks, the temperature of the air goes up and hence the relative humidity decreases. Outside air with relative humidity higher than ASHRAE recommended level is brought into the server room. Even thought the humidity of the air is higher than the recommended level, RH at the “inlet” of the server is not disturbed. The outside air mixes with the data center space air and goes through the CRAC unit. In the CRAC unit, humidification or dehumidification takes place to control the moisture so that the air is within ASHRAE recommended region.

Similar plots for temperature and relative humidity can be plotted for other months of the year and other locations. The plots are provided in Appendix A.

4.2.7. Mass Fraction of water vapor contour

The relative humidity depends on the temperature and does not give a clear picture of humidification or dehumidification requirements. Instead of looking at the relative humidity, which is a function of temperature, a better idea of the humidification requirement can be obtained from absolute humidity plots. For illustrative purpose, three different seasons in the city of New York are considered. Mass fraction of water vapor in the outside air is plotted in figure 4.11 month of January to represent a cold dry weather.

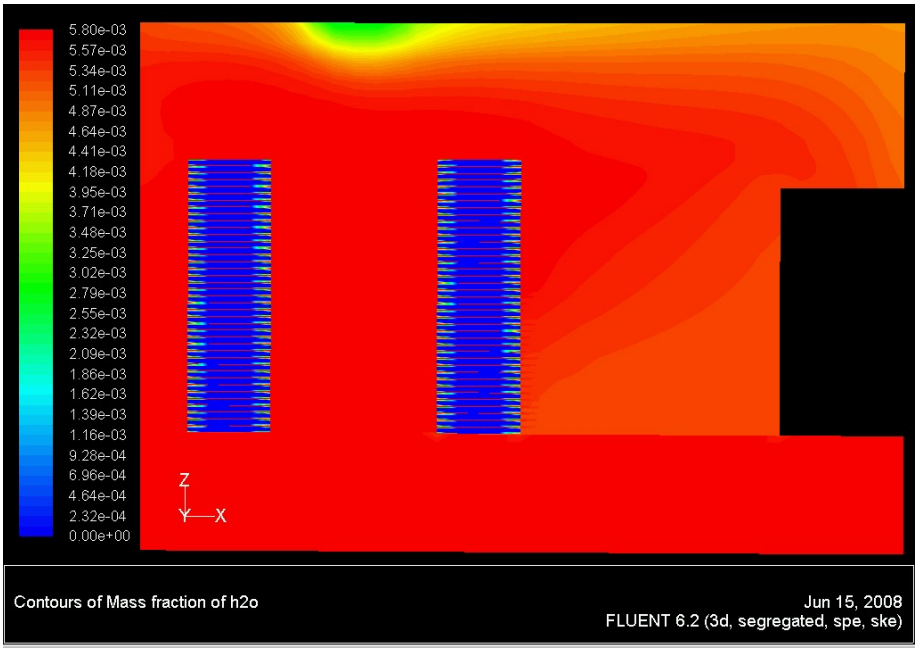

Figure 4.11 Mass fraction of water vapor in the month of January in New York

The plot shows that average humidity of the air lower than the data center space and hence humidification would be required. But even though the humidity of the incoming air is lower than the recommended humidity level, it does not disturb the flow near the inlet of the racks.

Figure 4.12 shows the plot of mass fraction of water vapor in the month of April, which represents the month of spring season. The plot shows the humidity of the outside air is in the near vicinity of ASHRAE recommended region and hence the humidification requirement would be minimal. This can be seen in the energy saving plots that the energy required to replenish the water vapor in data center space is small.

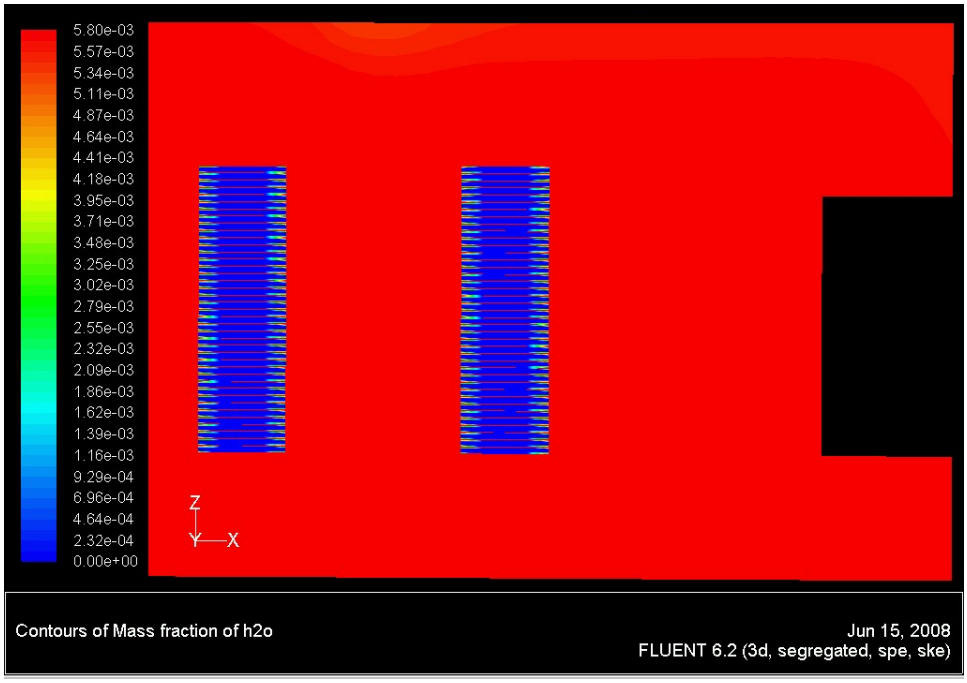

Figure 4.12 Mass fraction of water vapor in the month of April in New York

Figure 4.13 shows the plot of mass fraction of water vapor in the month of October, which represents the month of rainy season. The plot shows that the humidity of the outside air is higher than the ASHRAE recommended region and hence dehumidification is required in this case.

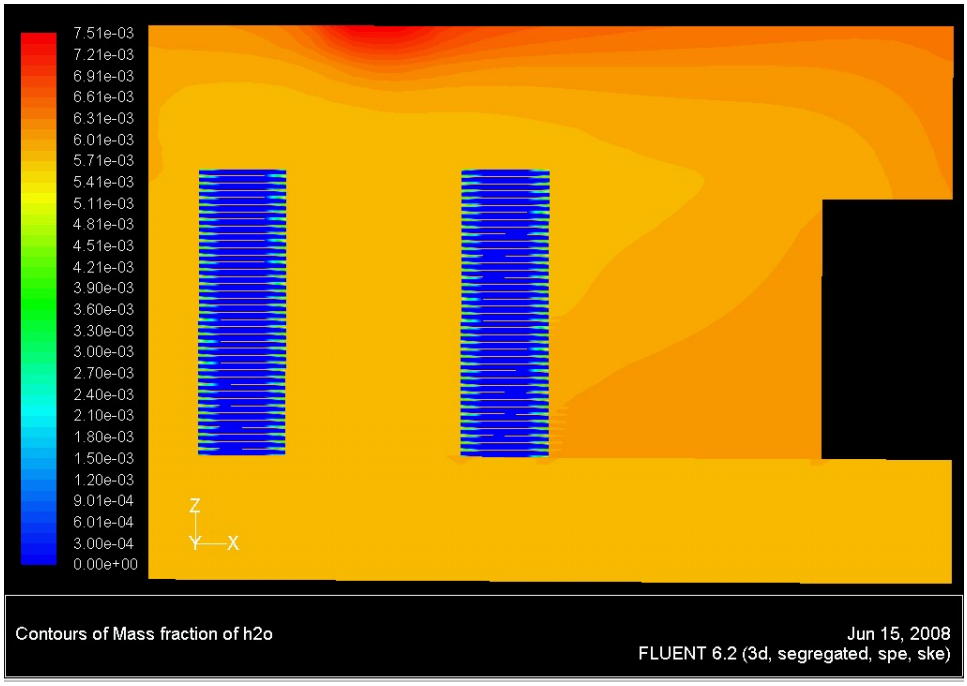

Figure 4.13 Mass fraction of water vapor in the month of October in New York

To analyze the above results, let us consider a simplified psychrometric chart as shown in figure 4.14.

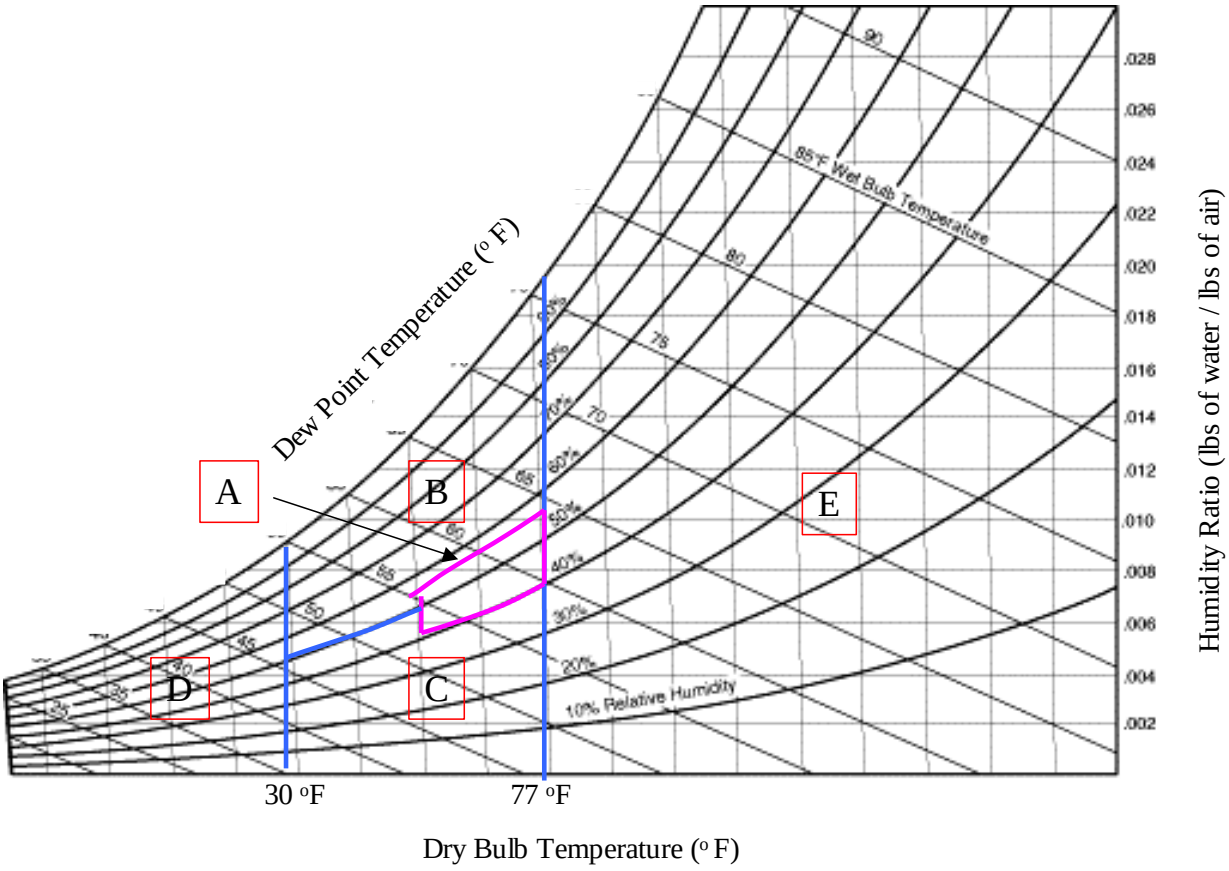

Figure 4.14. Psychrometric chart showing different regimes of economizer usage

The chart is divided into five sections depending on the air temperature and humidity. When the outside air temperature and humidity are located in region A, the economizer can be used at 100 %. The chillers and humidifiers are not needed in this region. If the outside air temperature and humidity falls in region B, outside air still can be used to directly feed into the data center space. However, since the humidity of the air is higher, dehumidification would be required before it is supplied back to the data center space through the perforated tiles. If the outside air temperature and humidity fall in

region C, the air would require humidification to meet the ASHRAE recommended humidity level.

If the outside air temperature falls in the region D, the outside air and return air might need blending to achieve the air temperature in region A, B or C. If the air in region D is directly used, modulation of the flow rate would be required. Otherwise, this might lead to the space air temperature below the recommended level and anti-freeze action might be required. So adjusting the dampers would be required to reduce the amount of air brought into the space. If the outside air temperature falls in region E, it is not suitable to be used for cooling the data center. The dampers must be adjusted to close the inlet and outlet of the economizer.

4.3. Effect of Mass Flow Rate and Temperature

Pareto analysis is a statistical technique in decision-making that is used for selection of a limited number of tasks that produce significant overall effect. The tool estimates the benefit delivered by each action, then selects a number of the most effective actions. A Pareto chart is used to graphically summarize and display the relative importance of the differences between groups of data. A Pareto chart is constructed by segmenting the range of the data into groups (also called segments, bins or categories).

To evaluate the effect of the mass flow rate and the temperature on savings of energy of the data center, a transfer function was build. Figure 4.15 shows the Pareto of effect of temperature and mass flow rate for the given data center design. It shows amount of effect each factor has on the saving. The numbers show the slope of the transfer function between the energy saving and air temperature and mass flow rate of the air. The effect of temperature of the air is higher than that of the mass flow rate. Hence a greater savings can be realized by small decrease in the air temperature.

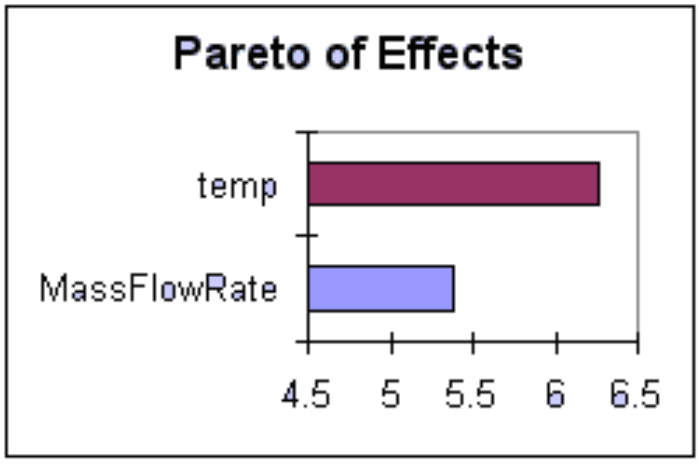

Figure 4.15. Temperature and mass flow rate effect on the CRAC energy saving

For process improvement, a key concept is understanding the relationship of inputs to outputs, the Y = f(x) relationship. This is also known as a “transfer function” or “prediction equation”. Transfer functions can be determined by several different methods. For the simplest processes, data is readily obtained from a process map. In some cases, they may be described from principles inherent in the design’s physics, chemistry or geometry. In less obvious situations, a model to describe the relationship between inputs and outputs using design of experiments is developed. A design of experiments approach was followed in this study to develop the transfer function. Useful information we can learn from the transfer function is exactly what effect each input factor is likely to have on an output. Fully understanding these relationships allows us to adjust a design to achieve a target and to choose settings that reduce variability. The plot in figure 4.16 shows the surface plot of the saving that can be obtained for different combinations of mass flow rate and air inlet temperature. This gives the transfer function of the saving from the air inlet temperature and mass flow rate. The saving in the energy can be predicted using the surface without actual numerical simulation of the conditions.

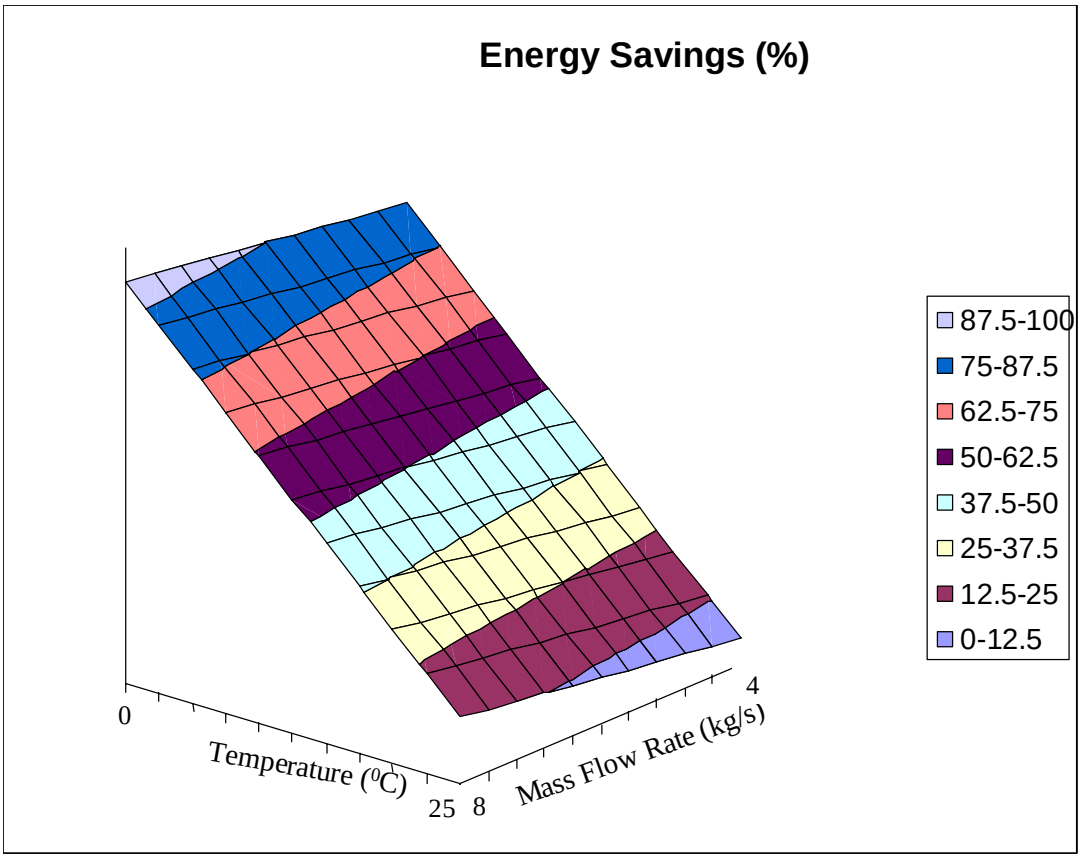

Figure 4.16. Surface plot for energy saving for temperature and mass flow rate variation

CHAPTER 5

CONCLUSION AND FUTURE WORK

5.1 Conclusions

The design of data center cooling systems with economizers is in its early stages. It is necessary to quantify the benefits that these systems can give and the parameters that affect their design and benefit. In this investigation, four different cities, Atlanta, New York, Seattle and Shanghai, were considered for evaluating the saving in energy that can be achieved if an airside economizer is implemented. Some key conclusions from the study are:

- The savings from the economizer depend largely on the local climate. As cold weather increases (from Atlanta to New York), the number of hours that the economizer is operating increases. The longer the cold weather, the better the economizer works.
- Assuming an average $0.08/kWh energy charge, the savings would be $14,000 / year (Atlanta) to $ 29,000 / year (New York) for a baseline consumption of 118 kW. Clearly, the savings in the cost is significant and larger for a colder location.
- A higher supply air temperature would greatly increase the energy savings. If the supply air temperature is raised from 20 ^{0}C to 25 ^{0}C, the economizer can be activated earlier providing more hours of free cooling.
- Even if the outside air relative humidity is not within the recommended ASHRAE limits [7], the air can be introduced into the data center space. The relative humidity distributions of all the cases considered show that for the specified mass flow rate, the humidity at the inlet of the server is not changed, provided the

CRAC units supply the air at humidity level within the recommended range. This would require humidification or dehumidification as necessary. This would result in added cost and offset the savings. However, a net saving of energy may still be possible.

- Particulate contamination would be a concern, though the literature [6] claims that the recommended level could be met by improvement in the filtration system.

5.2 Future Work

It is important to validate the claims of the simulation by doing full-scale experiments. Detailed analysis of the cost of infrastructure improvement for the implementation of the economizer would be worthwhile exploring to quantify payoff periods. CRAC and rack position optimization with the airside economizer in the data center would help improve the benefits of the system.

Appendix A

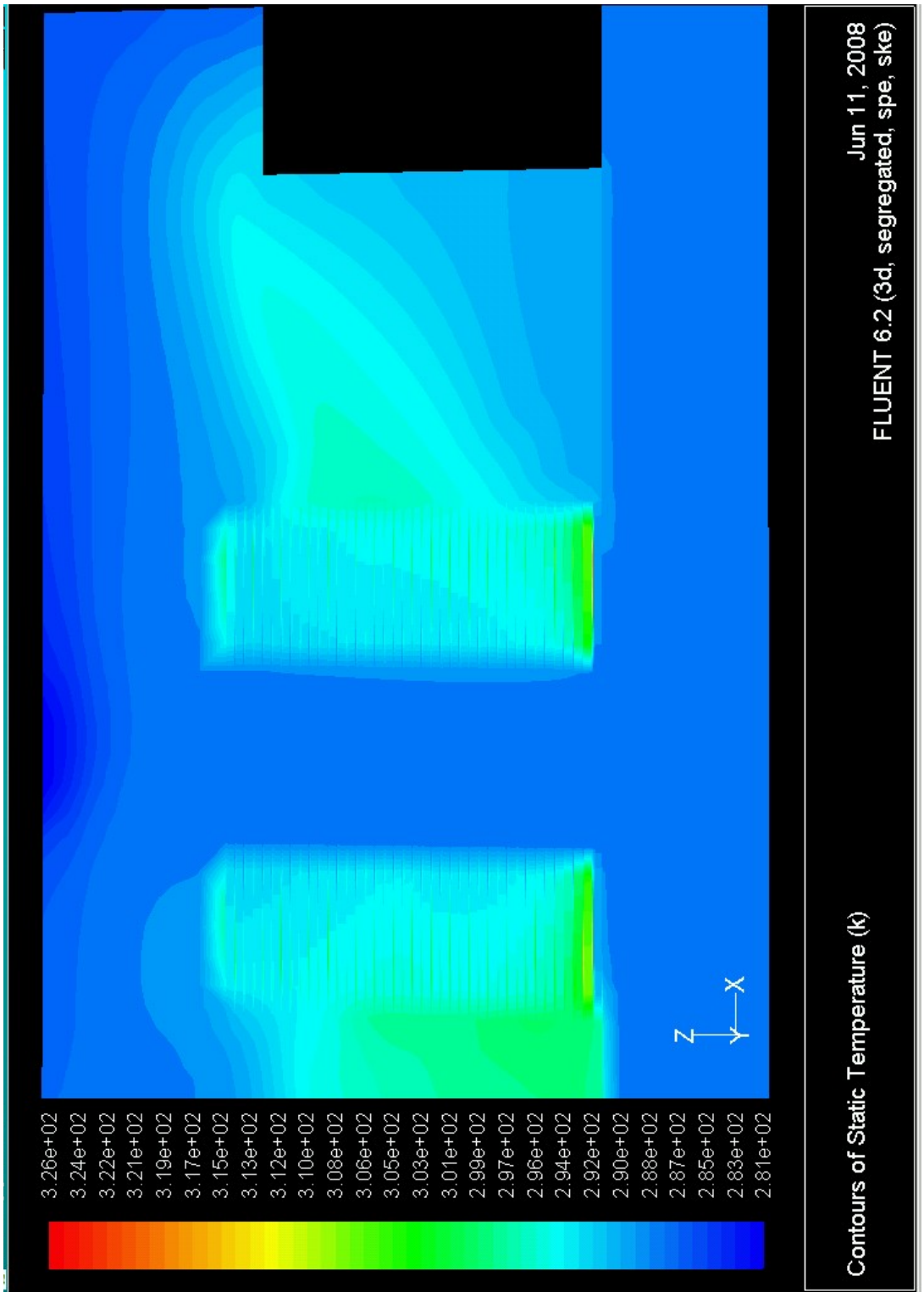
Contours of Static Temperature (k)
3.26e+02
3.24e+02
3.22e+02
3.21e+02
3.19e+02
3.17e+02
3.15e+02
3.13e+02
3.12e+02
3.10e+02
3.08e+02
3.06e+02
3.05e+02
3.03e+02
3.01e+02
2.99e+02
2.97e+02
2.96e+02
2.94e+02
2.92e+02
2.90e+02
2.88e+02
2.87e+02
2.85e+02
2.83e+02
2.81e+02
Z
X
FLUENT 6.2 (3d, segregated, spe, ske)
Jun 11, 2008

(a)

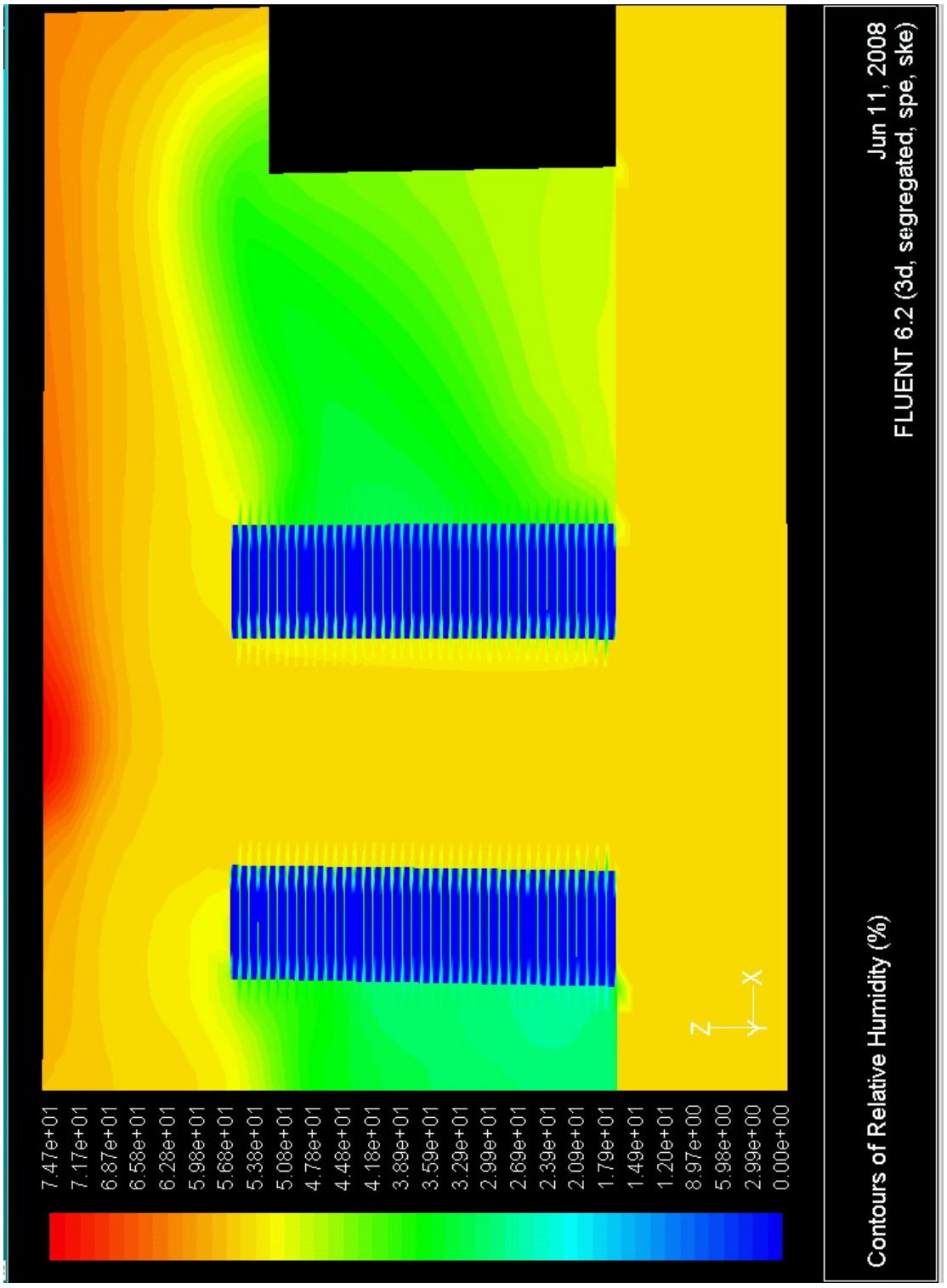

(b)

Figure A1. a) Temperature and b) RH plot through the vertical mid plane for the month of February inside the data center in Atlanta

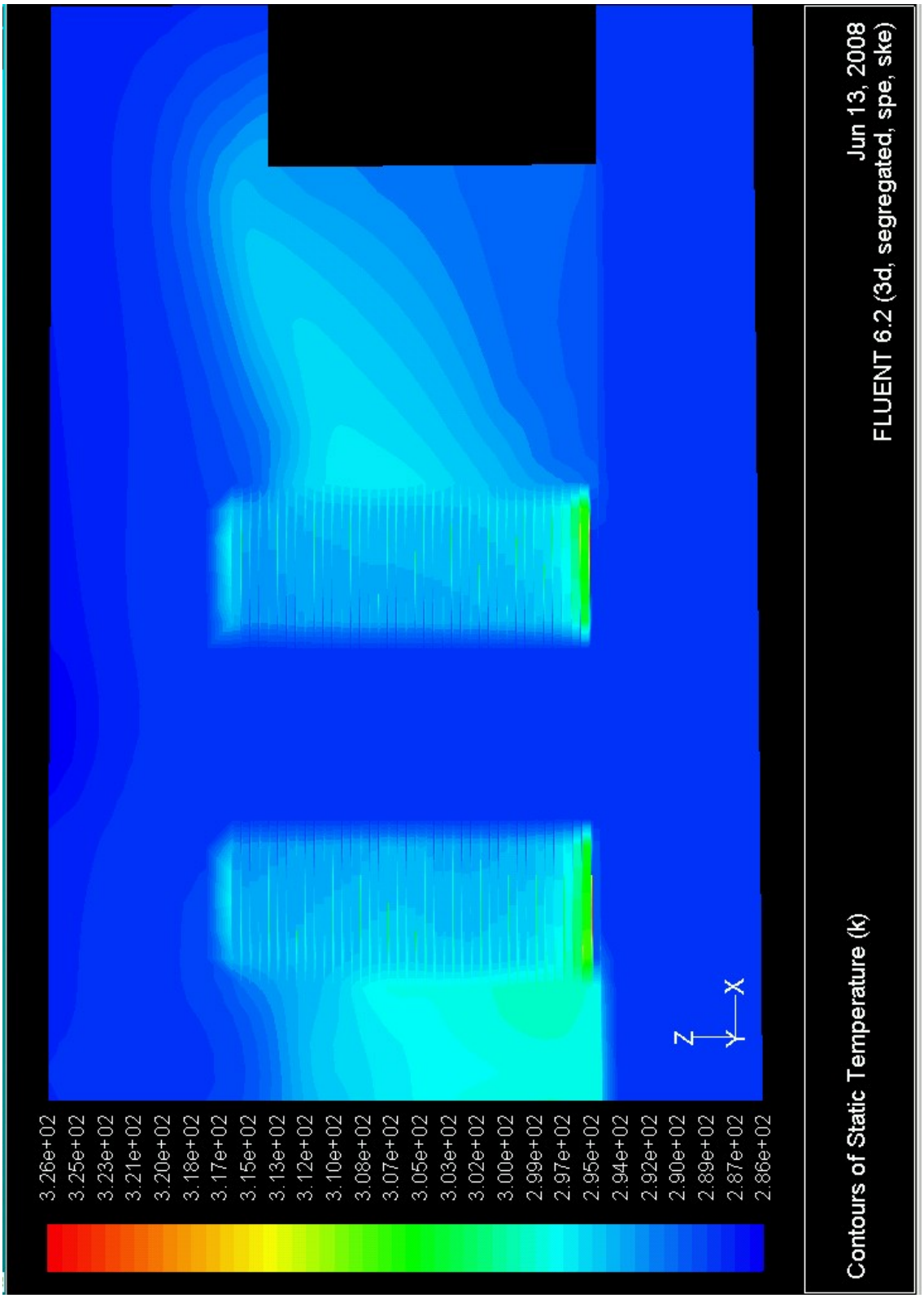
Contours of Static Temperature (k)
3.26e+02
3.25e+02
3.23e+02
3.21e+02
3.20e+02
3.18e+02
3.17e+02
3.15e+02
3.13e+02
3.12e+02
3.10e+02
3.08e+02
3.07e+02
3.05e+02
3.03e+02
3.02e+02
3.00e+02
2.99e+02
2.97e+02
2.95e+02
2.94e+02
2.92e+02
2.90e+02
2.89e+02
2.87e+02
2.86e+02
Z
Y
X
Jun 13, 2008
FLUENT 6.2 (3d, segregated, spe, ske)

(a)

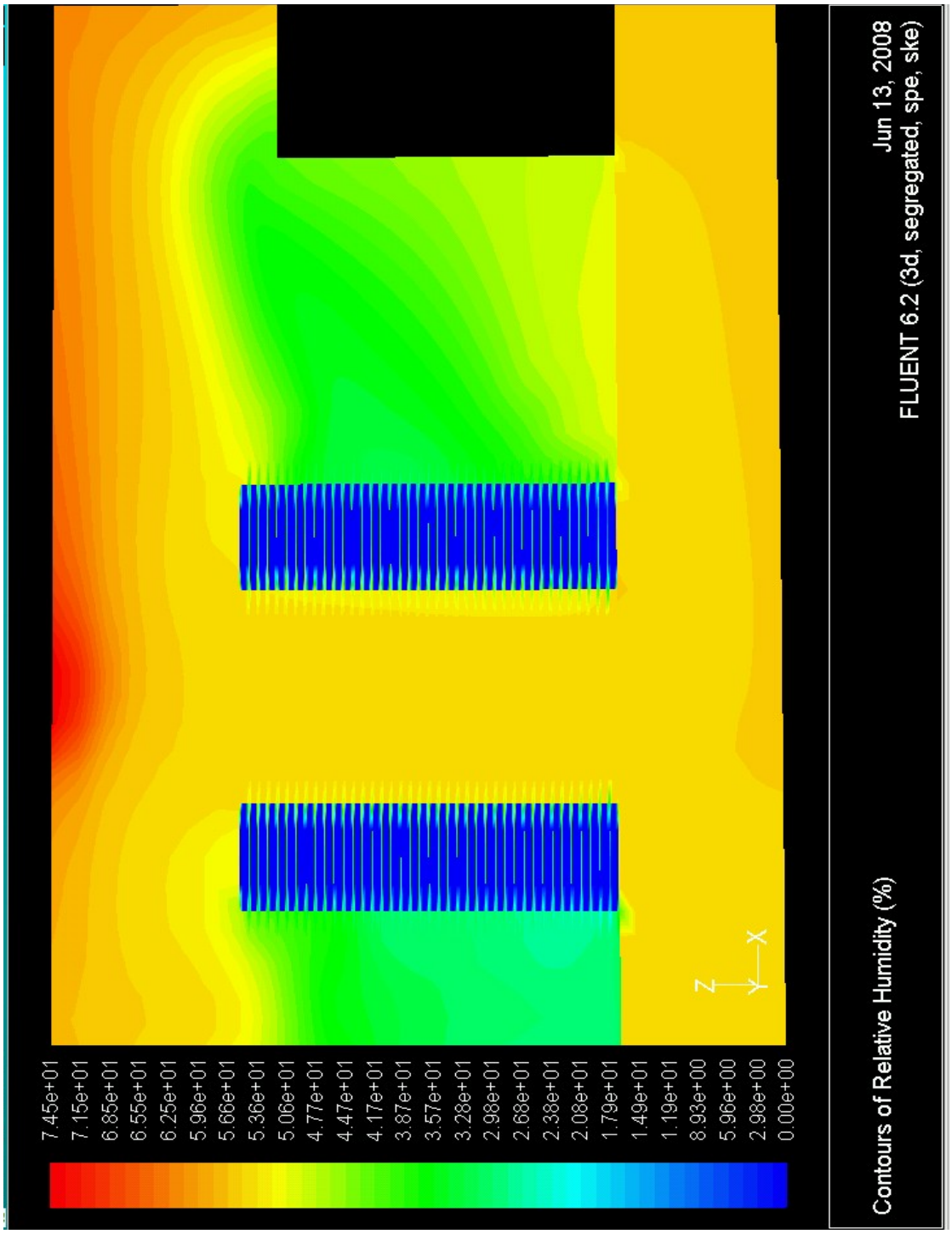

(b)

Figure A2. a) Temperature and b) RH plot through the vertical mid plane for the month of March inside the data center in Atlanta

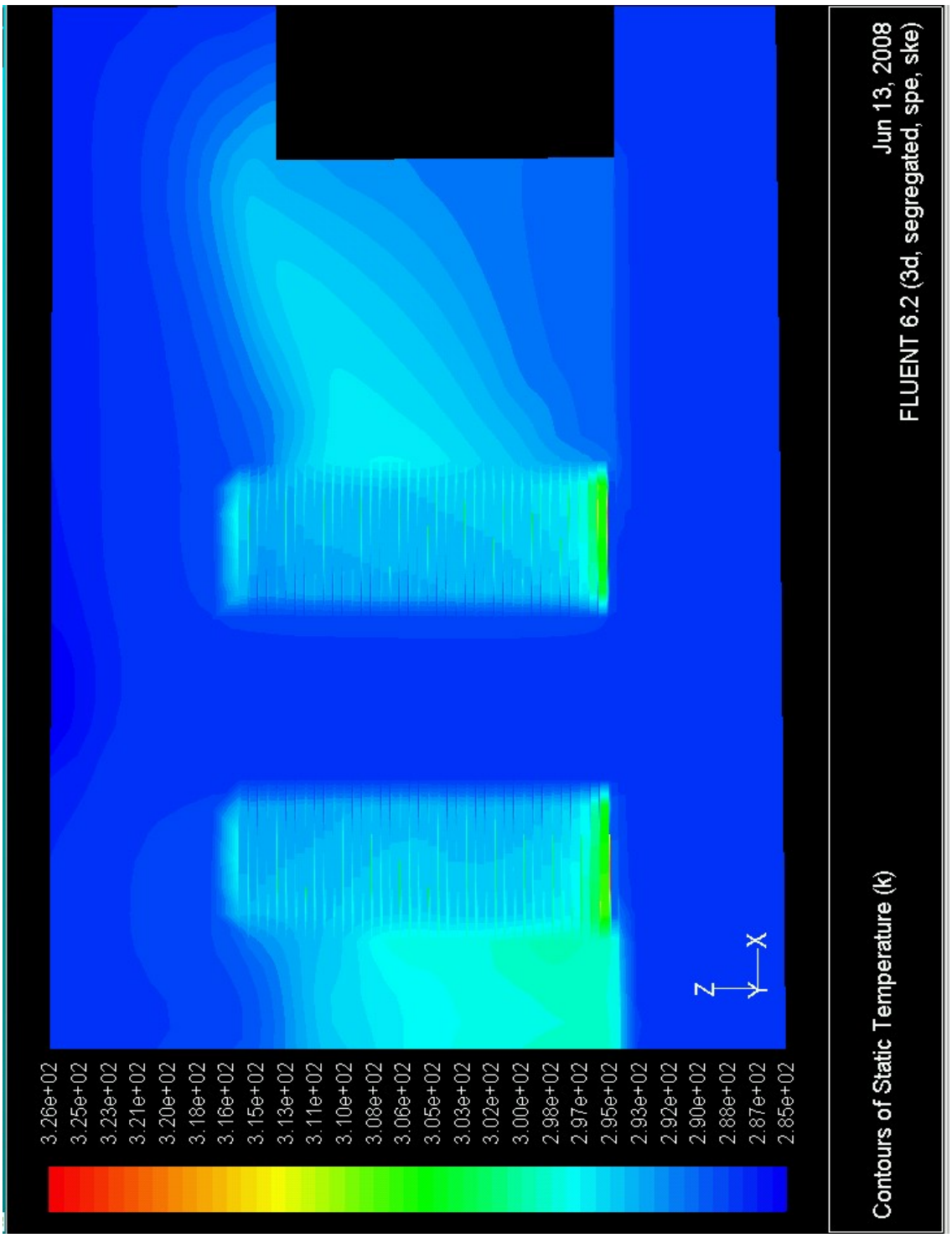
Contours of Static Temperature (k)
3.26e+02
3.25e+02
3.23e+02
3.21e+02
3.20e+02
3.18e+02
3.16e+02
3.15e+02
3.13e+02
3.11e+02
3.10e+02
3.08e+02
3.06e+02
3.05e+02
3.03e+02
3.02e+02
3.00e+02
2.98e+02
2.97e+02
2.95e+02
2.93e+02
2.92e+02
2.90e+02
2.88e+02
2.87e+02
2.85e+02
Z
X
Jun 13, 2008
FLUENT 6.2 (3d, segregated, spe, ske)

(a)

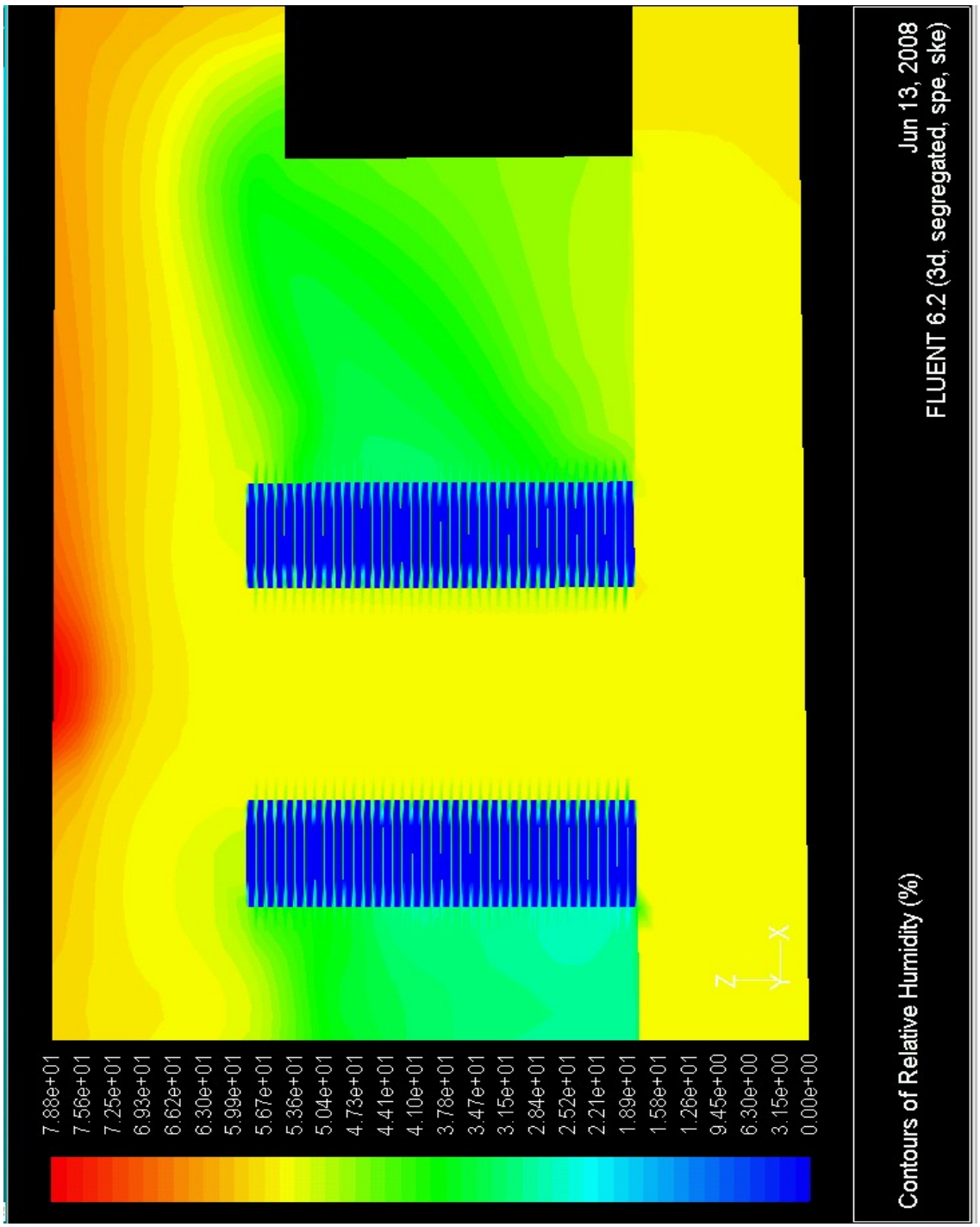

(b)

Figure A3. a) Temperature and b) RH plot through the vertical mid plane for the month of November inside the data center in Atlanta

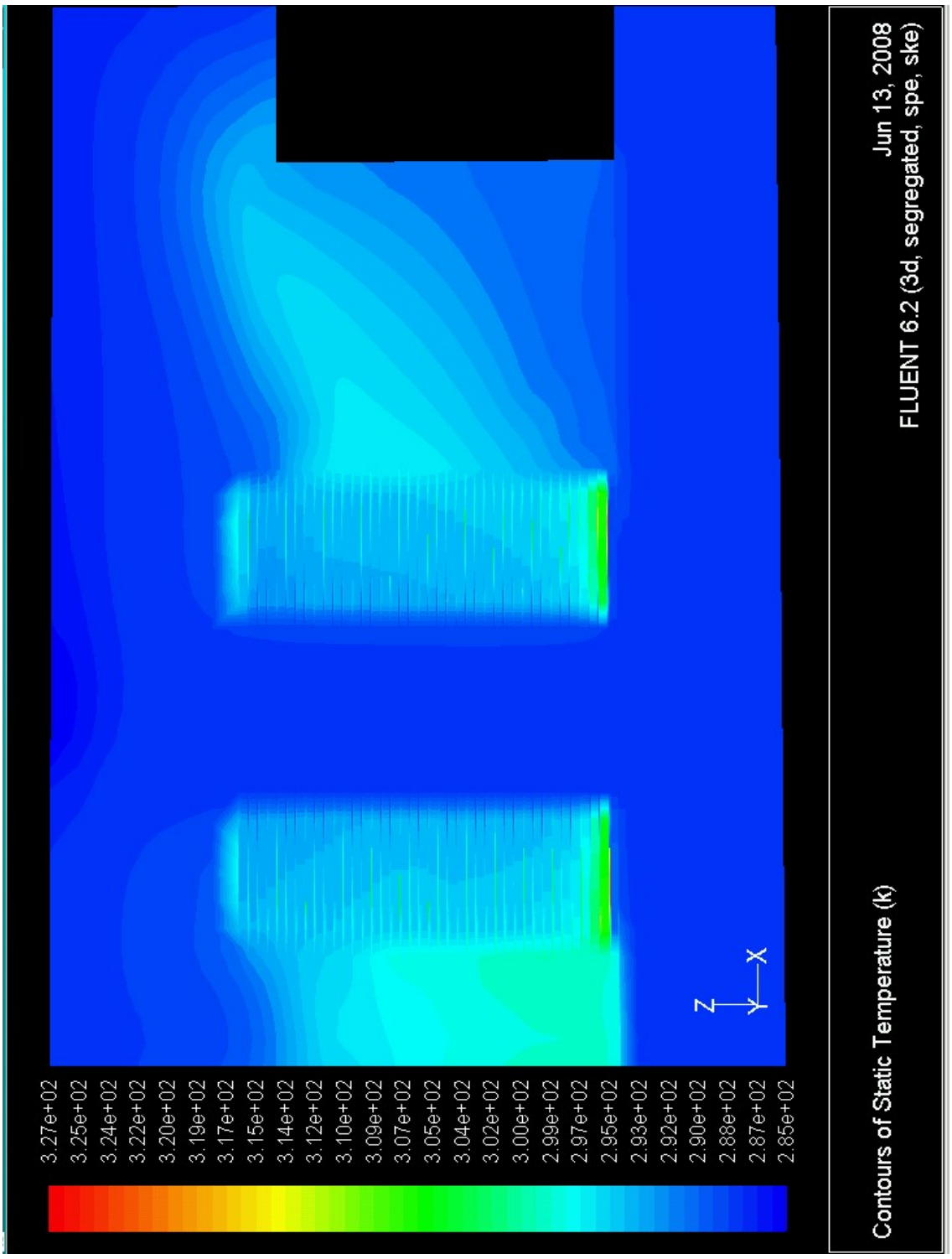
Contours of Static Temperature (k)
3.27e+02
3.25e+02
3.24e+02
3.22e+02
3.20e+02
3.19e+02
3.17e+02
3.15e+02
3.14e+02
3.12e+02
3.10e+02
3.09e+02
3.07e+02
3.05e+02
3.04e+02
3.02e+02
3.00e+02
2.99e+02
2.97e+02
2.95e+02
2.93e+02
2.92e+02
2.90e+02
2.88e+02
2.87e+02
2.85e+02
Z
Y
X
Jun 13, 2008
FLUENT 6.2 (3d, segregated, spe, ske)

(a)

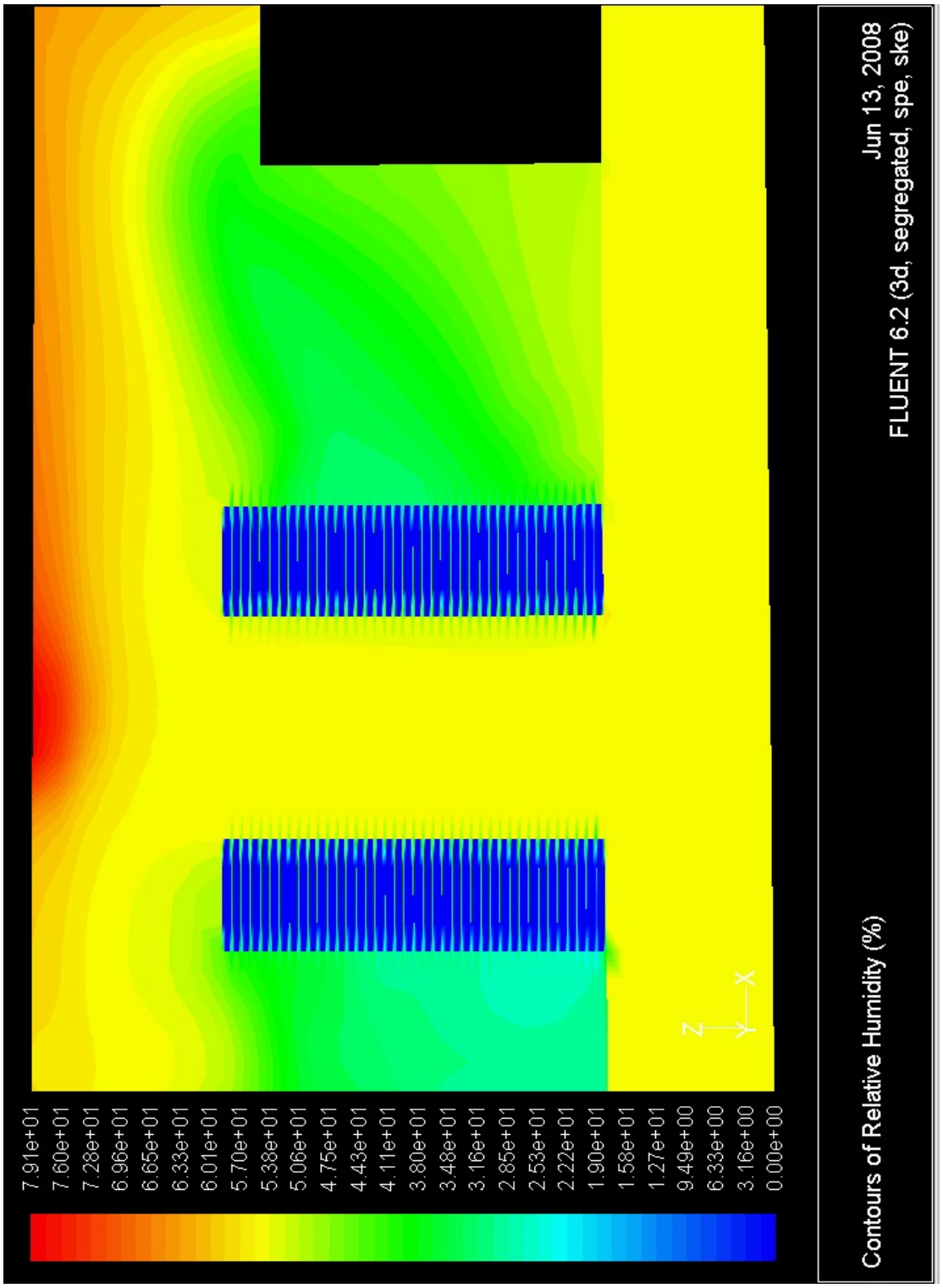

(b)

Figure A4. a) Temperature and b) RH through the vertical mid plane for the month of December inside the data center in Atlanta

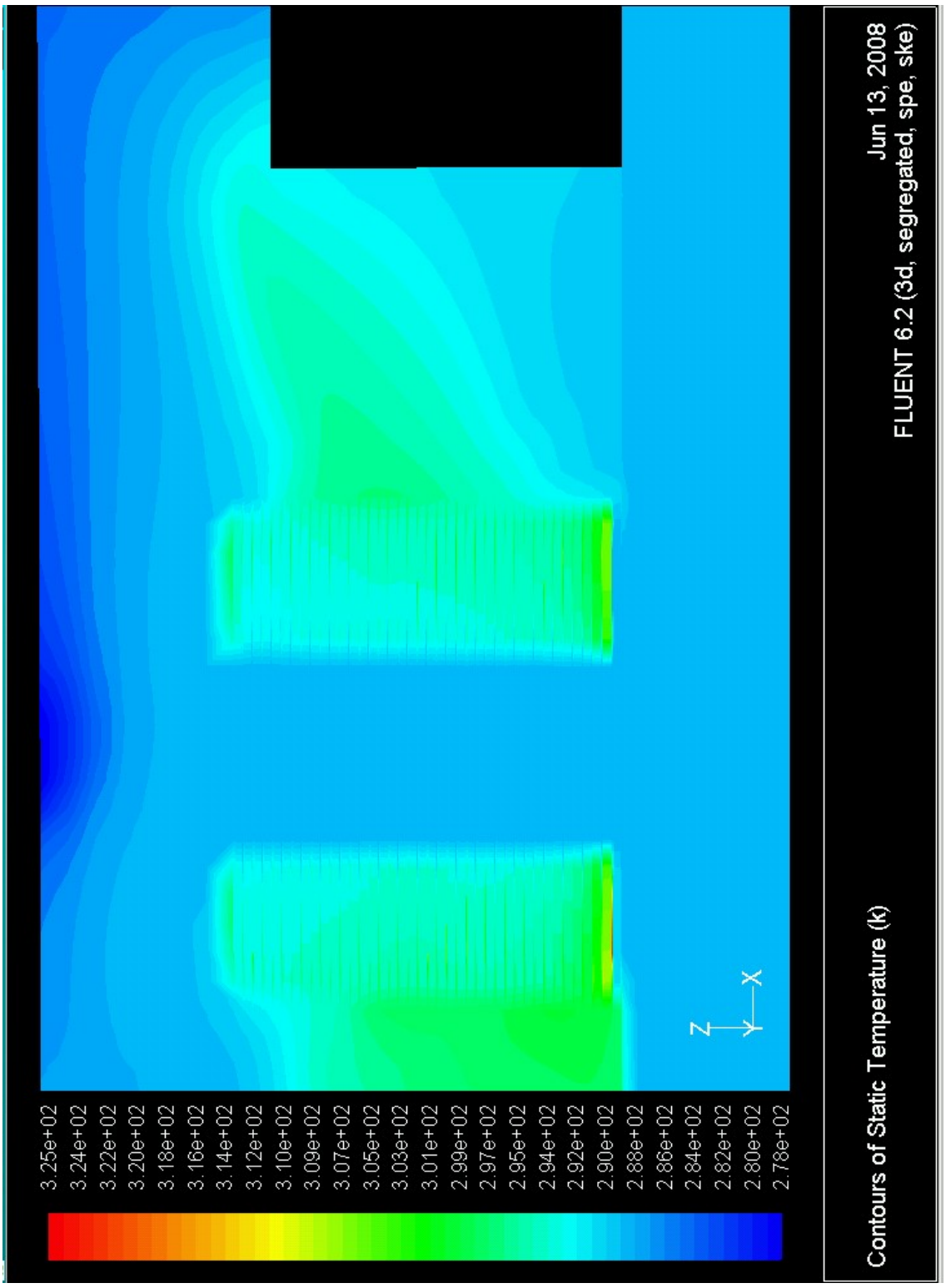
Contours of Static Temperature (k)
3.25e+02
3.24e+02
3.22e+02
3.20e+02
3.18e+02
3.16e+02
3.14e+02
3.12e+02
3.10e+02
3.09e+02
3.07e+02
3.05e+02
3.03e+02
3.01e+02
2.99e+02
2.97e+02
2.95e+02
2.94e+02
2.92e+02
2.90e+02
2.88e+02
2.86e+02
2.84e+02
2.82e+02
2.80e+02
2.78e+02
Z
X
Jun 13, 2008
FLUENT 6.2 (3d, segregated, spe, ske)

(a)

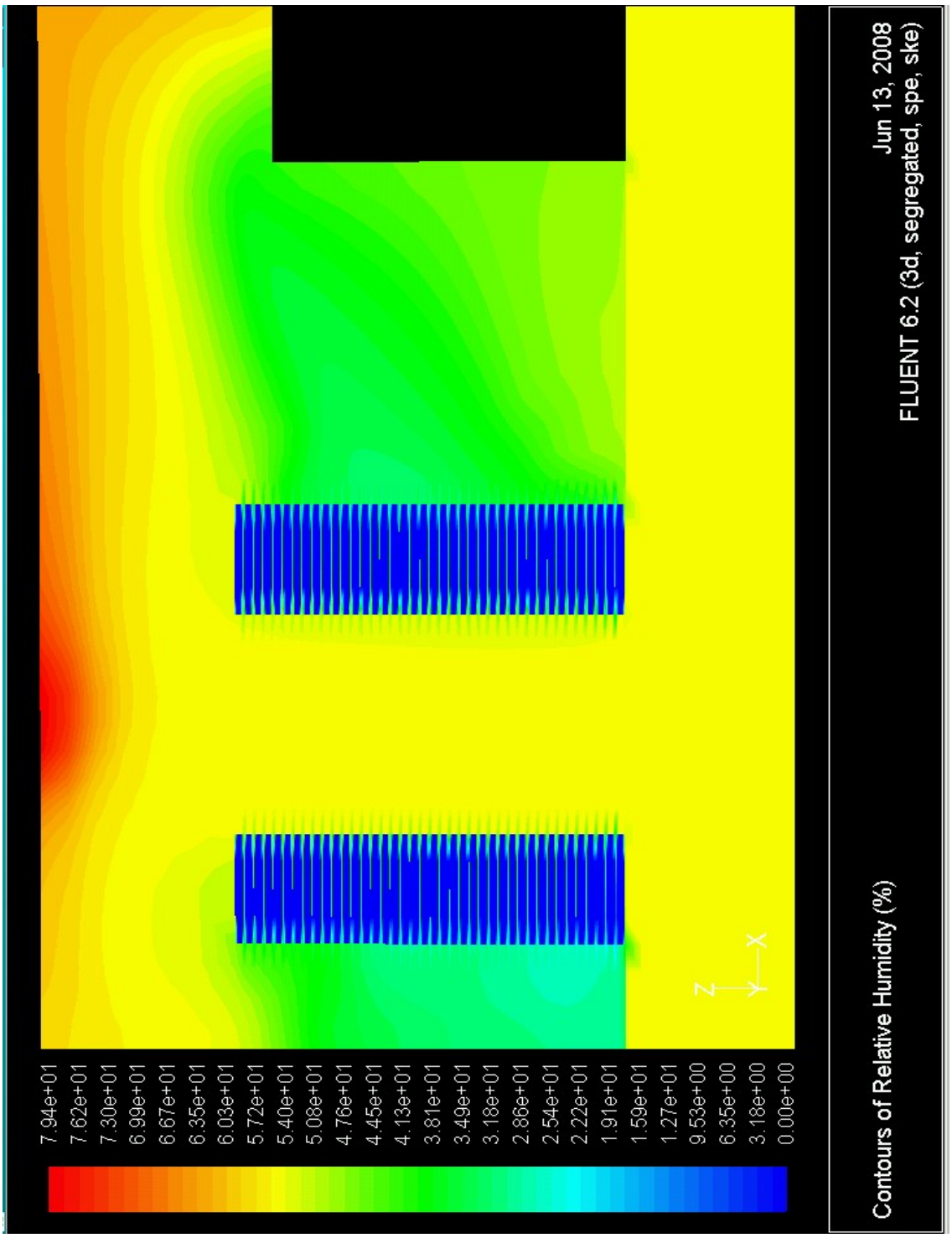

(b)

Figure A5. a) Temperature and b) RH plot through the vertical mid plane for the month of January inside the data center in Seattle

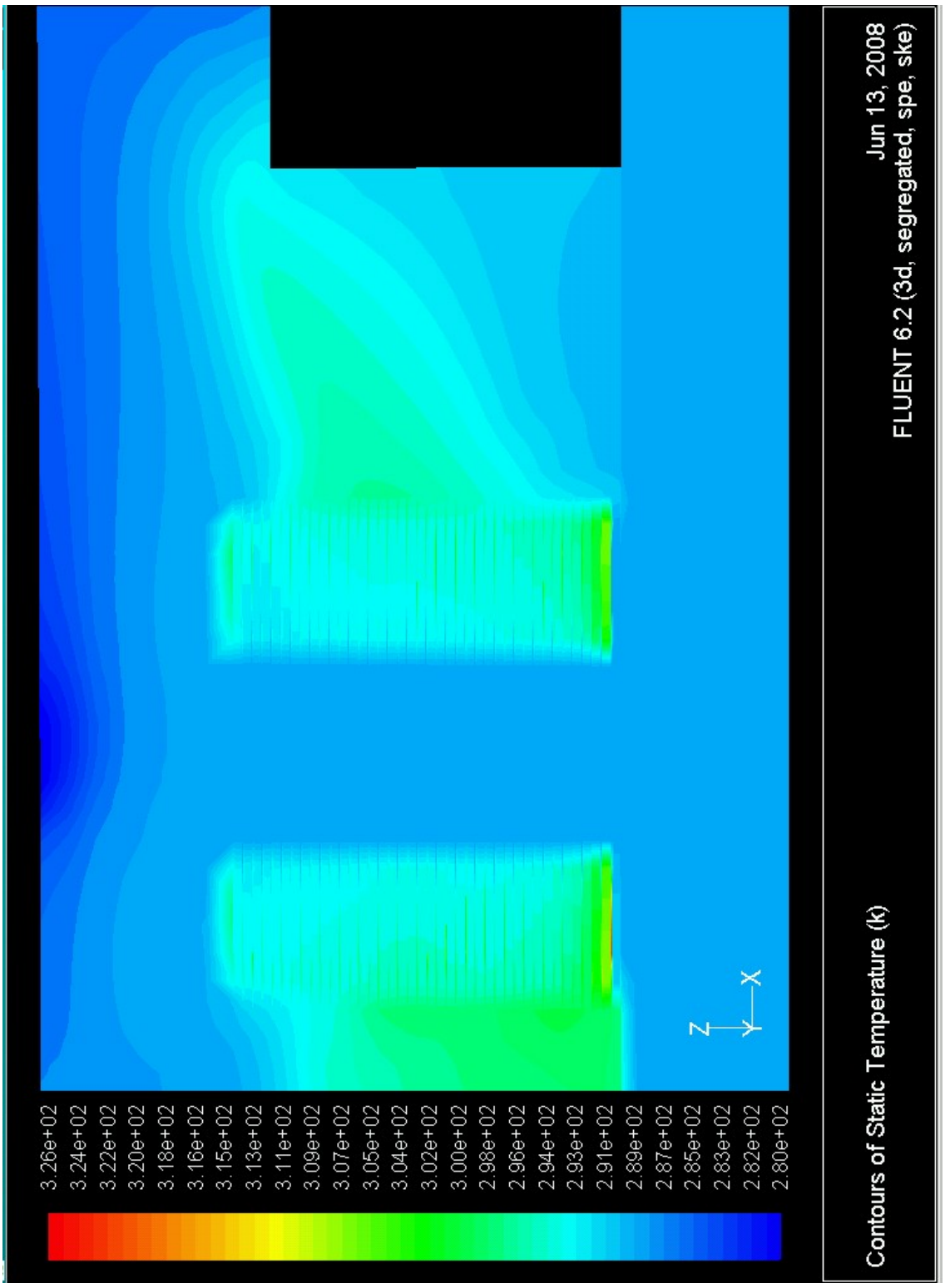
Contours of Static Temperature (k)
3.26e+02
3.24e+02
3.22e+02
3.20e+02
3.18e+02
3.16e+02
3.15e+02
3.13e+02
3.11e+02
3.09e+02
3.07e+02
3.05e+02
3.04e+02
3.02e+02
3.00e+02
2.98e+02
2.96e+02
2.94e+02
2.93e+02
2.91e+02
2.89e+02
2.87e+02
2.85e+02
2.83e+02
2.82e+02
2.80e+02
Z
Y
X
FLUENT 6.2 (3d, segregated, spe, ske)
Jun 13, 2008

(a)

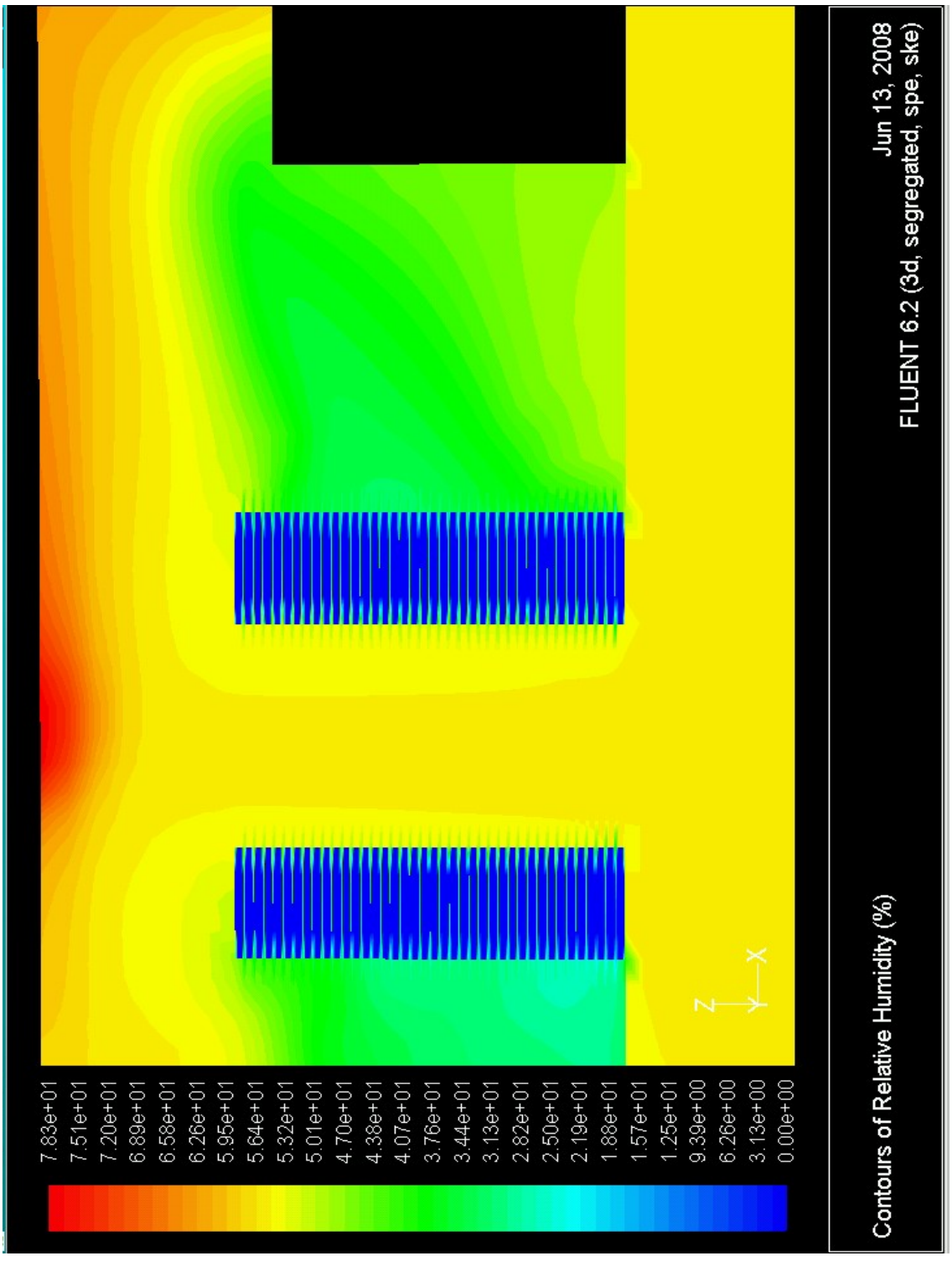

(b)

Figure A6. a) Temperature and b) RH plot through the vertical mid plane for the month of February inside the data center in Seattle

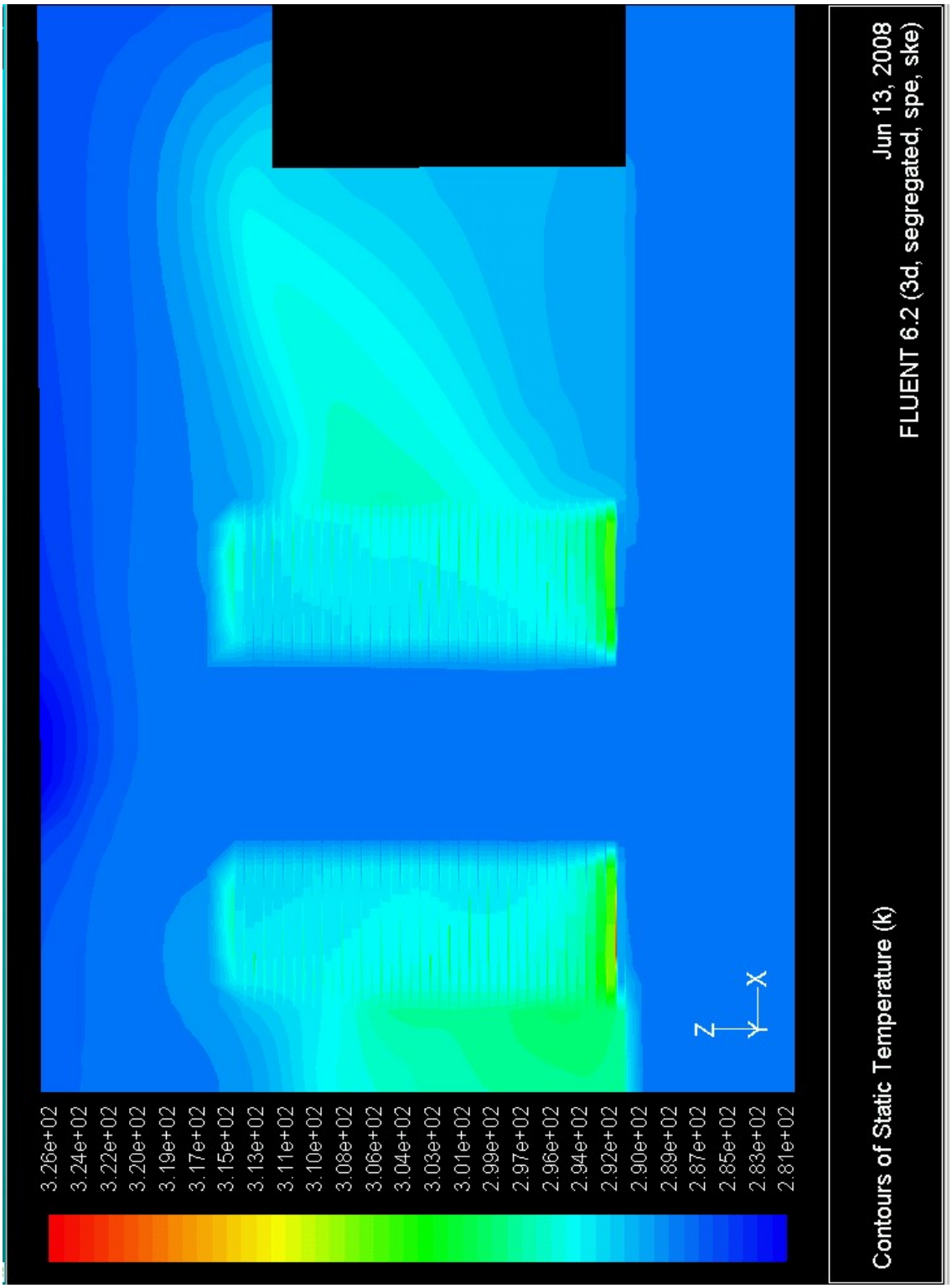
Contours of Static Temperature (k)
3.26e+02
3.24e+02
3.22e+02
3.20e+02
3.19e+02
3.17e+02
3.15e+02
3.13e+02
3.11e+02
3.10e+02
3.08e+02
3.06e+02
3.04e+02
3.03e+02
3.01e+02
2.99e+02
2.97e+02
2.96e+02
2.94e+02
2.92e+02
2.90e+02
2.89e+02
2.87e+02
2.85e+02
2.83e+02
2.81e+02
Z
Y
X
Jun 13, 2008
FLUENT 6.2 (3d, segregated, spe, ske)

(a)

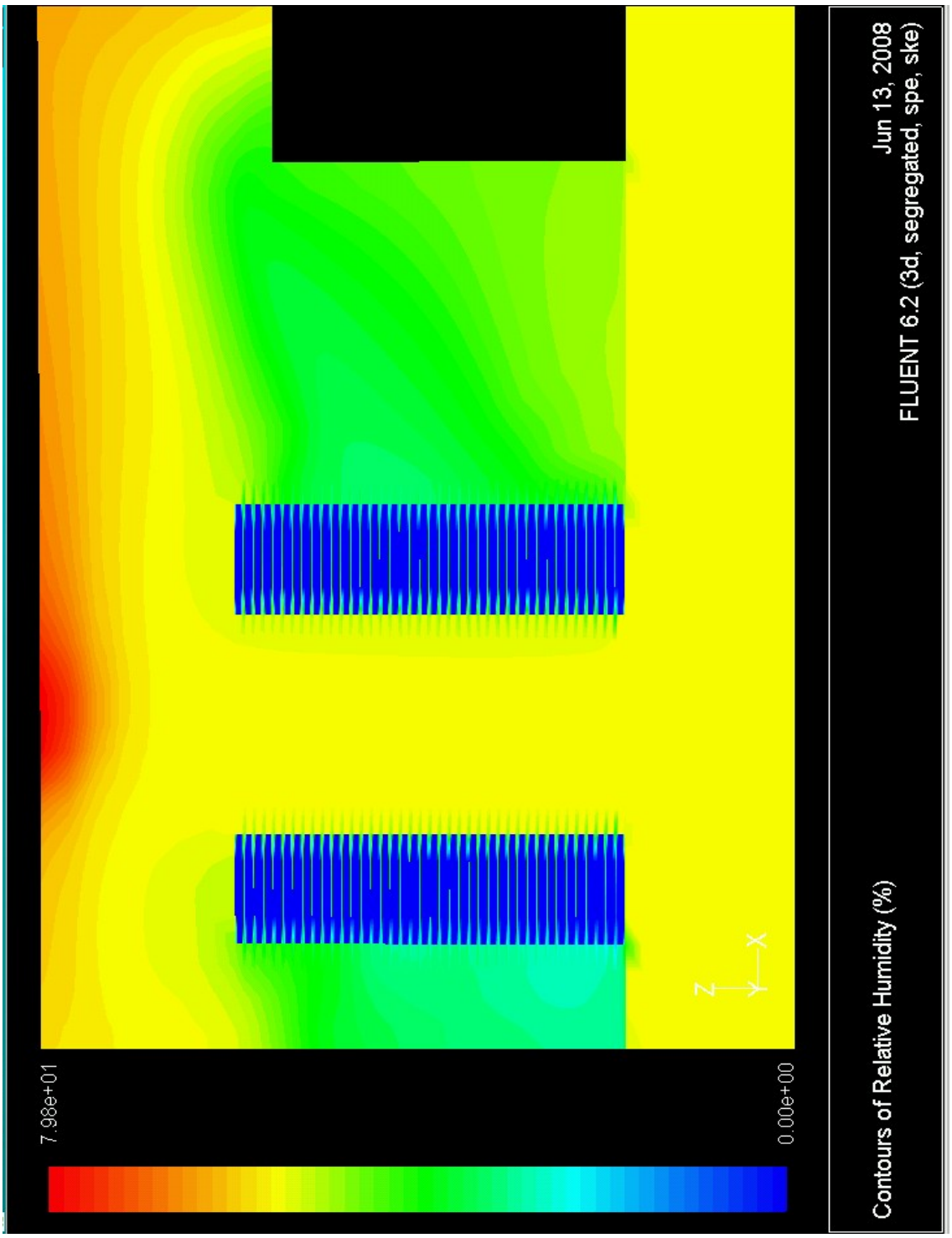

(b)

Figure A7. a) Temperature and b) RH plot through the vertical mid plane for the month of March inside the data center in Seattle

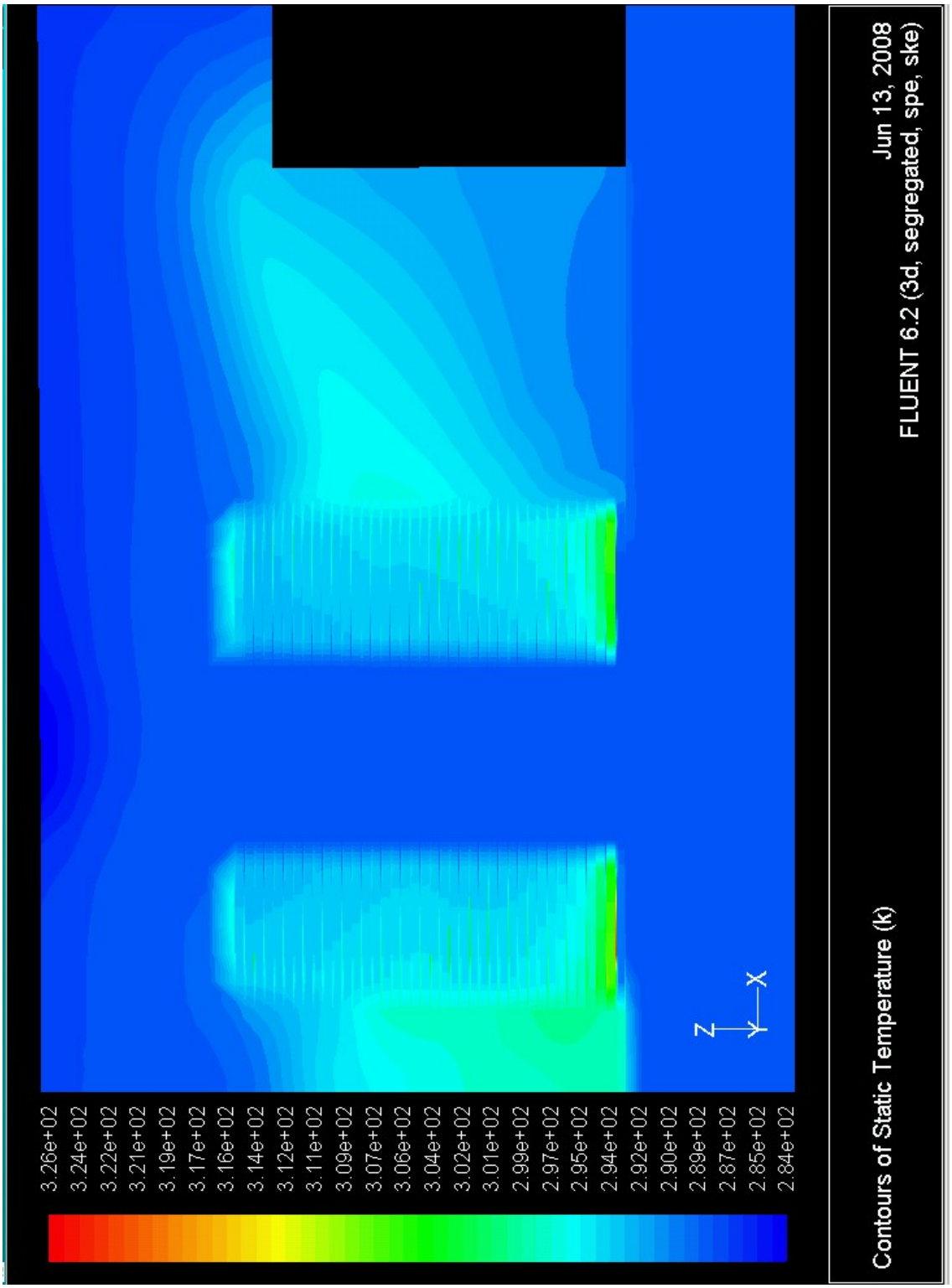
Contours of Static Temperature (k)
3.26e+02
3.24e+02
3.22e+02
3.21e+02
3.19e+02
3.17e+02
3.16e+02
3.14e+02
3.12e+02
3.11e+02
3.09e+02
3.07e+02
3.06e+02
3.04e+02
3.02e+02
3.01e+02
2.99e+02
2.97e+02
2.95e+02
2.94e+02
2.92e+02
2.90e+02
2.89e+02
2.87e+02
2.85e+02
2.84e+02
Z
X
Jun 13, 2008
FLUENT 6.2 (3d, segregated, spe, ske)

(a)

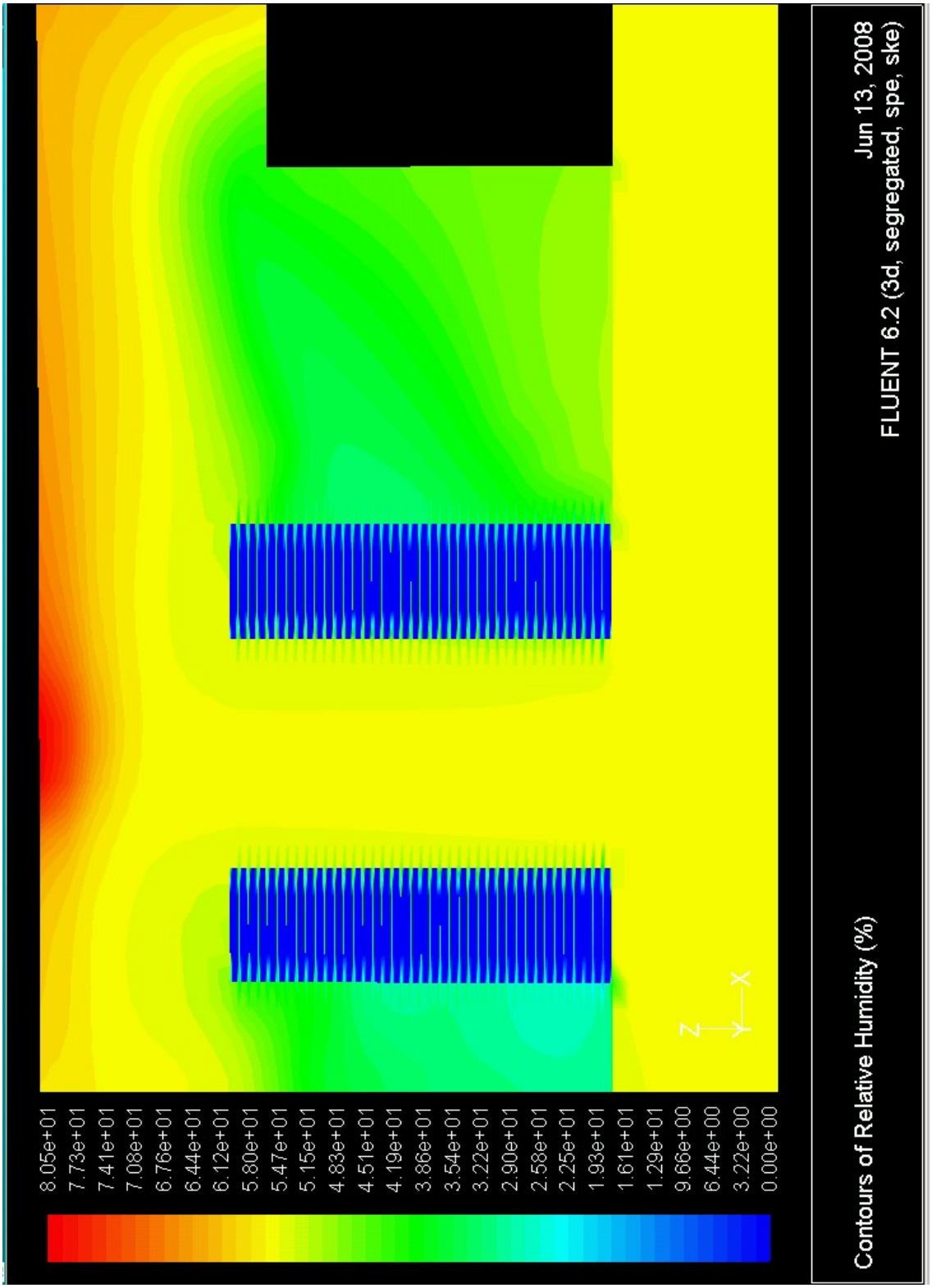

(b)

Figure A8. a) Temperature and b) RH plot through the vertical mid plane for the month of April inside the data center in Seattle

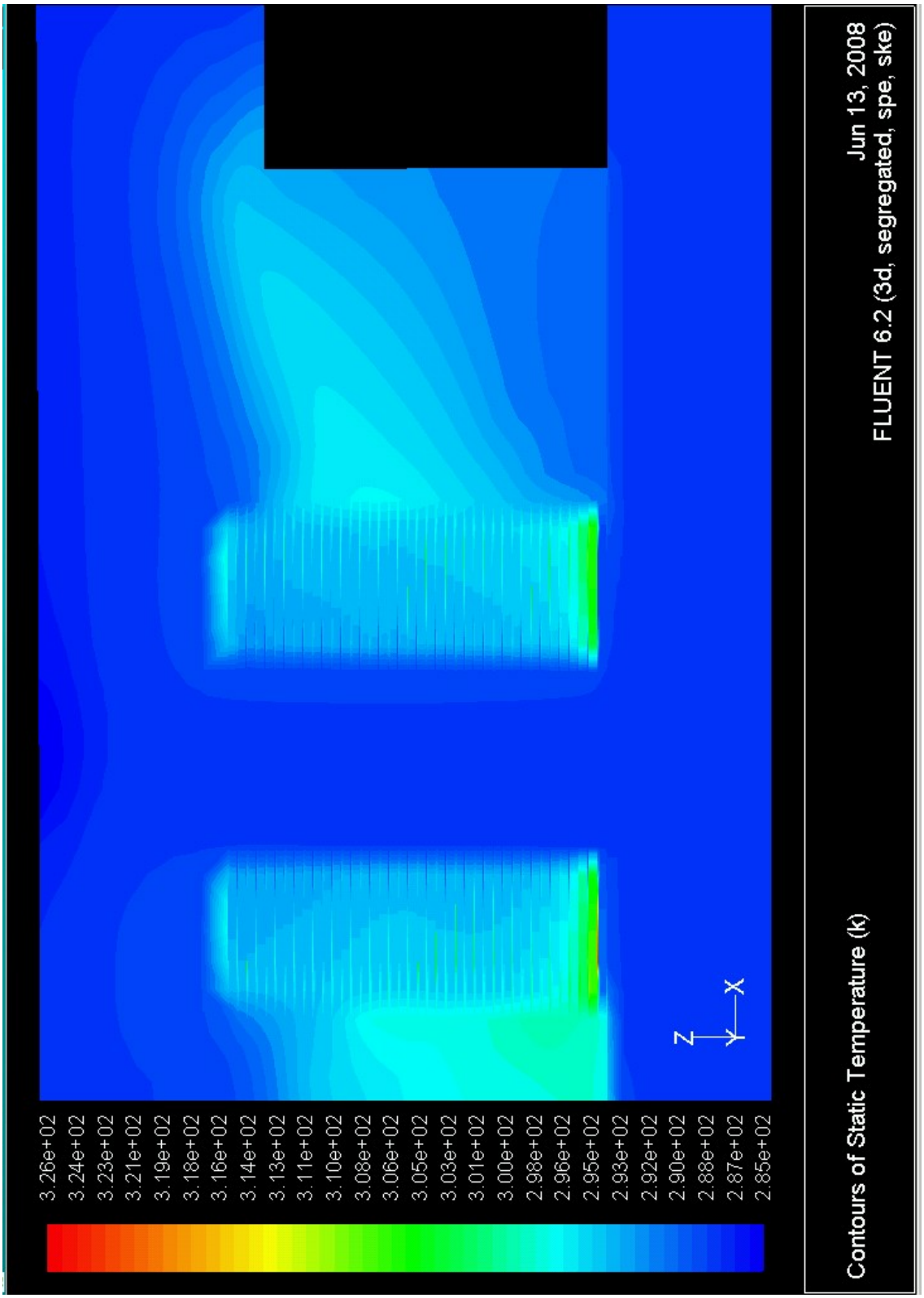
Contours of Static Temperature (k)
3.26e+02
3.24e+02
3.23e+02
3.21e+02
3.19e+02
3.18e+02
3.16e+02
3.14e+02
3.13e+02
3.11e+02
3.10e+02
3.08e+02
3.06e+02
3.05e+02
3.03e+02
3.01e+02
3.00e+02
2.98e+02
2.96e+02
2.95e+02
2.93e+02
2.92e+02
2.90e+02
2.88e+02
2.87e+02
2.85e+02
Z
X
Jun 13, 2008
FLUENT 6.2 (3d, segregated, spe, ske)

(a)

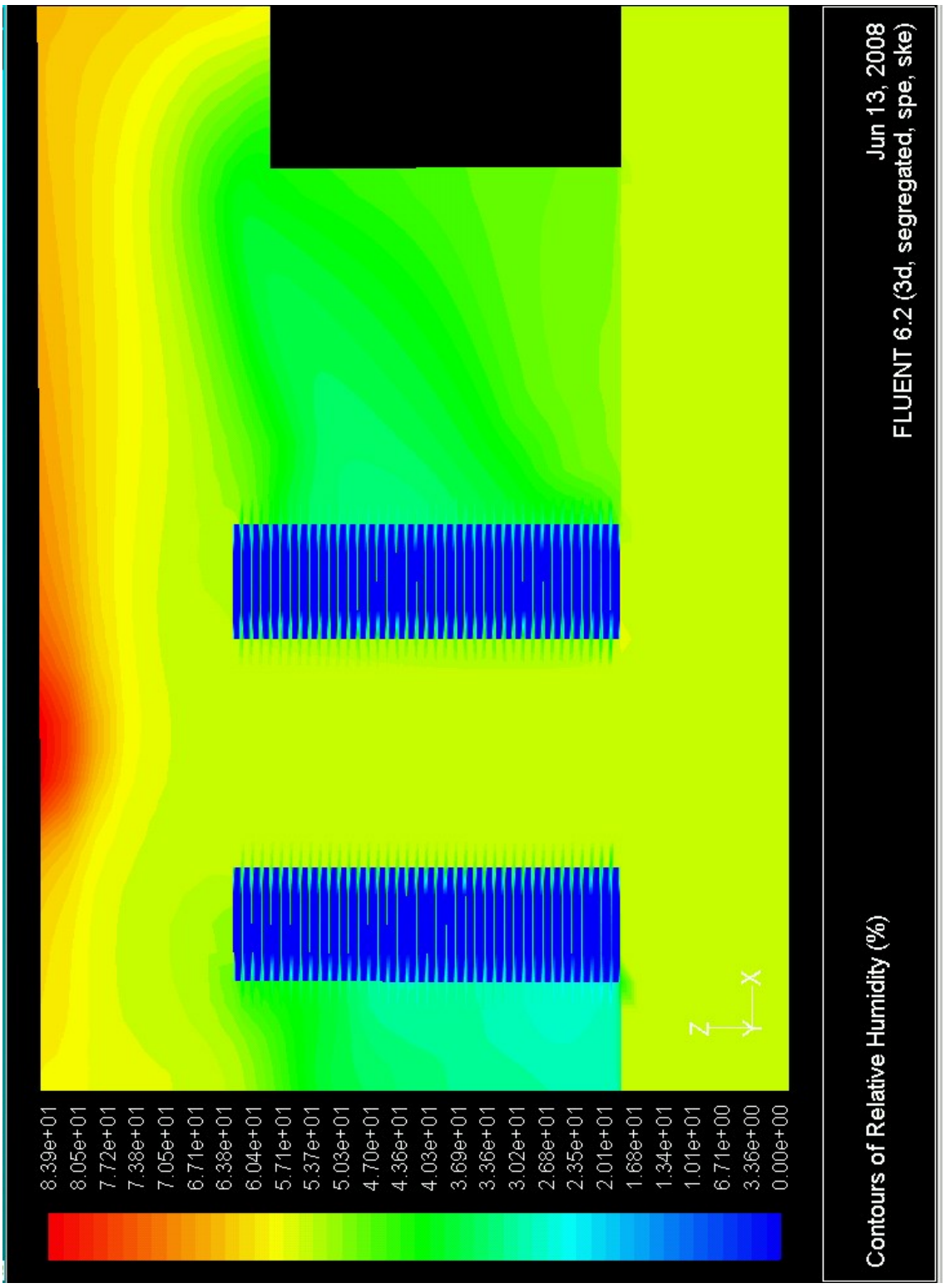

(b)

Figure A9. a) Temperature and b) RH plot through the vertical mid plane for the month of October inside the data center in Seattle

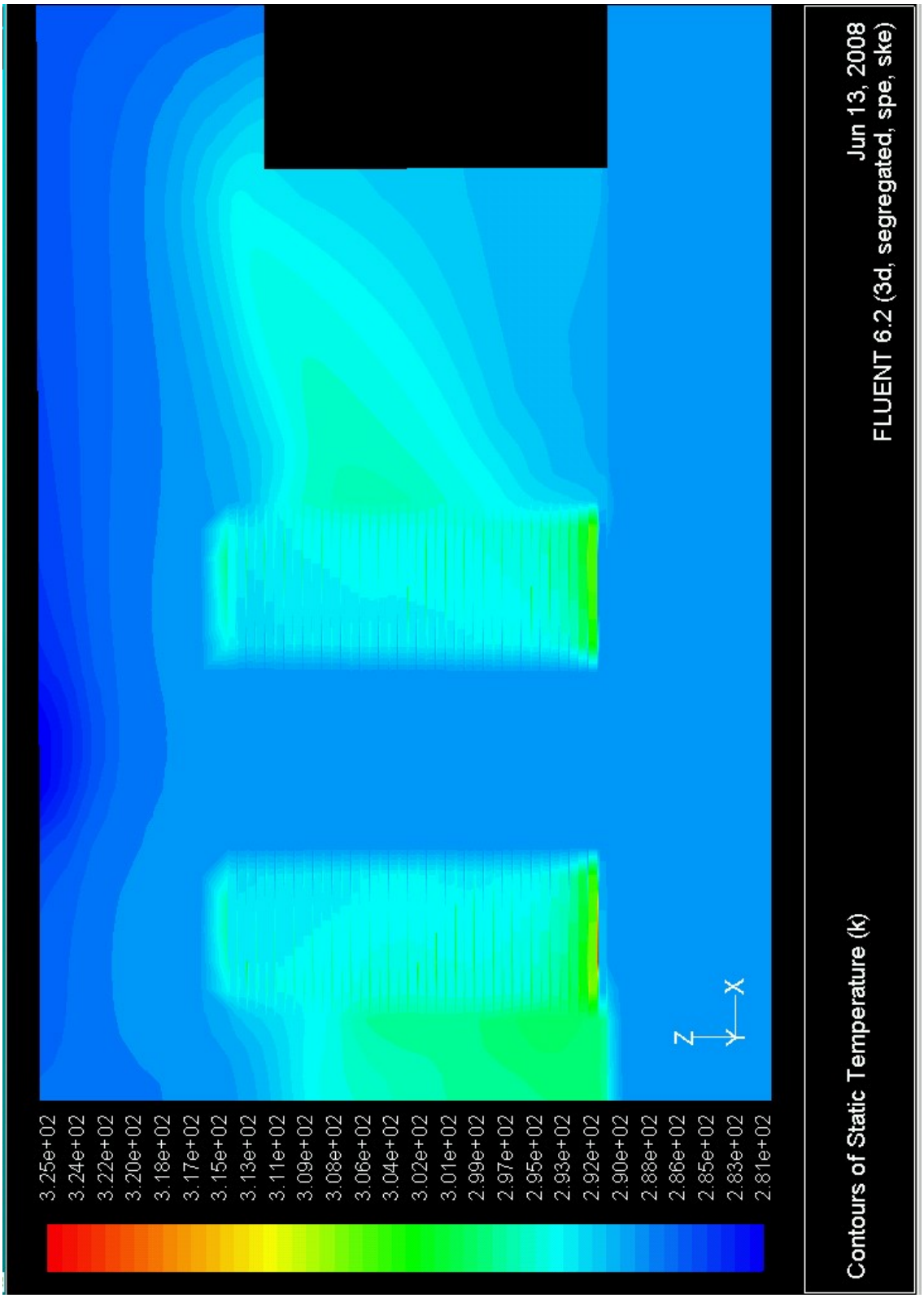
Contours of Static Temperature (k)
3.25e+02
3.24e+02
3.22e+02
3.20e+02
3.18e+02
3.17e+02
3.15e+02
3.13e+02
3.11e+02
3.09e+02
3.08e+02
3.06e+02
3.04e+02
3.02e+02
3.01e+02
2.99e+02
2.97e+02
2.95e+02
2.93e+02
2.92e+02
2.90e+02
2.88e+02
2.86e+02
2.85e+02
2.83e+02
2.81e+02
Z
X
Jun 13, 2008
FLUENT 6.2 (3d, segregated, spe, ske)

(a)

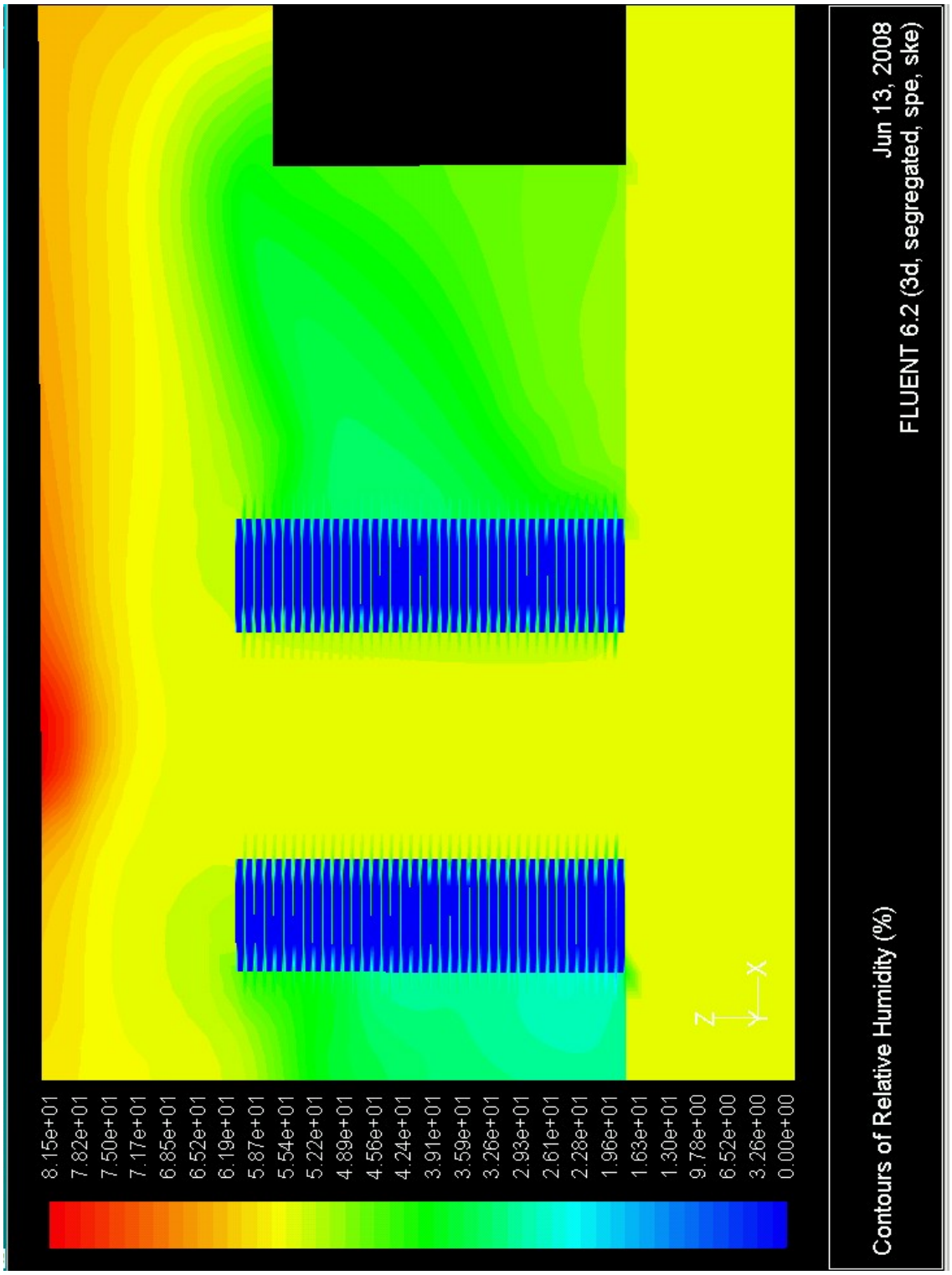

(b)

Figure A10. a) Temperature and b) RH plot through the vertical mid plane for the month of November inside the data center in Seattle

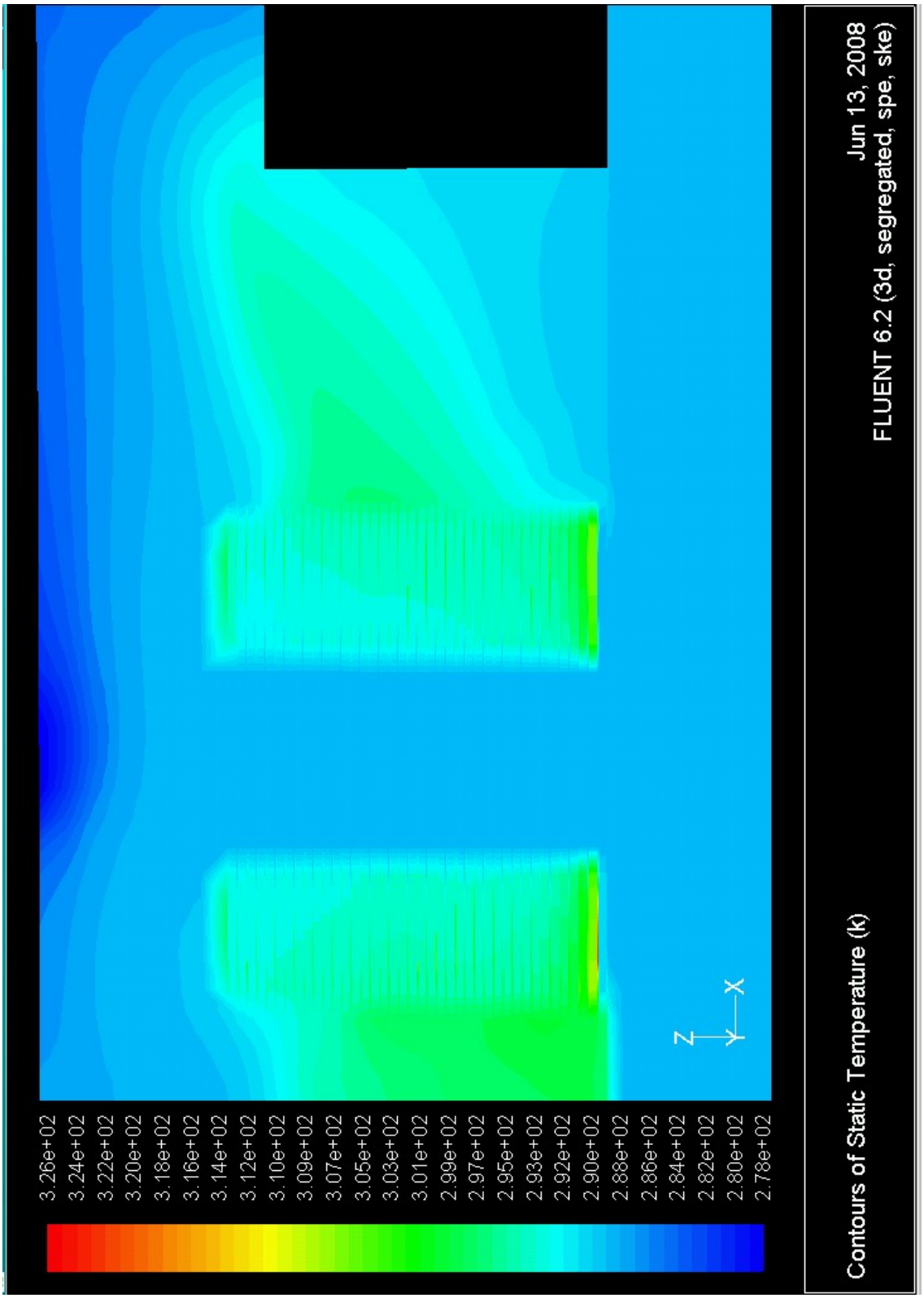
Contours of Static Temperature (k)
3.26e+02
3.24e+02
3.22e+02
3.20e+02
3.18e+02
3.16e+02
3.14e+02
3.12e+02
3.10e+02
3.09e+02
3.07e+02
3.05e+02
3.03e+02
3.01e+02
2.99e+02
2.97e+02
2.95e+02
2.93e+02
2.92e+02
2.90e+02
2.88e+02
2.86e+02
2.84e+02
2.82e+02
2.80e+02
2.78e+02
Z
X
Jun 13, 2008
FLUENT 6.2 (3d, segregated, spe, ske)

(a)

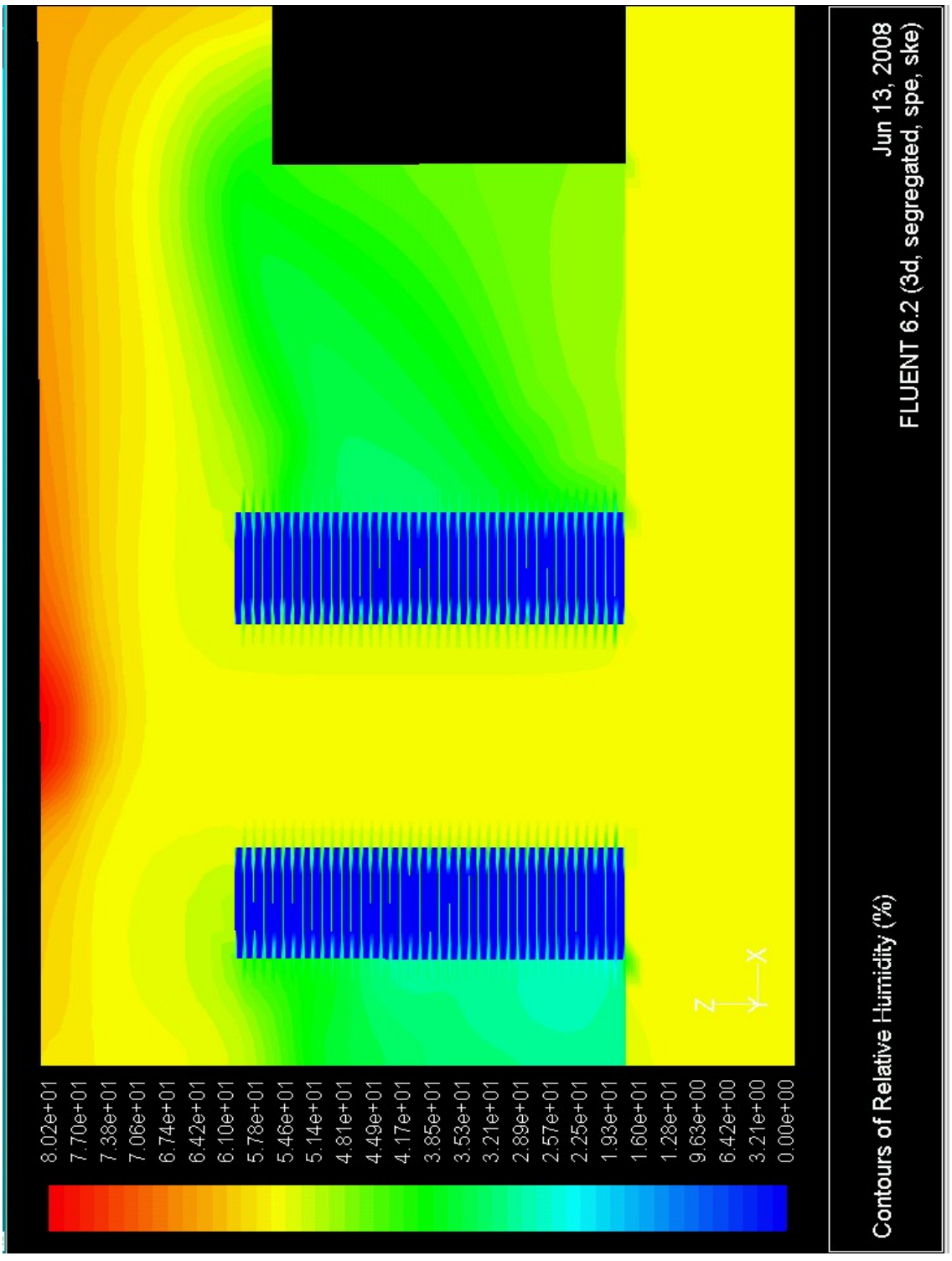

(b)

Figure A11. a) Temperature and b) RH plot through the vertical mid plane for the month of December inside the data center in Seattle

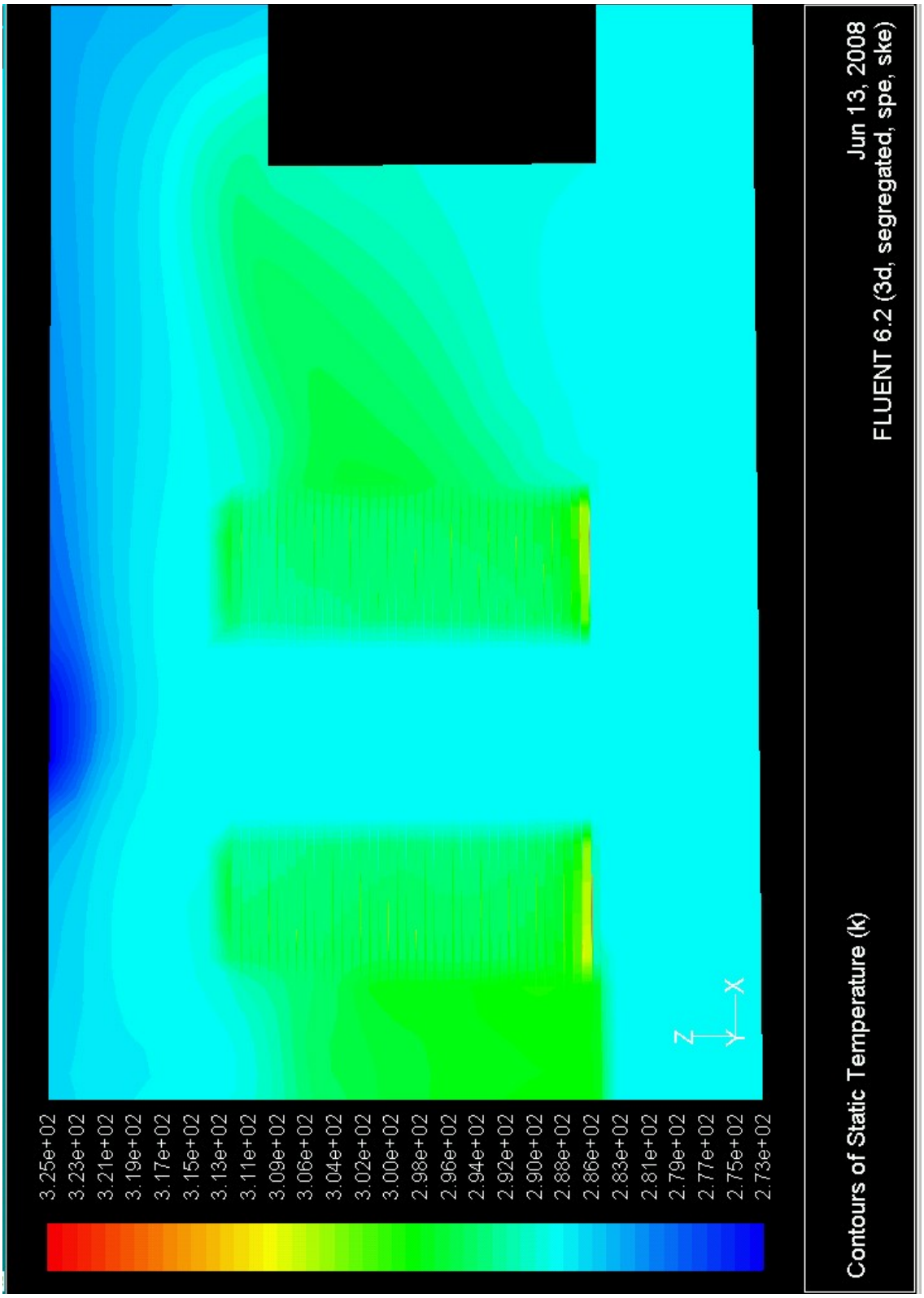
Contours of Static Temperature (k)
3.25e+02
3.23e+02
3.21e+02
3.19e+02
3.17e+02
3.15e+02
3.13e+02
3.11e+02
3.09e+02
3.06e+02
3.04e+02
3.02e+02
3.00e+02
2.98e+02
2.96e+02
2.94e+02
2.92e+02
2.90e+02
2.88e+02
2.86e+02
2.83e+02
2.81e+02
2.79e+02
2.77e+02
2.75e+02
2.73e+02
Z
Y
X
Jun 13, 2008
FLUENT 6.2 (3d, segregated, spe, ske)

(a)

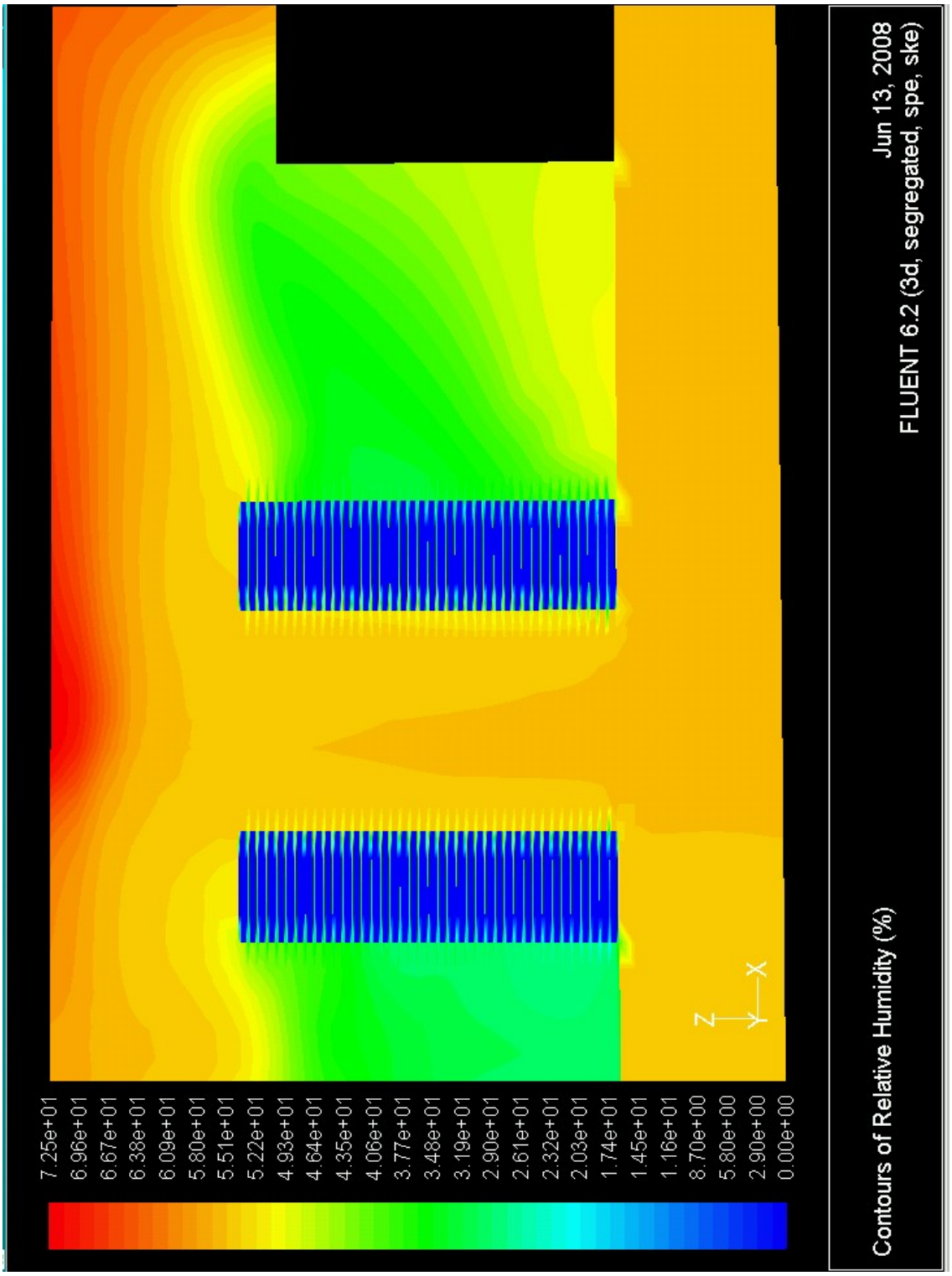

(b)

Figure A12. a) Temperature and b) RH plot through the vertical mid plane for the month of January inside the data center in New York

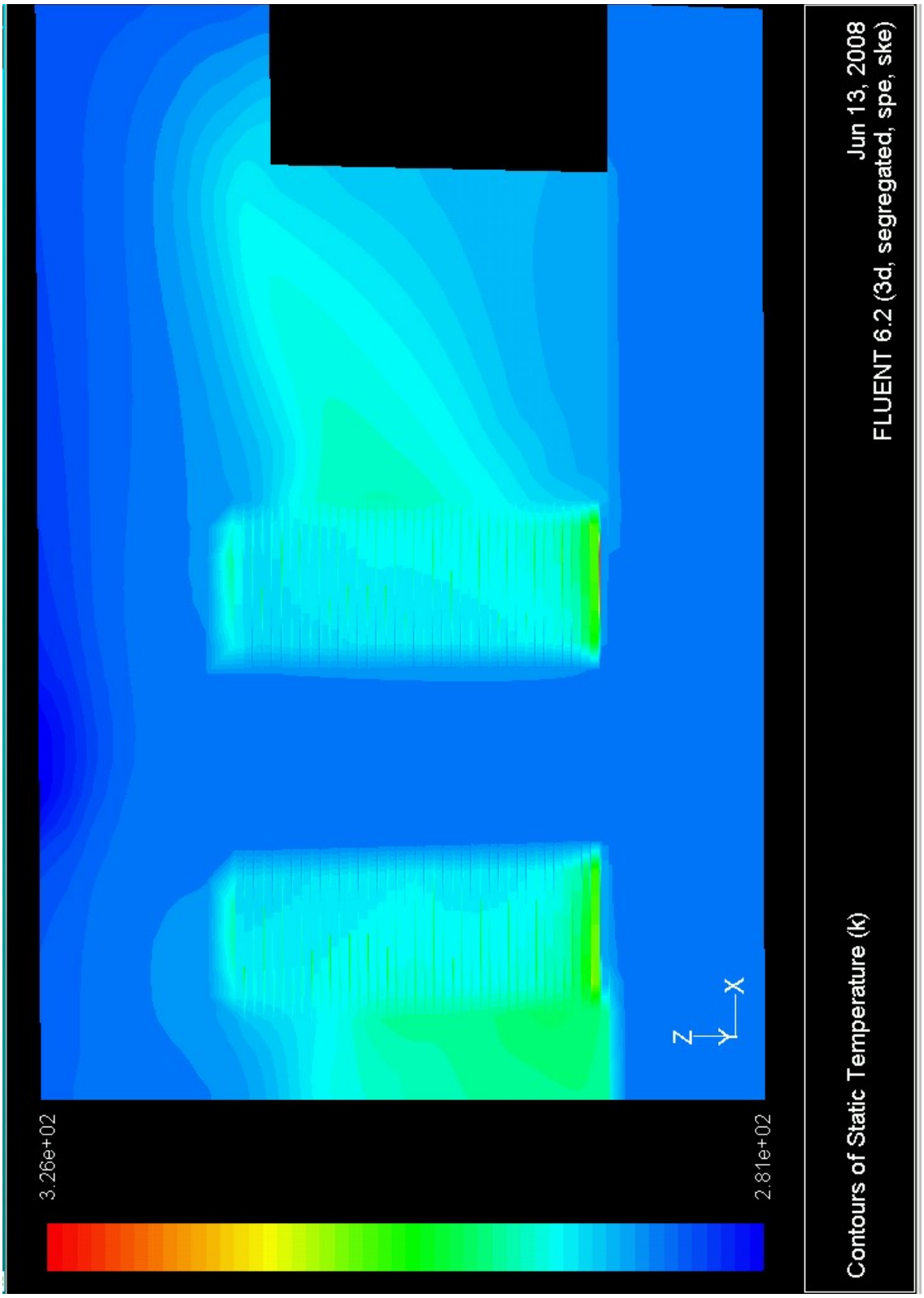
Contours of Static Temperature (k)
3.26e+02
2.81e+02
Z
X
Jun 13, 2008
FLUENT 6.2 (3d, segregated, spe, ske)

(a)

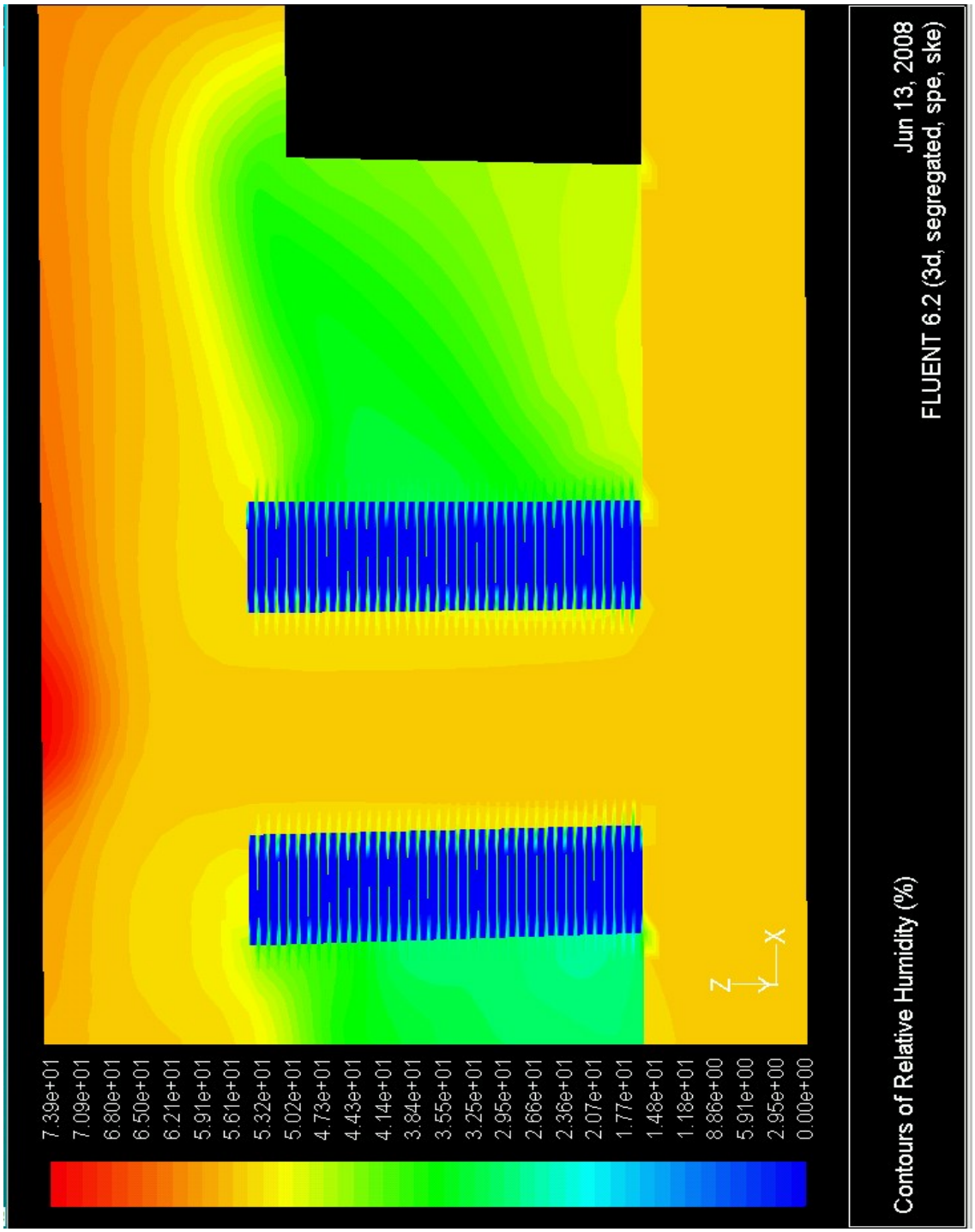

(b)

Figure A13. a) Temperature and b) RH plot through the vertical mid plane for the month of February inside the data center in New York

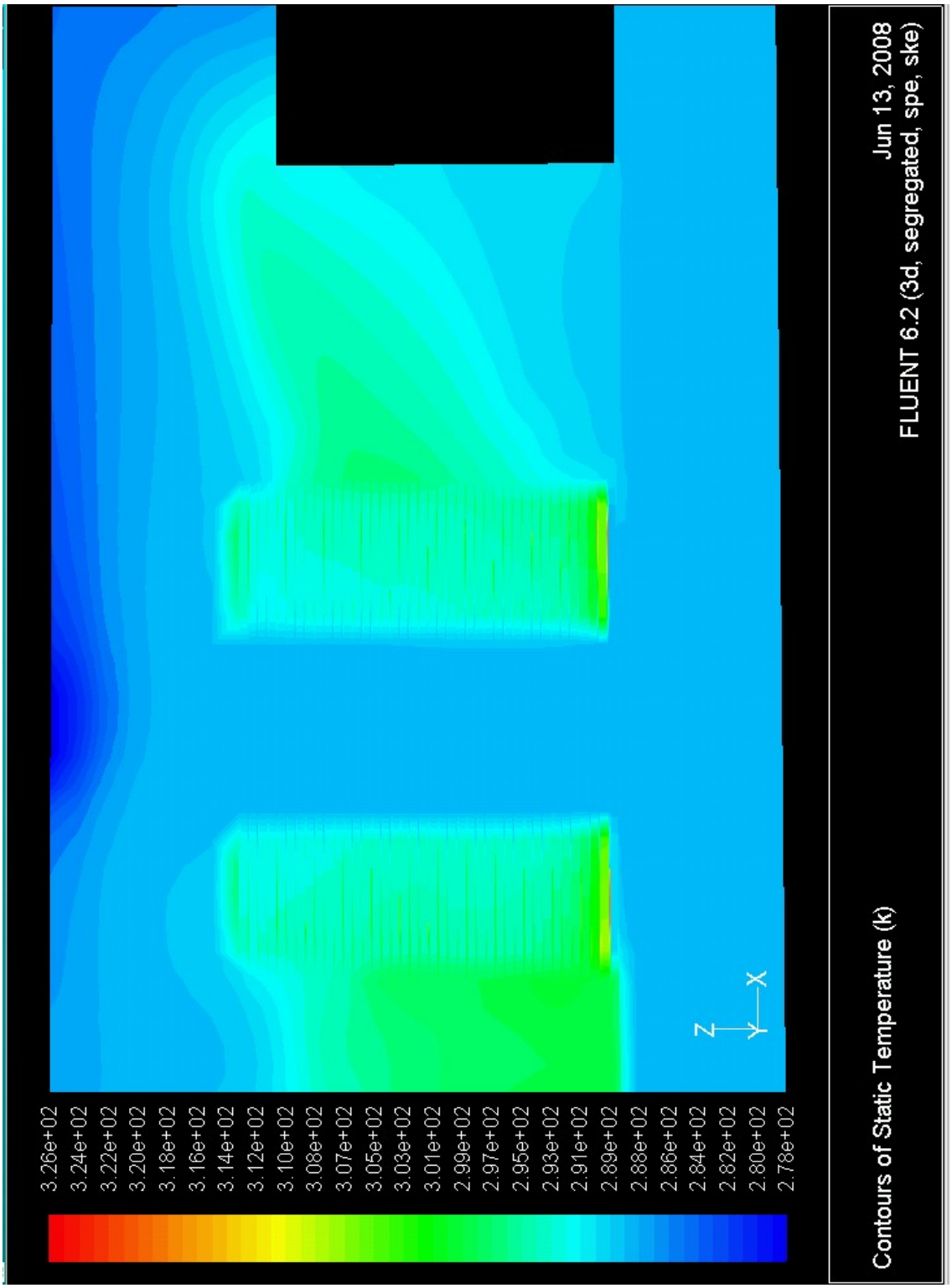
Contours of Static Temperature (k)
3.26e+02
3.24e+02
3.22e+02
3.20e+02
3.18e+02
3.16e+02
3.14e+02
3.12e+02
3.10e+02
3.08e+02
3.07e+02
3.05e+02
3.03e+02
3.01e+02
2.99e+02
2.97e+02
2.95e+02
2.93e+02
2.91e+02
2.89e+02
2.88e+02
2.86e+02
2.84e+02
2.82e+02
2.80e+02
2.78e+02
Z
Y
X
Jun 13, 2008
FLUENT 6.2 (3d, segregated, spe, ske)

(a)

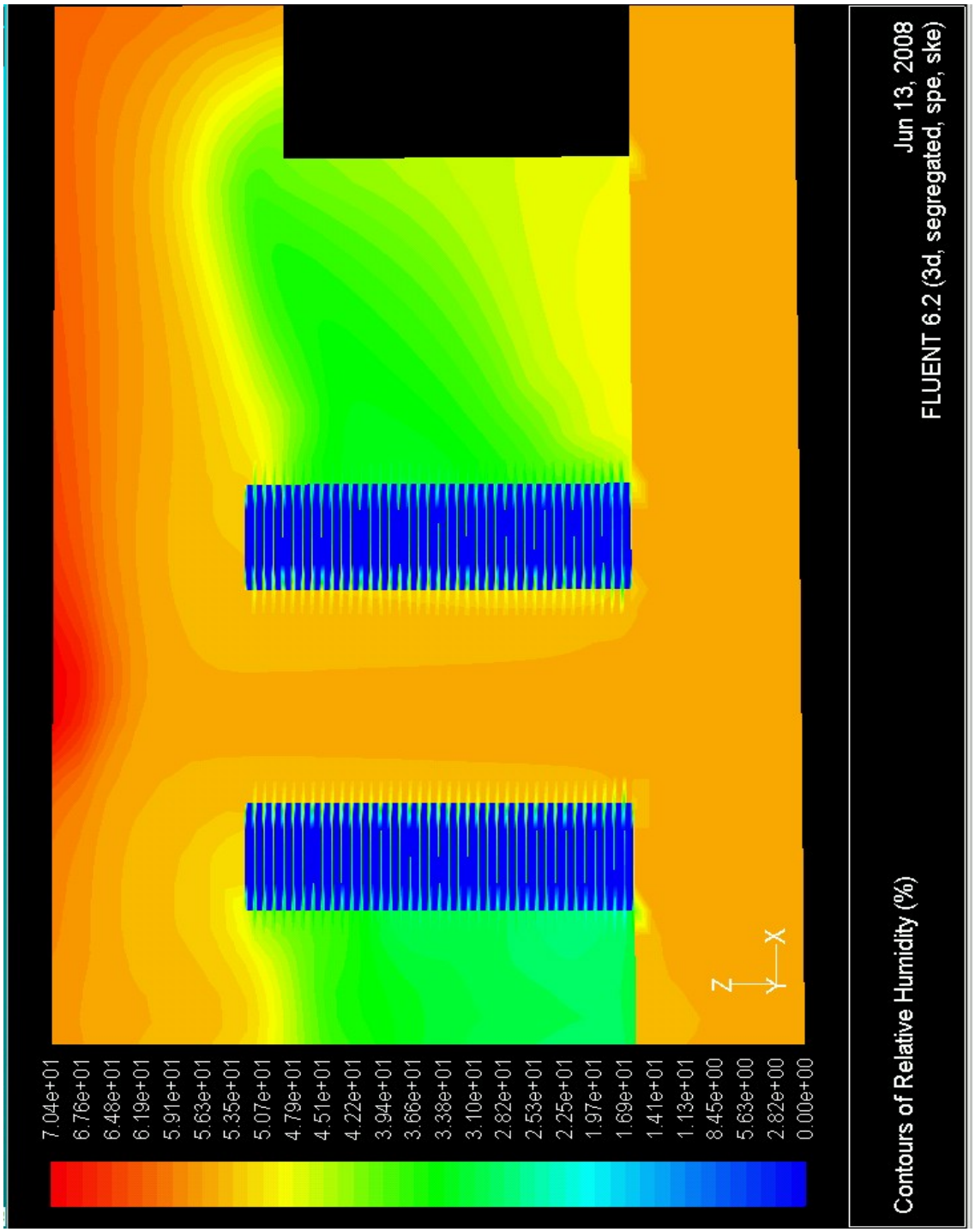

(b)

Figure A14. a) Temperature and b) RH plot through the vertical mid plane for the month of March inside the data center in New York

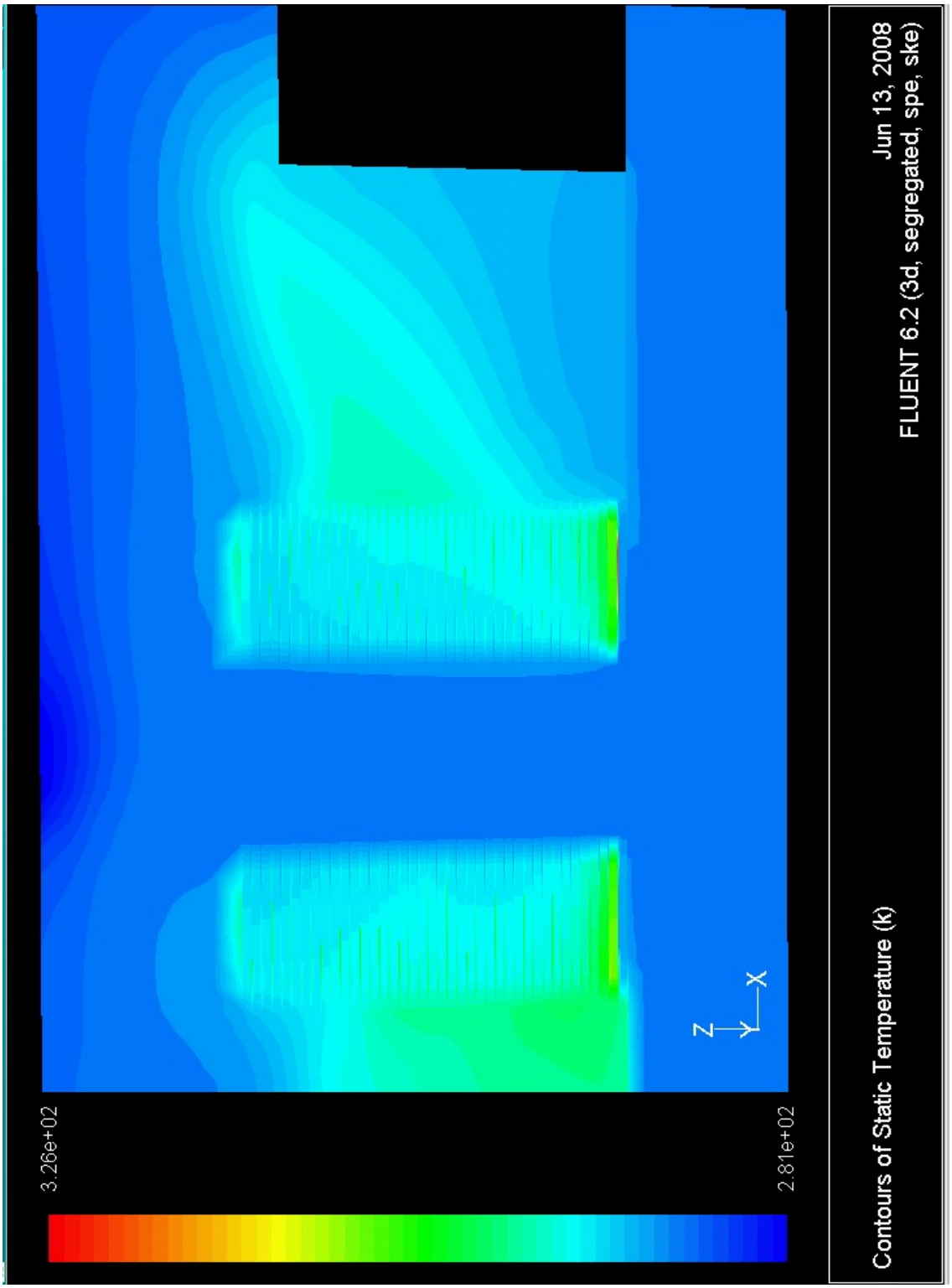
Contours of Static Temperature (k)
Jun 13, 2008
FLUENT 6.2 (3d, segregated, spe, ske)
3.26e+02
2.81e+02
Z
Y
X

(a)

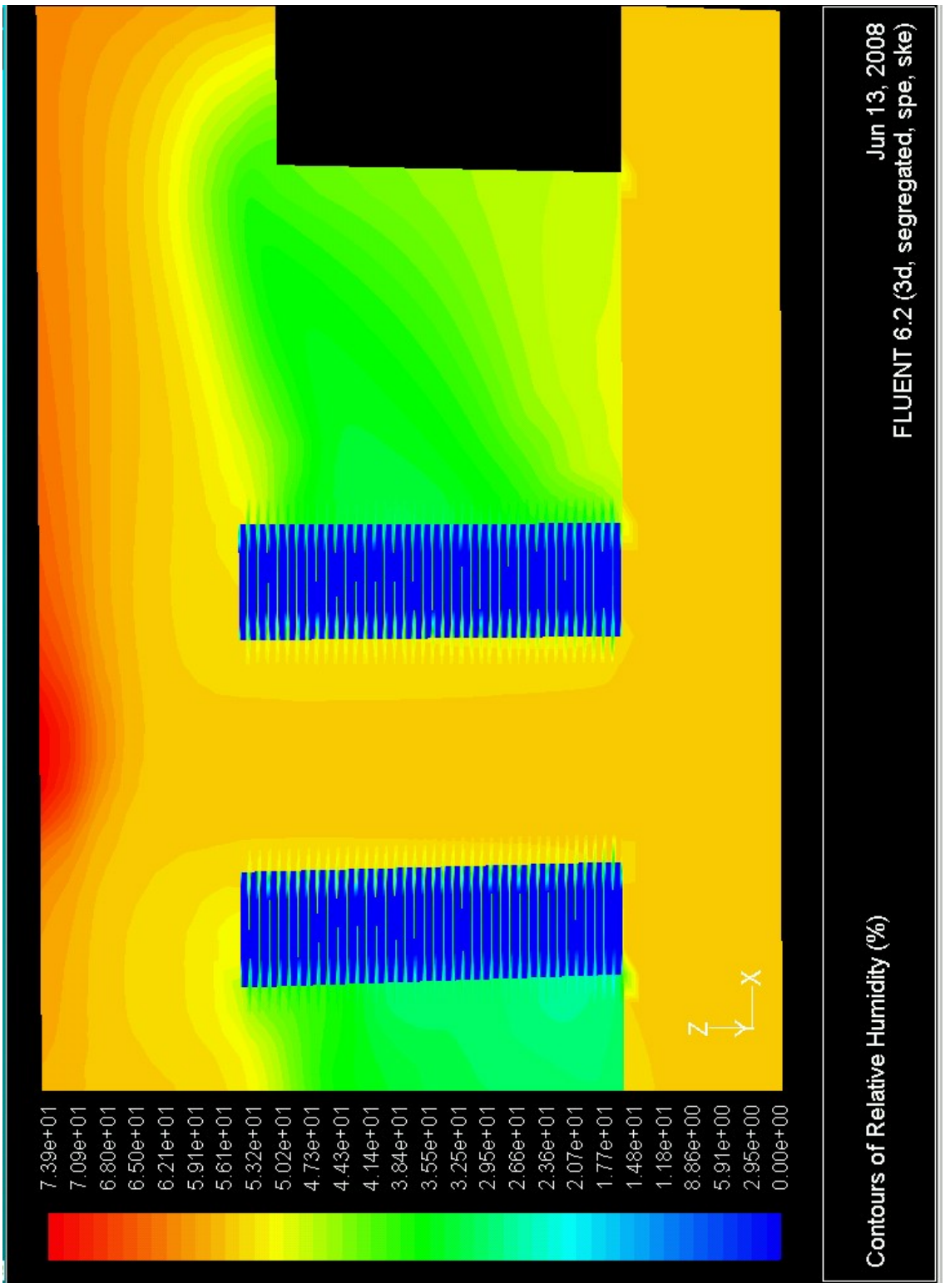

(b)

Figure A16. a) Temperature and b) RH plot through the vertical mid plane for the month of November inside the data center in New York

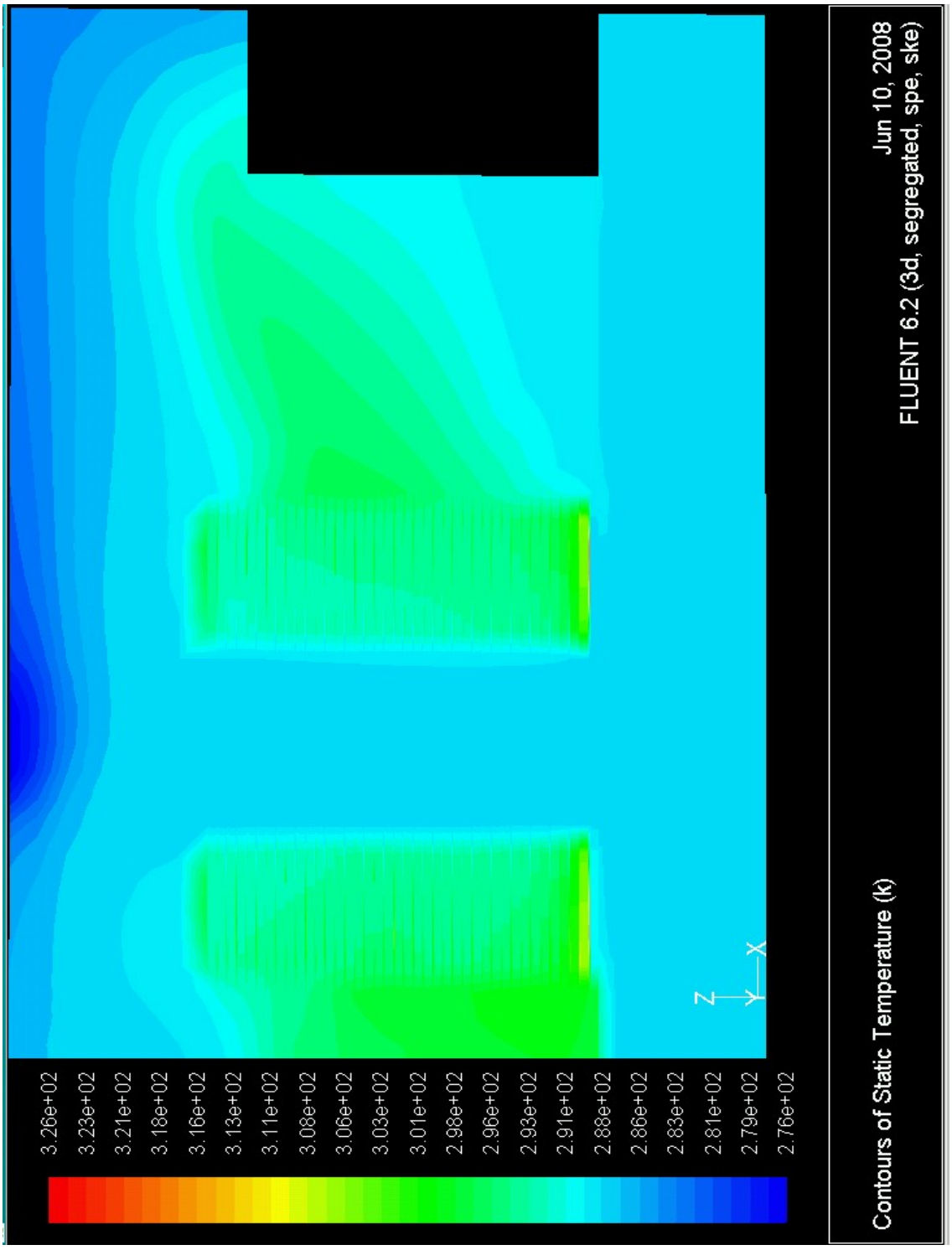
Contours of Static Temperature (k)
3.26e+02
3.23e+02
3.21e+02
3.18e+02
3.16e+02
3.13e+02
3.11e+02
3.08e+02
3.06e+02
3.03e+02
3.01e+02
2.98e+02
2.96e+02
2.93e+02
2.91e+02
2.88e+02
2.86e+02
2.83e+02
2.81e+02
2.79e+02
2.76e+02
Z
X
Jun 10, 2008
FLUENT 6.2 (3d, segregated, spe, ske)

(a)

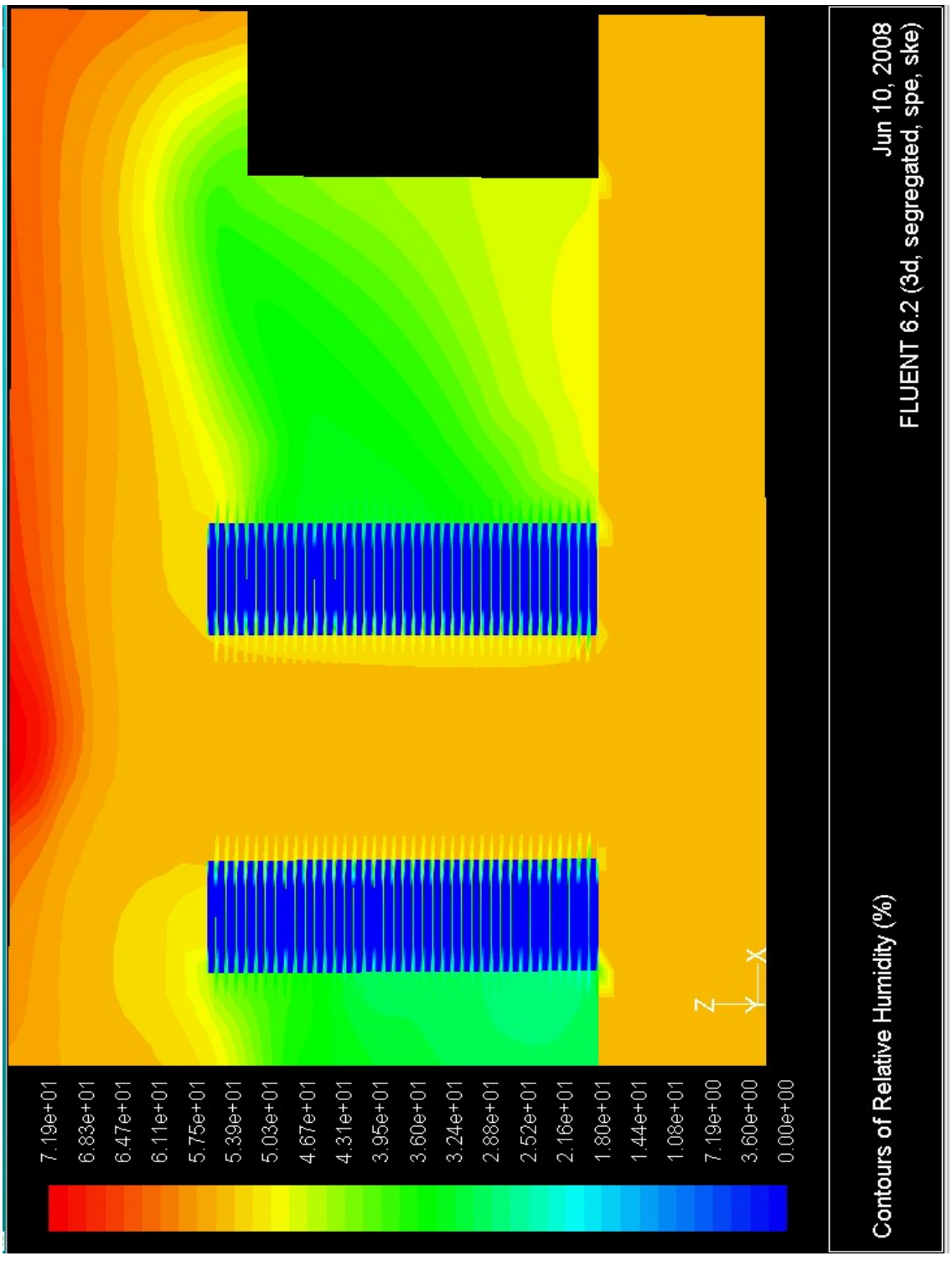

(b)

Figure A17. a) Temperature and b) RH plot through the vertical mid plane for the month of December inside the data center in New York

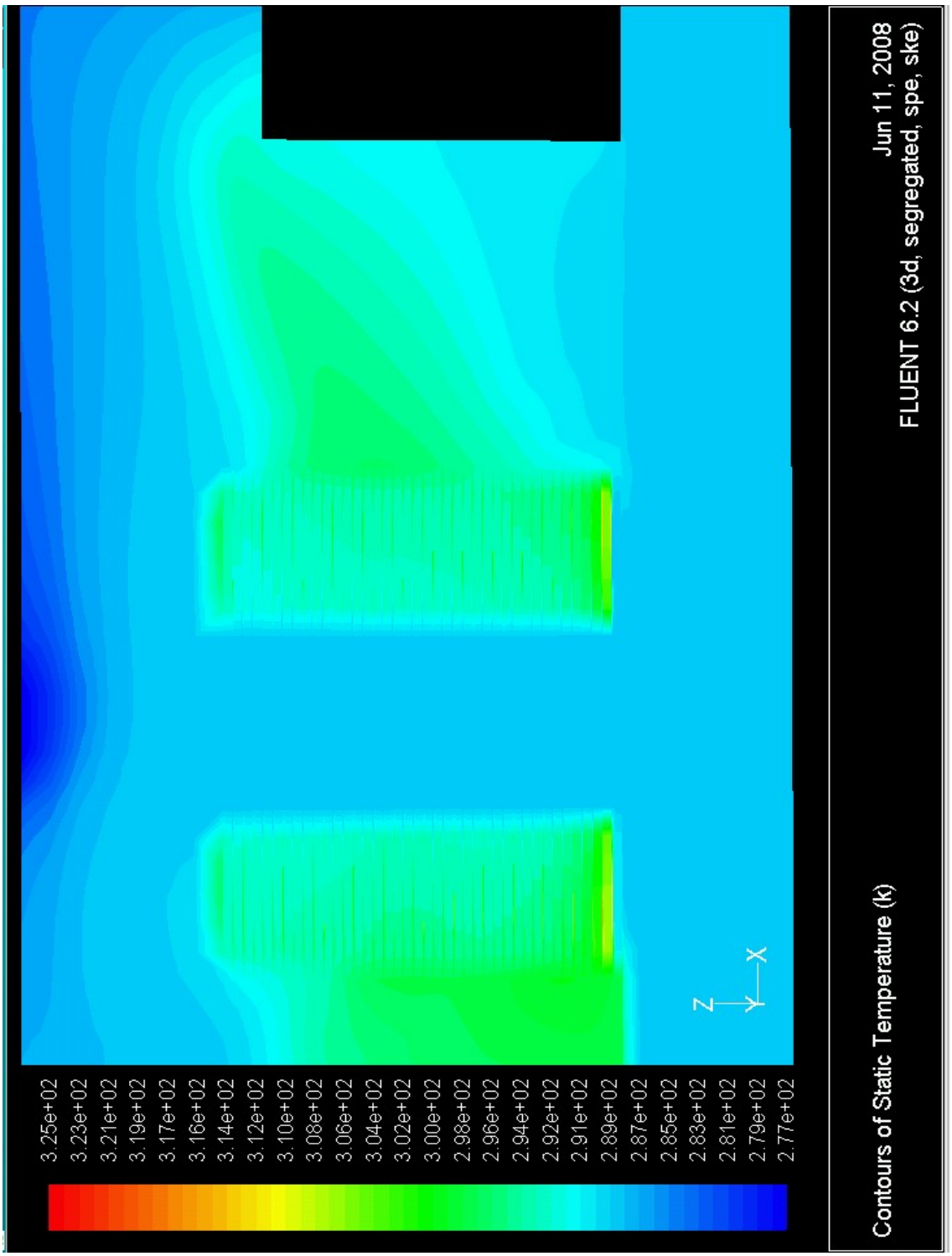
Contours of Static Temperature (k)
3.25e+02
3.23e+02
3.21e+02
3.19e+02
3.17e+02
3.16e+02
3.14e+02
3.12e+02
3.10e+02
3.08e+02
3.06e+02
3.04e+02
3.02e+02
3.00e+02
2.98e+02
2.96e+02
2.94e+02
2.92e+02
2.91e+02
2.89e+02
2.87e+02
2.85e+02
2.83e+02
2.81e+02
2.79e+02
2.77e+02
Z
X
FLUENT 6.2 (3d, segregated, spe, ske)
Jun 11, 2008

(a)

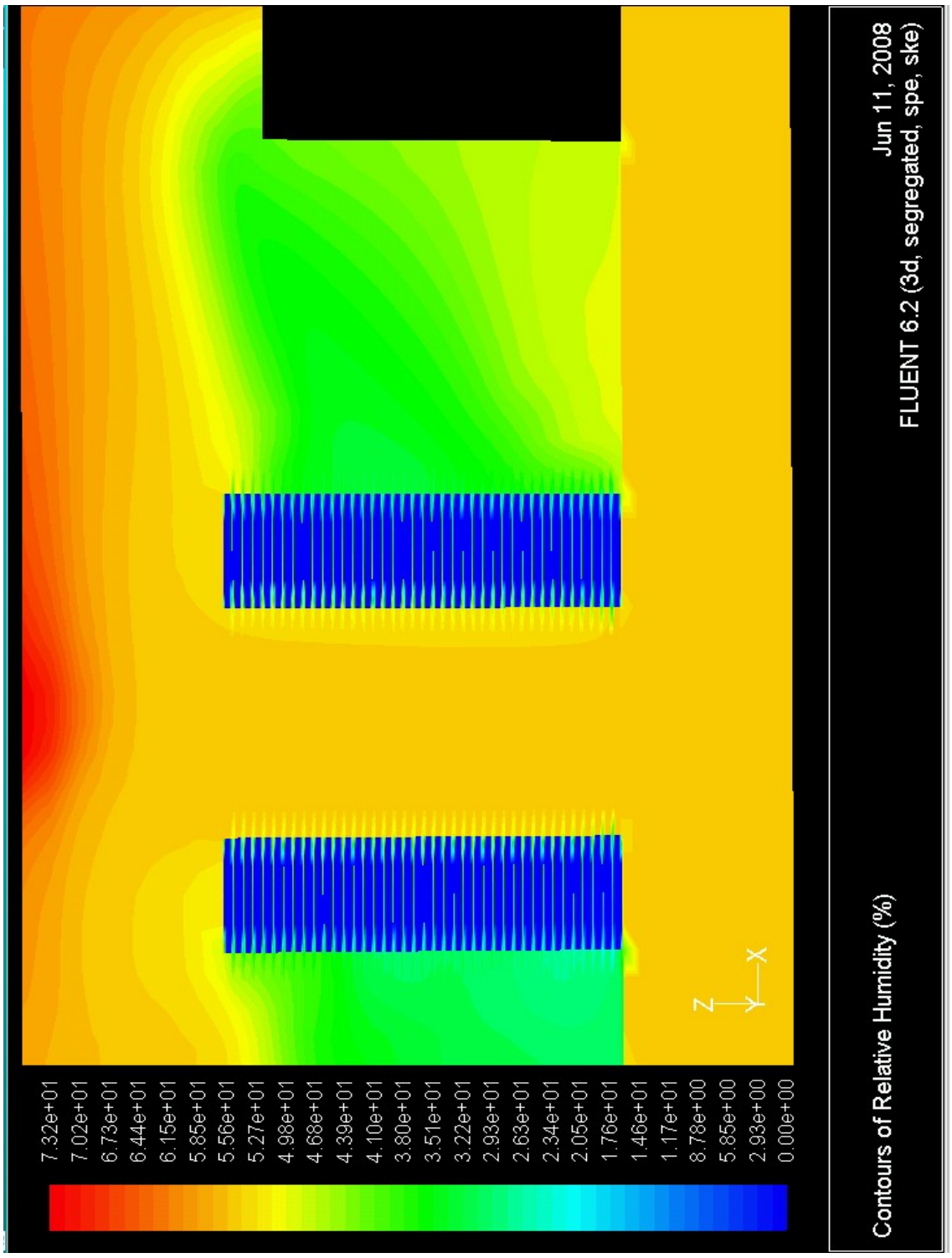

(b)

Figure A18. a) Temperature and b) RH plot through the vertical mid plane for the month of January inside the data center in Shanghai

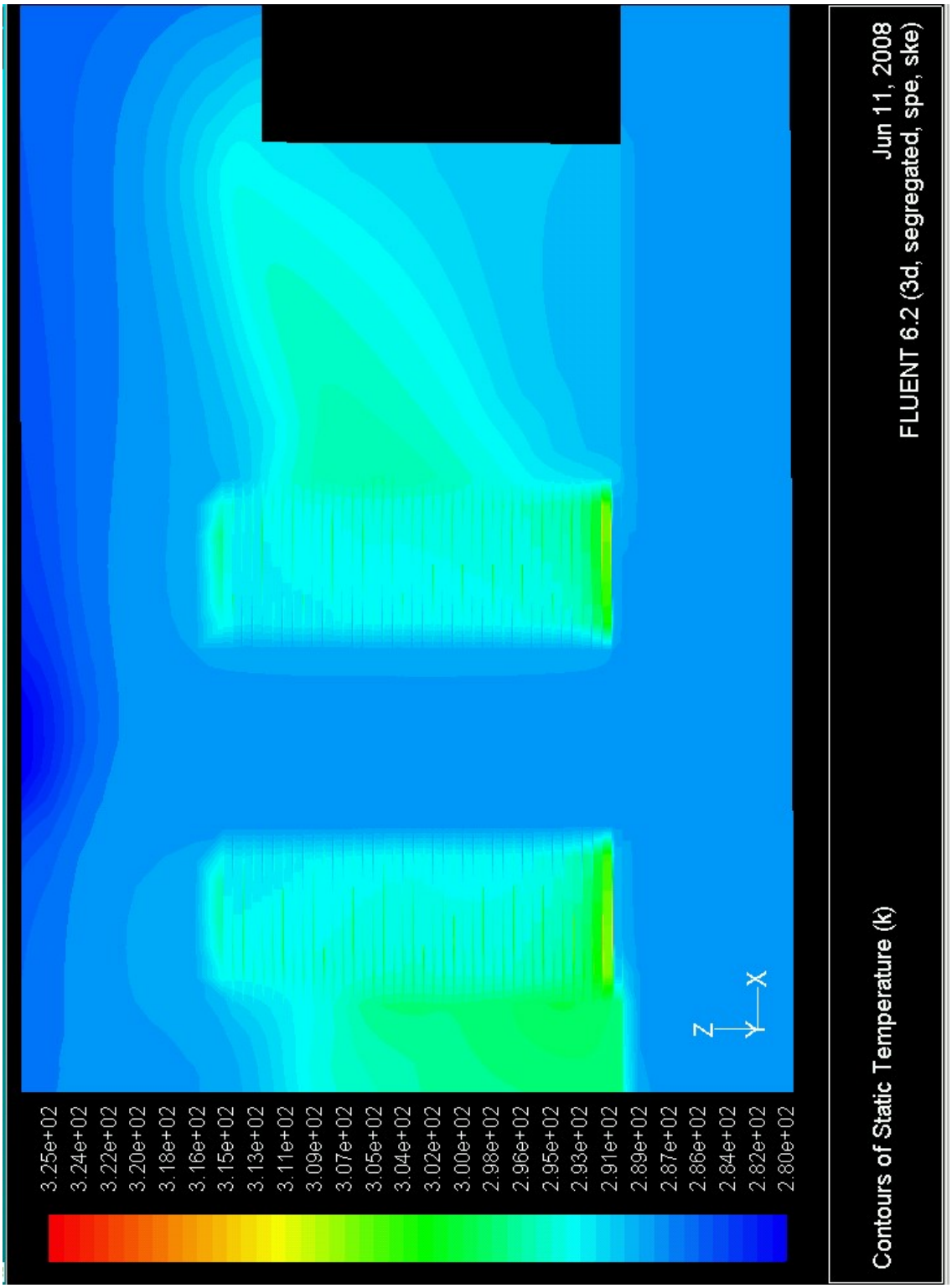
Contours of Static Temperature (k)
3.25e+02
3.24e+02
3.22e+02
3.20e+02
3.18e+02
3.16e+02
3.15e+02
3.13e+02
3.11e+02
3.09e+02
3.07e+02
3.05e+02
3.04e+02
3.02e+02
3.00e+02
2.98e+02
2.96e+02
2.95e+02
2.93e+02
2.91e+02
2.89e+02
2.87e+02
2.86e+02
2.84e+02
2.82e+02
2.80e+02
Z
X
Jun 11, 2008
FLUENT 6.2 (3d, segregated, spe, ske)

(a)

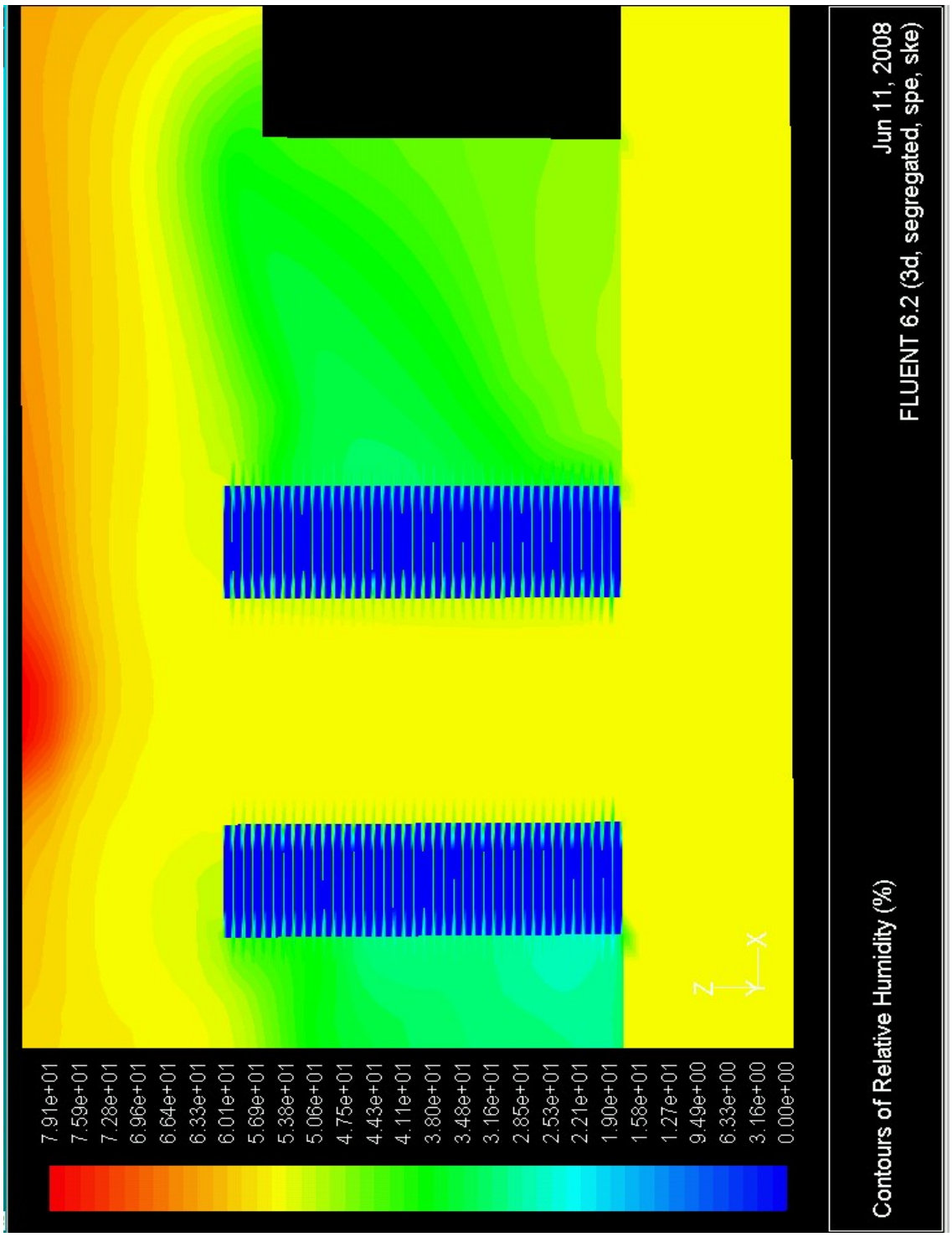

(b)

Figure A19. a) Temperature and b) RH plot through the vertical mid plane for the month of February inside the data center in Shanghai

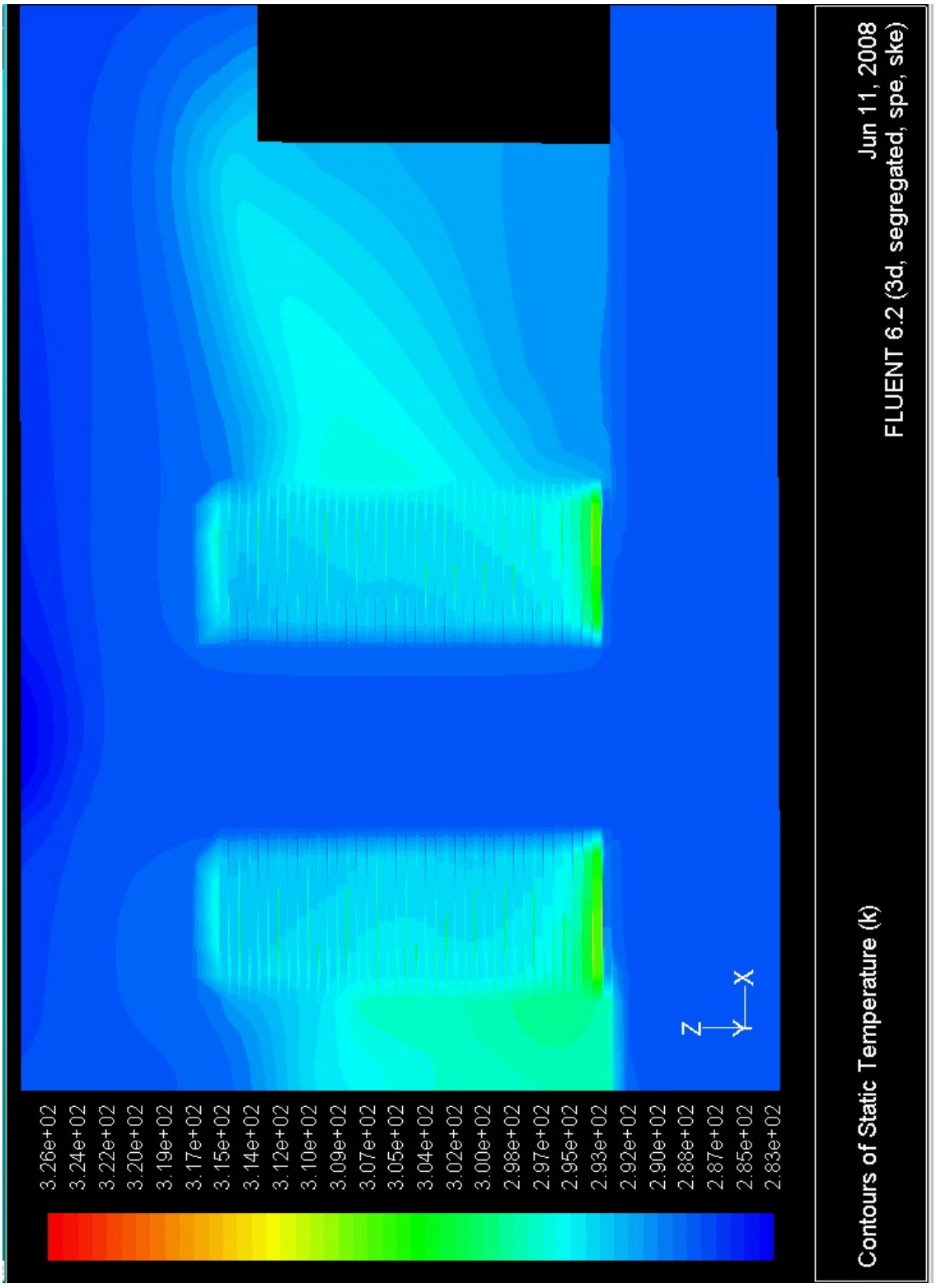
Contours of Static Temperature (k)
3.26e+02
3.24e+02
3.22e+02
3.20e+02
3.19e+02
3.17e+02
3.15e+02
3.14e+02
3.12e+02
3.10e+02
3.09e+02
3.07e+02
3.05e+02
3.04e+02
3.02e+02
3.00e+02
2.98e+02
2.97e+02
2.95e+02
2.93e+02
2.92e+02
2.90e+02
2.88e+02
2.87e+02
2.85e+02
2.83e+02
Z
X
Jun 11, 2008
FLUENT 6.2 (3d, segregated, spe, ske)

(a)

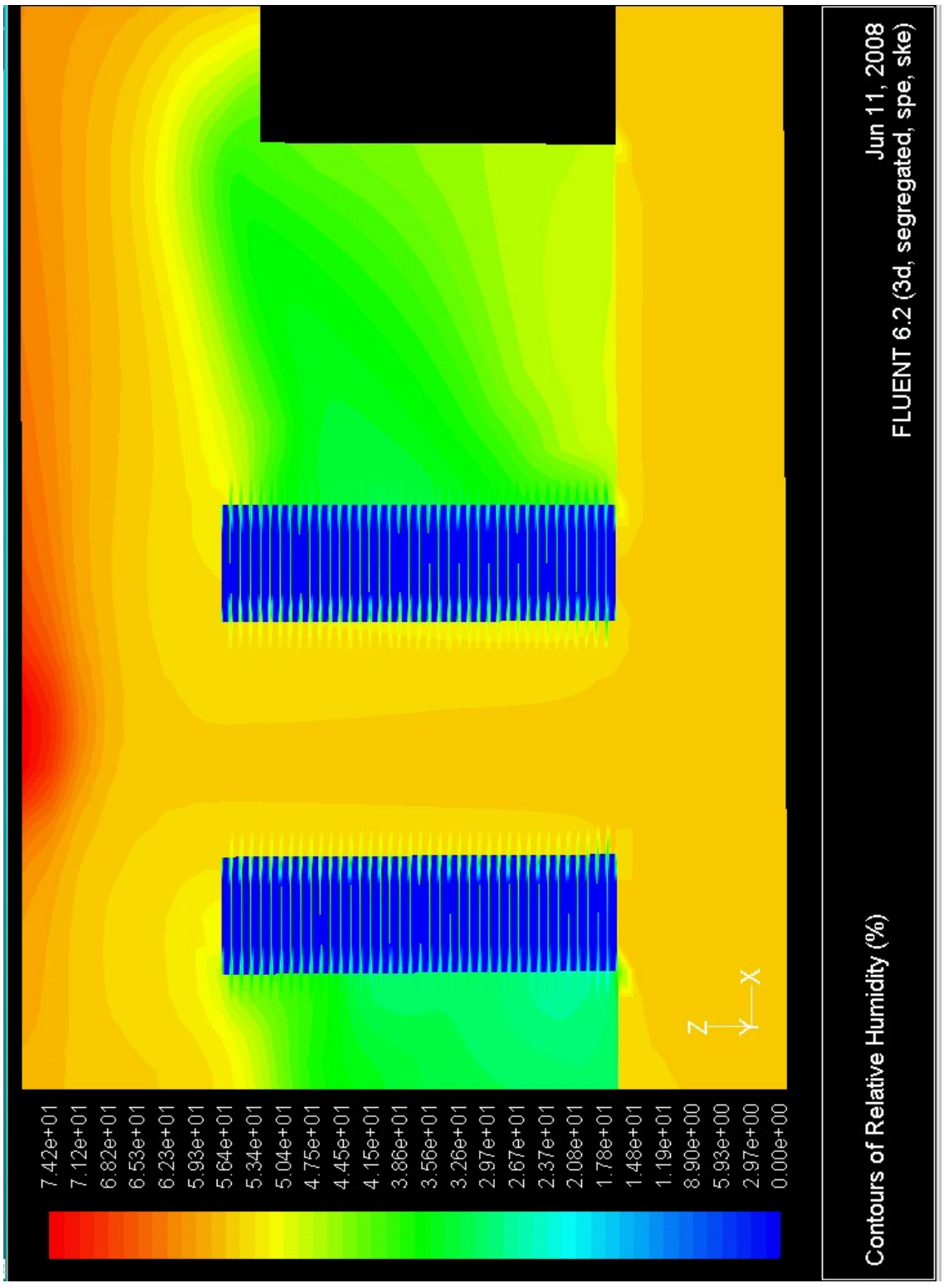

(b)

Figure A20. a) Temperature and b) RH plot through the vertical mid plane for the month of March inside the data center in Shanghai

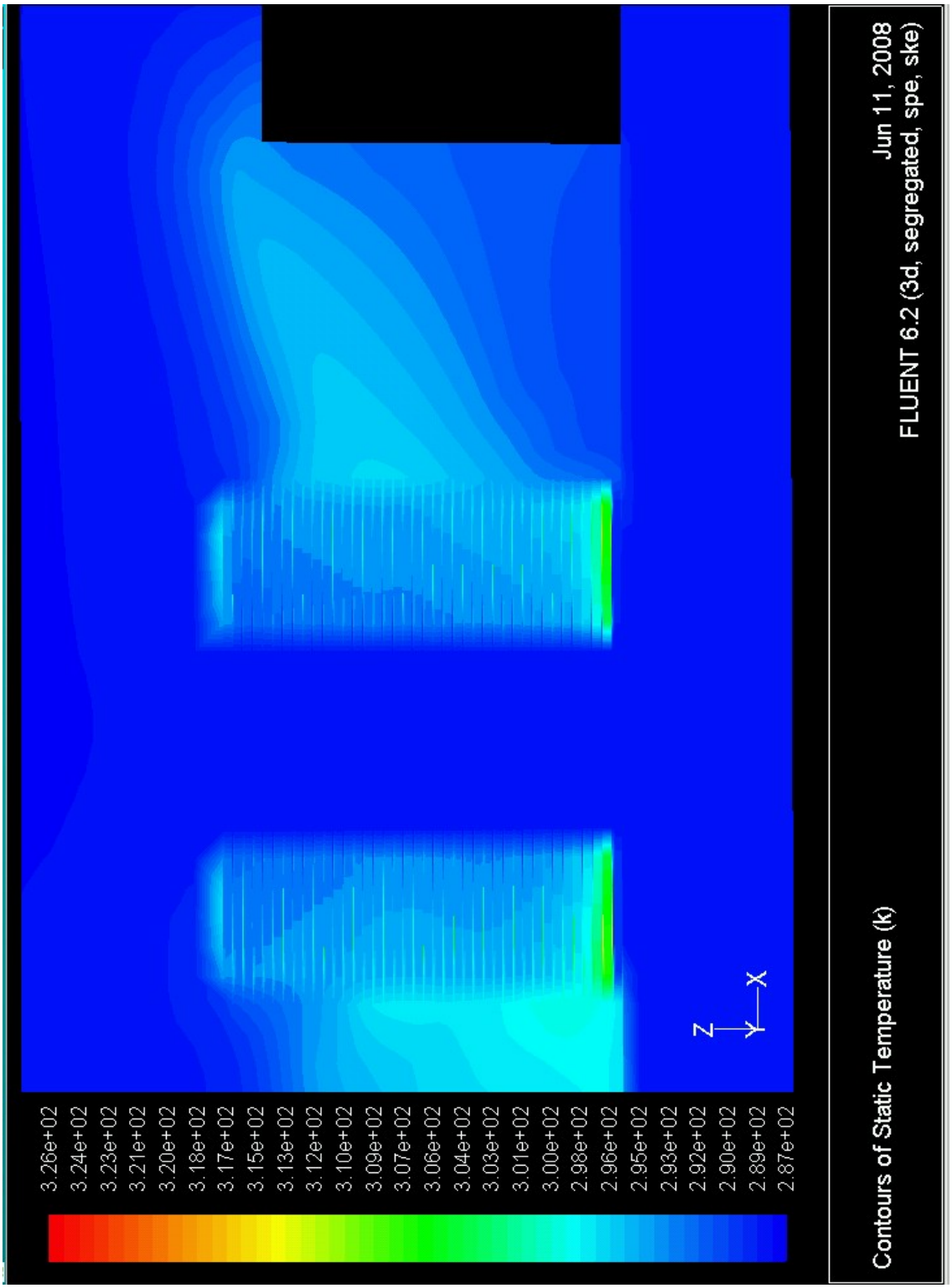
Contours of Static Temperature (k)
3.26e+02
3.24e+02
3.23e+02
3.21e+02
3.20e+02
3.18e+02
3.17e+02
3.15e+02
3.13e+02
3.12e+02
3.10e+02
3.09e+02
3.07e+02
3.06e+02
3.04e+02
3.03e+02
3.01e+02
3.00e+02
2.98e+02
2.96e+02
2.95e+02
2.93e+02
2.92e+02
2.90e+02
2.89e+02
2.87e+02
Z
X
Jun 11, 2008
FLUENT 6.2 (3d, segregated, spe, ske)

(a)

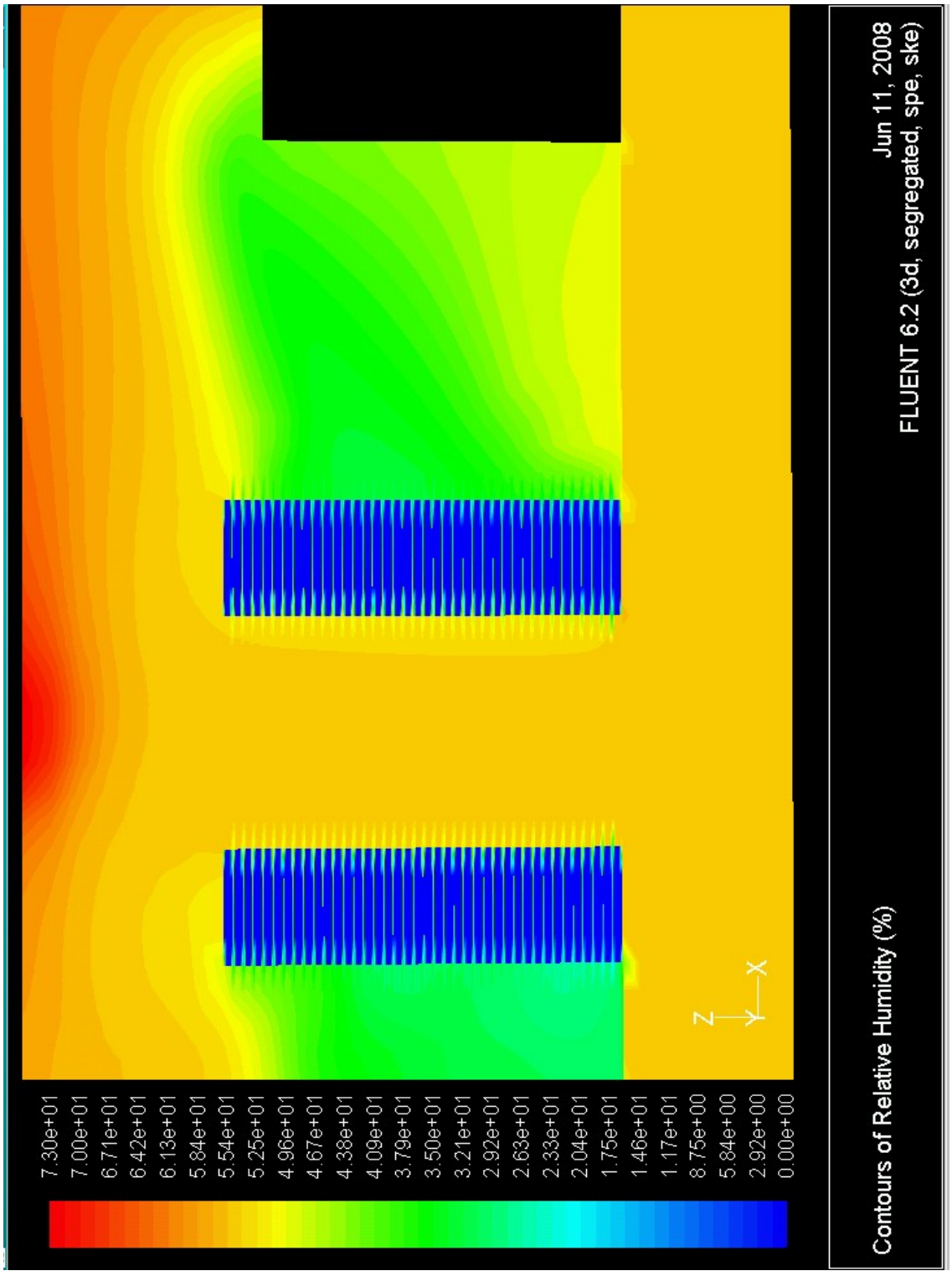

(b)

Figure A21. a) Temperature and b) RH plot through the vertical mid plane for the month of November inside the data center in Shanghai

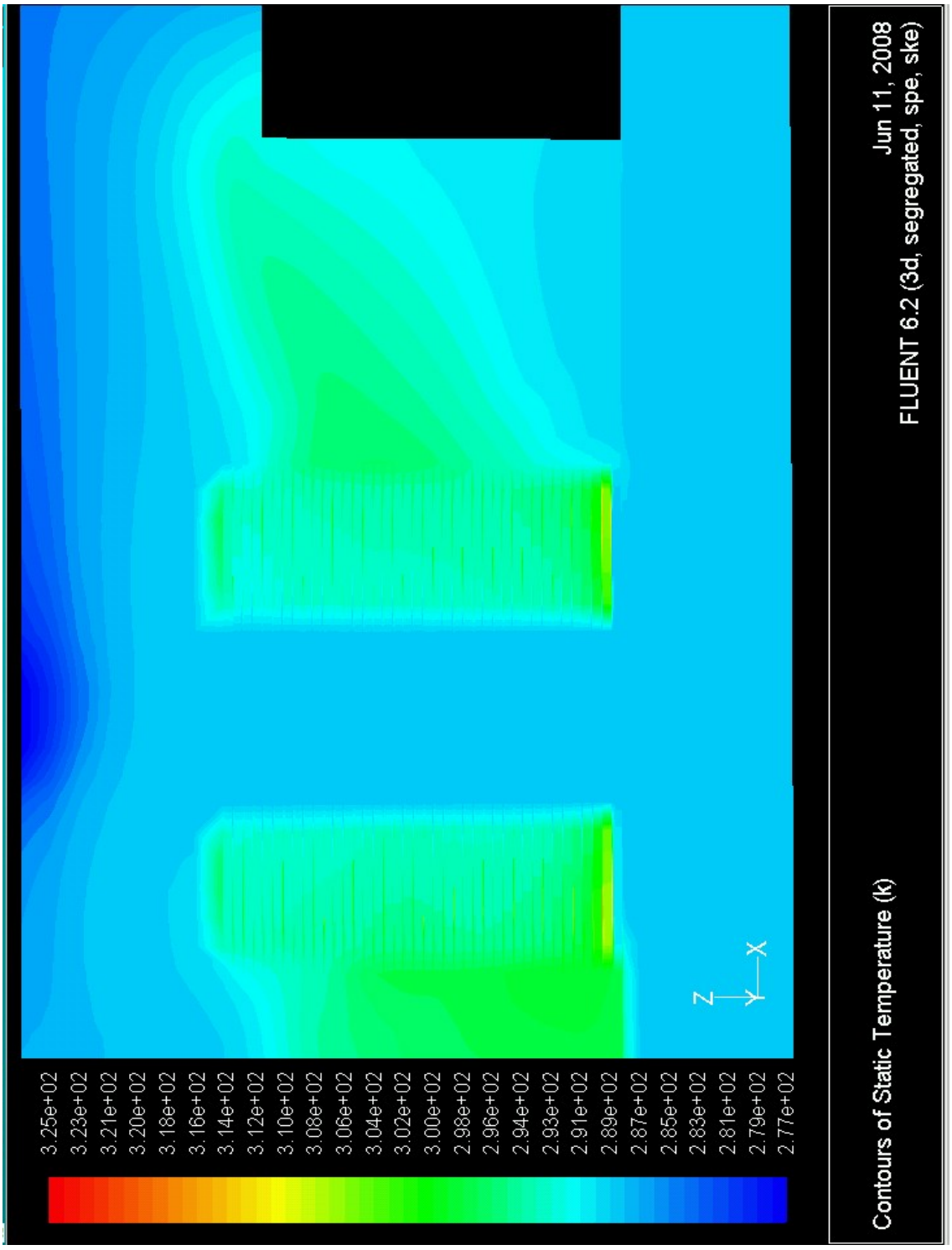
Contours of Static Temperature (k)
3.25e+02
3.23e+02
3.21e+02
3.20e+02
3.18e+02
3.16e+02
3.14e+02
3.12e+02
3.10e+02
3.08e+02
3.06e+02
3.04e+02
3.02e+02
3.00e+02
2.98e+02
2.96e+02
2.94e+02
2.93e+02
2.91e+02
2.89e+02
2.87e+02
2.85e+02
2.83e+02
2.81e+02
2.79e+02
2.77e+02
Z
X
Jun 11, 2008
FLUENT 6.2 (3d, segregated, spe, ske)

(a)

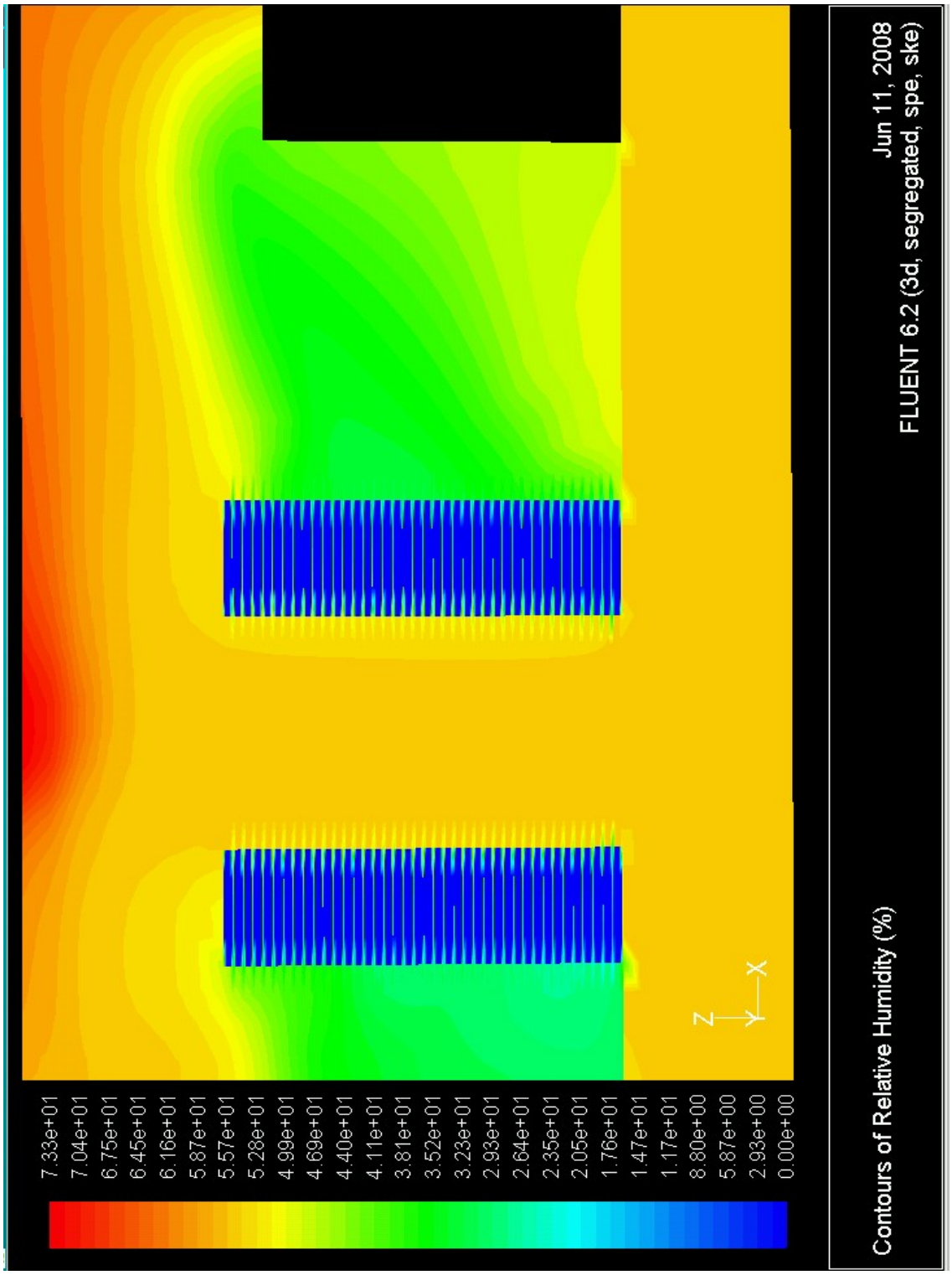

(b)

Figure A22. a) Temperature and b) RH plot through the vertical mid plane for the month of December inside the data center in Shanghai

Appendix B

Table 7: Power consumption calculation of CRAC for Atlanta

Atlanta					
Month	Cooling power (kW)	Humidification /Dehumidification Power (kW)	Fan Power (kW)	Baseline Power usage by CRAC units (kW)	% Saving
January	40.90	21.68	1.50	118.38	47.14697
February	60.50	9.50	1.50	118.38	40.87084
March	67.89	25.61	1.50	118.38	21.02033
November	67.85	25.25	1.50	118.38	21.39631
December	57.10	5.11	1.50	118.38	47.45951

Table 8: Power consumption calculation of CRAC for New York

New York					
Month	Cooling power (kW)	Humidification /Dehumidification Power (kW)	Fan Power (kW)	Baseline Power usage by CRAC units (kW)	% Saving
January	0.00	21.68	1.50	118.38	80.42
February	7.18	28.30	1.50	118.38	68.76
March	40.82	20.99	1.50	118.38	46.52
April	81.40	11.58	1.50	118.38	20.20
October	68.44	40.47	1.50	118.38	6.74
November	67.10	11.04	1.50	118.38	32.73
December	24.50	25.09	1.50	118.38	56.84

Table 9: Power consumption calculation of CRAC for Seattle

Seattle					
Month	Cooling power (kW)	Humidification /Dehumidification Power (kW)	Fan Power (kW)	Baseline Power usage by CRAC units (kW)	% Saving
January	43.80	11.30	1.50	118.38	52.19
February	54.00	9.01	1.50	118.38	45.50
March	67.70	4.22	1.50	118.38	37.98
April	67.93	17.07	1.50	118.38	26.93
October	68.48	29.02	1.50	118.38	16.37
November	63.80	4.08	1.50	118.38	41.39
December	43.20	11.04	1.50	118.38	52.92

Table 10: Power consumption calculation of CRAC for Shanghai

Shanghai					
Month	Cooling power (kW)	Humidification /Dehumidification Power (kW)	Fan Power (kW)	Baseline Power usage by CRAC units (kW)	% Saving
January	55.90	22.93	1.50	118.40	32.15
February	66.58	10.68	1.50	118.40	33.47
March	68.08	12.42	1.50	118.40	30.74
November	67.75	44.55	1.50	118.40	3.89
December	52.50	21.26	1.50	118.40	36.44

REFERENCES

[1] Lawrence Berkeley National Laboratory and Rumsey Engineers, Data Center Power Use: A Review of the Historical Data, 2004 http://hightech.lbl.gov/benchmarking-dc.html

[2] Lawrence Berkeley National Laboratory and Rumsey Engineers, 2003, "Data Center Energy Benchmarking Case Study", http://datacenters.lbl.gov/

[3] The Uptime Institute, 2004, "Heat Density Trends in Data Processing, Computer Systems and Telecommunications Equipment", http://www.upsite.com/TUIpages/tuiwhite.html

[4] Litvak, Mitrofanov, Hamara, Sounders, Modeling of Martian seasonal caps from HEND/ODYSSEY data, 2004, Advances in Space Research, Volume 36, Issue 11, p 2156-2161

[5] Weschler, C. J., and H. C. Shields, Experiments probing the influence of air exchange rates on secondary organic aerosols derived from indoor chemistry, 2003,Atmos. Environ., Volume 37, p5621-5631

[6] Tschudi, W., Data Center Economizer Contamination and Humidity Study, LNBN/Pacific Gas & Electric

[7] ASHRAE TC 9.9 2004, Thermal Guidelines for Data Processing Environments

[8] Patel, C. D., Bash, C. E., Belady, C., Stahl, L., and Sullivan, D., 2001, "Computational Fluid Dynamics Modeling of High Compute Density Data Centers to Assure System Inlet Air Specifications", Proc. of IPACK'01 - The Pacific Rim / ASME International Electronics Packaging Technical Conference and Exhibition Kauai, HI

[9] Schmidt, R. R., Karki, K. C., Kelkar, K. M., Radmehr, A., and Patankar, S. V., 2001, "Measurements and Predictions of the Flow Distribution Through Perforated Tiles in Raised Floor Data Centers", Proc. of IPACK'01 - The Pacific Rim / ASME International Electronics Packaging Technical Conference and Exhibition, Kauai, HI

[10] Schmidt, R. R. and Shaukatullah, H., 2002, "Computer and Telecommunications

Equipment Room Cooling: A Review of the Literature", Proc. of ITHERM 2002 - Eight Intersociety Conference on Thermal and Thermomechanical Phenomena in Electronic Systems, San Diego, CA

[11] Schmidt, R. R., Karki, K. C., and Patankar, S. V., 2004, "Raised-Floor Data Center: Perforated Tile Flow Rates for Various Tile Layouts", Proc. of ITHERM 2004 - Ninth Intersociety Conference on Thermal and Thermomechanical Phenomena in Electronic Systems, Las Vegas, NV, USA

[12] Radmehr, A., Schmidt, R. R., Karki, K. C., and Patankar, S. V., 2005, "Distributed Leakage Flow in Raised-Floor Data Centers", Proc. of IPACK'05 - International Electronic Packaging Technical Conference and Exhibition, San Franciso, CA

[13] Van Gilder, J. W. and Schmidt, R. R., 2005, "Airflow Uniformity Through Perforated Tiles in a Rasied-Floor Data Center", Proc. of IPACK'05 - International Electronic Packaging Technical Conference and Exhibition, San Francisco, CA

[14] Patel, C. D., Sharma, R., Bash, C. E., and Beitelmal, A., 2002, "Thermal Considerations in Cooling of Large Scale High Compute Density Data Centers", Proc. of ITHERM 2002 - Eight Intersociety Conference on Thermal and Thermomechanical Phenomena in Electronic Systems, San Diego, CA

[15] Schmidt, R. R. and Cruz, E., 2002, "Raised-Floor Compouter Data Center: Effect on Rack Inlet Temperatures of Chilled Air Exiting form Both the Hot and Cold Aisles", Proc. of ITHERM 2002 - Eight Intersociety Conference on Thermal and Thermomechanical Phenomena in Electronic Systems, San Diego, CA

[16] Schmidt, R. R. and Cruz, E., 2003, "Cluster of High Powered Racks within a Raised Floor Computer Data Center: Effects of Perforated Tiles Flow Distribution on Rack Inlet Air Temperature", Proc. of IMECE’03 – ASME International Mechanical Engineering Congress and R&D Exposition, Washington D.C

[17] Schmidt, R. R. and Iyengar, M., 2005, "Effect of Data Center Layout on Rack Inlet Air Temperatures", Proc. of IPACK'05 - International Electronic Packaging Technical Conference and Exhibition, San Francisco, CA

[18] Bhopte, S., Agonafer, D., Schmidt, R. R., and Sammakia, B., 2005, "Optimization

of Data Center Room Layout to Minimize Rack Inlet Air Temperature", Proc. of IPACK'05 - International Electronic Packaging Technical Conference and Exhibition, San Francisco, CA

[19] Rambo, J. and Joshi, Y., 2003, "Physical Models in Data Center Airflow Simulations", *Proc. of IMECE'03* – ASME International Mechanical Engineering Congress and R&D Exposition, Washington D.C.

[20] Iyengar, M., Schmidt, R. R., Sharma, A., McVicker, G., Shrivastava, S., Sri-Jayantha, S., Amemiya, Y., Dang, H., Chainer, T., and Sammakia, B., 2005, "Thermal Characterization of Non-Raised Floor Air Cooled Data Centers Using Numerical Modeling", Proc. of IPACK'05 - International Electronic Packaging Technical Conference and Exhibition, San Francisco, CA

[21] Shrivastava, S., Sammakia, B., Schmidt, R. R., and Iyengar, M., 2005, "Comparative Analysis of Different Data Center Airflow Management Configurations", Proc. of IPACK'05 - International Electronic Packaging Technical Conference and Exhibition, San Francisco, CA

[22] Rambo, J. and Joshi, Y., 2003, "Multi-Scale Modeling of High Power Density Data Centers", Proc. of IPACK'03 - The Pacific Rim / ASME International Electronics Packaging Technical Conference and Exhibition, Kauai, HI

[23] Rambo, J. and Joshi, Y. 2006, "Thermal Modeling of Technology Infrastructure Facilities: A Case Study of Data Centers", in: The Handbook of Numerical Heat Transfer: Vol II, W.J. Minkowycz, E.M. Sparrow, and J.Y. Murthy (Eds.), Taylor and Francis, New York

[24] Sharma, R. K., Bash, C. E., and Patel, C. D., 2002, "Dimensionless Parameters for the Evaluation of Thermal Design and Performance of Large-Scale Data Centers", AIAA, **AIAA-2002-3091**

[25] Sharma, R., Bash, C. E., Patel, C. D., and Beitelmal, M., 2004, "Experimental Investigation of Design and Performance of Data Centers", Proc. of ITHERM 2004 - Ninth Intersociety Conference on Thermal and Thermomechanical Phenomena in Electronic Systems, Las Vegas, NV

[26] Norota, M., Hayama, H., Enai, M., Mori, T., and Kishita, M., 2003, "Research on Efficiency of Air Conditioning System for Data Center", Proc. of INTELEC'03 -

25th International Telecommunications Energy Conference,, Yokohama, Japan

[27] Shah, A., Carey, V. P., Bash, C. E., and Patel, C. D., 2003, "Exergy Analysis of Data Center Thermal Management Systems", Proc. of IMECE'03 – ASME International Mechanical Engineering Congress and R&D Exposition, Washington, D.C.

[28] Shah, A. J., Carey, V. P., Bash, C. E., and Patel, C. D., 2005, "Exergy-Based Optimization Strategies for Multi-Component Data Center Thermal Management: Part I: Analysis", Proc. of IPACK'05 - International Electronic Packaging Technical Conference and Exhibition, San Francisco, CA

[29] Shah, A. J., Carey, V. P., Bash, C. E., and Patel, C. D., 2005, "Exergy-Based Optimization Strategies for Multi-Component Data Center Thermal Management: Part II: Application and Validation", Proc. of IPACK'05 - International Electronic Packaging Technical Conference and Exhibition, San Francisco, CA.

[30] Liebert Corporation, 2007, "Utilizing Economizers Effectively in the Data Center"

[31] Pacific Gas and Electric Company, 2006, "High Performance Data Centers, A Design Guidelines Scorebook"

[32] Vali Sorell, P.E., 2007, "OA Economizers For Data Centers", ASHRAE Journal

[33] Künzel, H.M., Zirkelbach D., Sedlbauer K., 2003, "Predicting Indoor Temperature and Humidity Conditions Including Hygrothermal Interactions with the Building Envelope", Proc. of 1st International Conference on Sustainable Energy and Green Architecture, Building Scientific Research Center (BSRC), King Mongkut's University Thonburi, Bangkok

[34] Peter Rumsey, 2007, "Using Airside Economizers to Chill Data Center Colling Bills." http://www.greenercomputing.com/columns_third.cfm?NewsID=35825

[35] U.S. Department of Energy, Energy Efficiency and Renewable Energy, http://www.energycodes.gov/implement/tech_assist_reports.stm

[36] Chivers, K.J., 1965, "Semi-automatic apparatus for study of temperature dependent phase separators", Journal of Sci Insrtu. Vol 42

[37] Buchanan, I.S., Apte, M.G., 2006, “Air Filter Materials and Building Related Systems in the BASE Study”, Environment Energy Technology Division, Indoor Environment Department, LNBN

[38] Seathon, I., Hot-Air Isolation Cools High-Density Data Centers http://cim.pennnet.com/display_article/305139/27/ARTCL/none/none/Hot-air-isolation-cools-high-density-data-centers/

[39] Garday, D., 2007, “Reducing Data Center Energy Consumption with Wet Side Economizers”, White Paper, Intel Information Technology

[40] Brandemuehl, M. J., Braun, J.E., “The Impact of Demand-Controlled and Economizer Ventilation Strategies on Energy Use in Buildings”, ASHRAE Transaction 1999, Vol 105, part 2

[41] Sloan, J., 2007, “Data Center-Full Time Air Economizer”, Proc. of ASHRAE 2007 Annual Meeting

[42] Rambo, J. D., Joshi, Y.K., 2003, “Multi-Scale Modeling of High Power Density Data Centers”, Porc of InterPACK’03

[43] Sharma, R.K., Bash, C.E., Patel, C.D., 2002, “Dimensionless Parameters for the Evaluation of Thermal Design and Performance of Large-Scale Data Centers”, 8th AIAA/ASME Joint Thermophysics and Heat Transfer Conference

[44] Bean, J., Dunlap, K., “Closed Coupled Rows Save Energy”, http://www.comnews.com/features/2007_april/0407close-coupled.aspx

[45] Schmidt, R.R., Cruz, E.E., “Challenges in Data Center Thermal Management”, IBM Journal of Research and Development, http://www.research.ibm.com/journal/rd/494/schmidt.html

[46] Kjelgaard, M., 2003, “Airside Economizers and Adiabatic Humidifier: a Better Choice?”, Weather Report, http://findarticles.com/p/articles/mi_m0BPR/is_4_20/ai_99751142

[47] 2005 ASHARE Handbook Fundamentals, 2005

[48] Teitel, M., Tanny, J., 1999, “Natural Ventilation of Greenhouses: Experiments and Model”, Agriculture and Forest Meterology, vol 96.